UNIVERSITÀ DEGLI STUDI DI MILANO

Facoltà di Medicina e Chirurgia

Dipartimento di Chimica, Biochimica e Biotecnologie per la Medicina

Settore Scientifico Disciplinare BIO/10

SCUOLA DI DOTTORATO IN SCIENZE BIOCHIMICHE, NUTRIZIONALI E METABOLICHE

DOTTORATO DI RICERCA IN BIOCHIMICA

CICLO XXIII

TESI DI DOTTORATO DI RICERCA

APPROACHES TO THE STUDY OF GLYCOLIPID BIOCHEMICAL MECHANISMS OF ACTION

Docente Guida: Prof. Fiamma RONCHETTI

Coordinatore: Prof. Francesco BONOMI

Candidato:
Dott. Riccardo DI BRISCO
Matr. n. R07798

Anno Accademico 2009-2010

INDEX

OVERVIEW

With this work I want to give an explanation of the role of glycolipids in biological processes, paying particular attention to their involvement in various biochemical mechanisms.

This thesis will be divided into two sections in which I discuss in the first one, the involvement of glycolipids in the process of fertilization and in the second one I will pay attention on a new class of glycolipids that might be involved in immunoregulation processes.

In more details in the first section I will provide an overview of the biochemical role of sulfogactosylglicerolipid (SGG), present in the sperm head of different mammalian species, and its involvement in the process of fertilization.

Then I will discuss an approach with which one can interfere in this biochemical mechanism focusing on the possibility of using a new class of molecules that permit not only the inhibition of the fertilization process but that can also act against sexually transmitted diseases. In this scenario, then I will focus on the characteristics of antimicrobial peptides, in particular on the family of cathelicidin, and on their possible application in the inhibition of fertilization, by interaction with SGG, and at the same time the prevention of sexually transmitted diseases.

In the second section I will discuss on a new class of immunomodulating glycolipids with an atypical structure, produced by symbiotic bacteria in the marine sponge *Plakortis Simplex*, which releases a unique profile of cytokines.

In this scenario, then I will talk about simplexide and on the role in which is involved in the activation of peripheral blood mononuclear cells (PBMC), and the peculiar profile of cytokines released.

Then I will describe the synthesis of a fluorescent analogue of simplexide which will be made to evaluate the subcellular distribution of the glycolipid and to clarify its mechanism of action.

The part of the project related to the study of fertilization process was carried out in the laboratory of Prof.ssa Nongnuj Tanphaichitr at the Ottawa Research Institute (OHRI), Canada.

SECTION I

1. INTRODUCTION

1.1 Sulfogalactosylglycerolipid (SGG)

1-*O*-hexadecyl-2-*O*-hexadecanoyl-3-*O*-(3'-sulfo-β-D-galactopyranosyl)-*sn*-glycerol (SGG), also known as sulfogalactosylglycerolipid or seminolipid, is a sulfoglycolipid substantially present in male germ cells (10 mole% of total lipids) across all the mammalian species studied (Bou et al., 2006; Tanphaichitr et al., 2003; Ishizuka et al., 1973; Kornblatt et al., 1974; Suzuki et al., 1973). SGG consists of a glycerol backbone with 3-*O*-sulfated galactose at the *sn*-3 position and an alkyl and acyl chain (both mainly 16:0) at the *sn*-1 and *sn*-2 positions, respectively (Fig. 1) (Ishizuka et al., 1973).
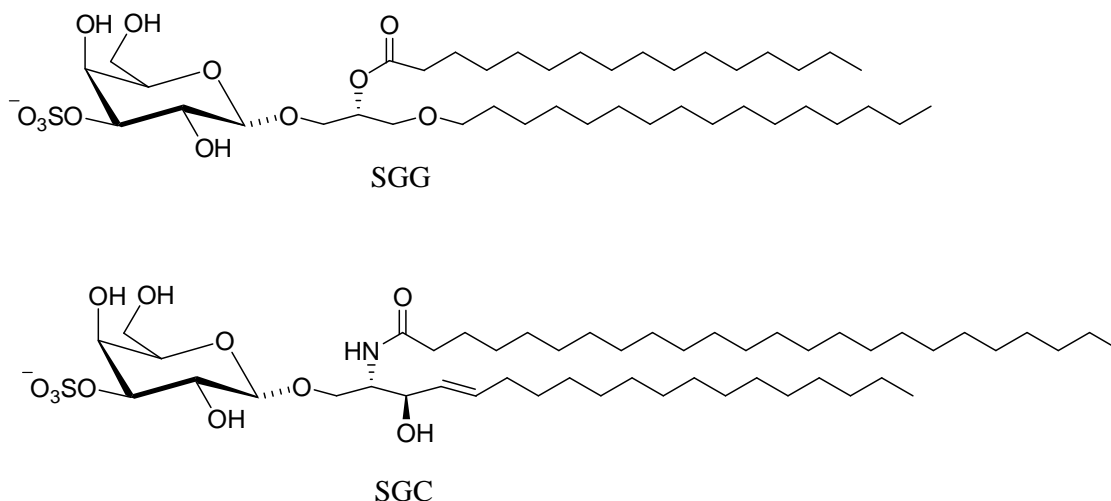
Fig. 1 Chemical structures of SGG and SGC.

Sulfogalactosylceramide (i.e., SGC or sulfatide), which can be structurally referred to SGG, is a major lipid component of the myelin sheath; it is also found in epithelial cells of the kidney and digestive tract as well as in male germ cells of lower vertebrates and invertebrates. SGC has the same galacto carbohydrate moiety as SGG but it has ceramide as a lipid backbone, unlike SGG (Fig. 1).

1.2 Biosynthesis of SGG and SGC

SGG and SGC have identical polar head groups but different lipid backbones (i.e., 1-*O*-hexadecyl 2-*O*-hexadecanoyl glycerol and ceramide, respectively). The biosynthesis of SGC, occurring mainly in the brain, involves two enzymes: UDP-galactose: ceramide galactosyltransferase (**CGT**; EC 2.4.1.62) and cerebroside sulfotransferase (**CST**; EC 2.8.2.11) (Fig. 2). CGT catalyzes the formation of galactosylceramide (GC) also known as cerebroside from ceramide with UDP-galactose as the galactose donor. CST catalyzes the synthesis of GC to SGC using 3'-phosphoadenosine -5'-phosphosulfate (PAPS) as sulfate donor. Accumulated evidence suggests that the biosynthetic pathway of SGG in the testis is similar to that of SGC described in the brain. Following the intratesticular injection of [^{14}C]palmitate, [^{14}C]galactose and [^{14}C]cetyl alcohol, both galactosylglycerol (GG) and SGG were radiolabeled, but the radioactivity peak of GG preceded that of SGG (Hsu et al., 1983). This suggested that SGG was synthesized from GG via sulfation. In fact, sulfotransferase, localized in the Golgi complexes of primary spermatocytes, has been described to catalyze this reaction using PAPS as a sulfate donor (Knapp et al., 1973), and the purification of testicular sulfotransferase has been reported (Sakac et al., 1992). The enzyme has a molecular mass of 56 kDa and is activated by phosphorylation (Sakac et al., 1992). The apparent sulfotransferase activity is sharply reduced in the mid-pachytene stage due to the appearance of a small molecular weight inhibitor (Lingwood, 1985), identified as a glycosyl phosphoinositide (Lingwood et al., 1994). Recently, Honke et al. (Honke et al., 2002) have shown that the testicular sulfotransferase is encoded by the same gene as that of cerebroside sulfotransferase (CST) present in the brain and kidney.
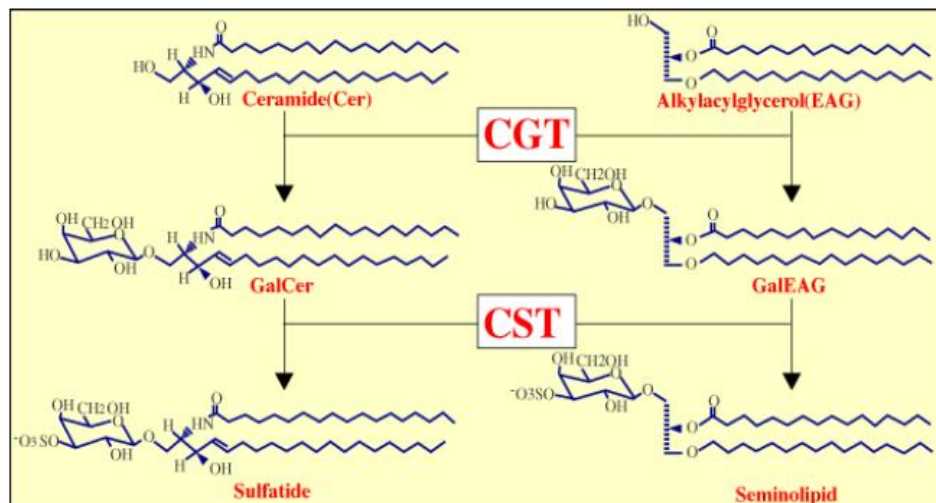

Fig. 2 Biosynthetic pathway of SGG/SGC.

Cst$^{-/-}$ mice genetically depleted of CST lacks SGC in brain, kidney and testis. A buildup of GG in testes of these mice also confirms that GG is the precursor of SGG (Honke et al., 2002).

In the metabolic radiolabeling studies of Hsu et al. (Hsu et al., 1983), a small amount of alkylacylglycerol (AAG) was detected and therefore AAG was postulated to be galactosylated to form GG. Lately, *Cgt*$^{-/-}$ mice have been generated (Coetzee et al., 1996a), and in these mice, GG and GC are not found in the testis and the brain, respectively (Coetzee et al., 1996a; Fujimoto et al., 2000). Thus, these findings indicate that formation of GG from AAG is via the same enzyme responsible for GC formation. UDP-galactose, a galactose donor for GC formation in the brain, is also likely to be the galactose donor for GG formation in the testis. Unlike CST, testicular CGT has not yet been characterized. However, CGT from the myelinating rat brain has been isolated and characterized as a 61-kDa high-mannose glycoprotein (Schulte and Stoffel, 1993). Localization of CGT using antibody made against N-terminus of CGT revealed that CGT is localized in the endoplasmic reticulum (ER) of CGT-transfected CHO cells (Sprong et al., 1998). This result agrees with the presence of the ER retrieval signal sequence KKXX at the C-terminal end of the enzyme (Nilsson and Warren, 1994). All these results suggest that the synthesis of GG by testicular CGT should also occur in this organelle.

1.3 Synthetic sites and cellular localization of SGG

Lines of evidence indicate that SGG is actively synthesized in early stages of primary spermatocytes during spermatogenesis (Kornblatt et al., 1974; Letts et al., 1978). Thin layer chromatography of isolated testicular glycolipids from 15-20-day-old rats, which just have primary spermatocytes appearing in their testes, showed the first appearance of SGG; this indicates that SGG is synthesized in primary spermatocytes (Kornblatt et al., 1974). To investigate SGG synthesis sites during spermatogenesis, Lett et al. (1978) also performed intratesticular injection of [^{35}S] sulfate into adult rats followed by isolation of spermatogenic cells using albumin gradient. The results revealed that early primary spermatocytes had a high degree of ^{35}S incorporation into SGG whereas late primary spermatocytes and spermatids showed minimal corporation of the radiolabel.

Once synthesized in early primary spermatocytes, SGG is transported from its site of synthesis via Golgi-derived vesicles towards the plasma membrane, and remains on plasma membrane throughout all the subsequent stages of germ cells (Tanphaichitr et al., 2003; Klugerman and Kornblatt, 1980; Lingwood et al., 1981; Shirley and Schachter, 1980). Indirect immunofluorescence (IIF) of frozen rat testis sections, using non-affinity purified rabbit anti-SGG IgG, revealed patchy staining patterns of SGG in fixed pachytene spermatocytes, and spermatids, but not in spermatogonia and Sertoli cells (Lingwood, 1981). Similar results were also described with loose spermatogenic cells released from minced rat testis (Lingwood et al., 1981). Subsequently, Lingwood reported SGG immunofluorescent staining in the rat epididymal sperm head (Lingwood, 1986). Using affinity purified rabbit polyclonal anti-SGG IgG antibody, patchy fluorescent staining patterns of SGG have also been described in live mouse primary spermatocytes, round and elongated spermatids, as well as in testicular and epididymal sperm (Tanphaichitr et al., 2003; Weerachatyanukul et al., 2003). In addition, SGG was shown to exist exclusively on the sperm head anterior plasma membrane overlying the acrosomal ridge and postacrosome of mature mouse sperm (White et al., 2000), pig sperm (Bou et al., 2006), and human sperm (Weerachatyanukul et al., 2001a). Biochemical studies demonstrated that SGG is present in isolated head anterior plasma membranes of pig, bull, stallion, and rooster sperm at appreciable amounts (i.e., < 10 mole% of total lipids) (Parks and Lynch, 1992). Since the anterior head plasma membrane is the ZP binding site of the

acrosome-intact sperm (Chen and Cardullo, 1994; Kerr et al., 2002; Yanagimachi, 1994), the results from both immunolocalization and biochemical studies implicate the function of SGG in the primary ZP binding.

1.4 Degradation of SGG during spermatogenesis

SGG and SGC are postulated to share similarity not only for their synthetic pathway, but also for the degradative pathway. The enzyme responsible for SGC desulfation is arylsulfatase A (ASA) (EC 3.1.6.8), a lysosomal enzyme with a molecular mass of 65-68 kDa. To desulfate sulfoglycolipids, ASA requires a sphingolipid activator protein, saposin B, which extract the target sulfoglycolipid from the membrane. The soluble sulfoglycolipid-saposin B complex can be recognized by ASA (Kolter and Sandhoff, 2005; von Figura et al., 2001). Saposin B is derived from its precursor protein, prosaposin (O'Brien and Kishimoto, 1991). The fact that ASA and saposin B are responsible for physiological degradation of SGC is obtained from phenotypes observed in metachromatic leukodystrophy (MLD) patients, genetically deficient in either ASA or, more rarely, saposin B. These patients have abnormal accumulation of SGC in the brain (the most affected organ) and other visceral organs. Similar but much milder phenotypes are also found in ASA deficient ($ASA^{-/-}$) mice (Molander-Melin et al., 2004; Schott et al., 2001).

Desulfation of SGG to GG by arylsulfatse A (ASA) has been shown *in vitro* by the enzymatic assay using purified human ASA (Fluharty et al., 1974) and isolated boar testis ASA (Yamato et al., 1974). Moreover, accumulation of SGG has been observed in testes of $ASA^{-/-}$ mice (Schott et al., 2001). Therefore, these findings suggest that SGG can be desulfated by ASA *in vivo*. In addition, accumulation of SGG was observed in testes of mice deficient in prosaposin, the precursor protein of saposin B (Tadano-Aritomi et al., 2003). These results suggest the role of saposin B in facilitating ASA action in SGG desulfation in the testis. Although where/how exactly testicular ASA functions in SGG degradation has yet to be determined, there is evidence suggesting that this action may occur in Sertoli cells. Immunolocalization studies on the testis sections revealed that ASA resides not only in the acrosomal process of spermatids but also in the lysosomes of Sertoli cells (Moviglia et al., 1982; Weerachatyanukul et al., 2003). Moreover, prosaposin has been found in lysosomes containing residual bodies in Sertoli cells (Morales et al., 1998). This co-presence of ASA and prosaposin implies that ASA and saposin B (derived from prosaposin) may act together in the degradation of membrane SGG from residual bodies, which are shed from differentiating spermatids and phagocytosed by Sertoli cells.

1.5 Roles of SGG in male reproduction

SGG and SGC have affinity to a number of cell adhesion proteins, extracellular matrix glycoproteins, growth factor, and microorganisms (see the details in Table 1).

Table 1: SGG/SGC binding molecule

Type	SGG/SGC-binding molecule	Note	Reference
Microorganisms and surface proteins of microorganisms	*Escherichia coli* Enterotoxin b	A protein in a specific *E. coli* strain that causes diarrhea in animals and humans	(Rousset et al., 1998)
	Mycoplasma hominis	A human pathogen that is transmitted sexually and causes infertility	(Olson and Gilbert, 1993)
	Circumsporozoite proteins*	A coat protein of malaria (plasmodia) sporozoites	(Pancake et al., 1992)
	Gp120	A surface glycoprotein of the human immunodeficiency virus (HIV-1)	(Brogi et al., 1995; Brogi et al., 1996)
	Mycoplasma pulmonis	Infertility-related mycoplasmas in rodents	(Lingwood et al., 1990)
Adhesive proteins	Properdin*	A globulin protein found in blood serum	(Holt et al., 1990)
	Antistatin*	A saliva protein from the leech that inhibits blood coagulation	(Holt et al., 1989)
	Thrombospondin*	A major component of platelet α granules	(Roberts, 1988)
	Von Willebrand factor*	A large plasma glycoprotein which binds to platelet and promotes platelet adhesion	(Roberts et al., 1986)
	L-selectin	A protein in the selectin family found on leukocytes	(Needham and Schnaar, 1993; Suzuki et al., 1993)
	P-selectin (CD62)	A protein in the selectin family found in granules in endothelial cells	(Bajorath et al., 1994; Needham and Schnaar, 1993)
	Cycotactin	A glial glycoprotein that plays roles in neural development of animals	(Crossin and Edelman, 1992)
	Amphoterin (p30)	A 30 kDa protein found in the rat cerebellum	(Mohan et al., 1992)
Extracellular matrix (ECM) glycoprotein	Laminin	A major noncollagenous glycoprotein of the basement membranes	(Roberts et al., 1985)
	Perlecan (C-terminal domain V)	An abundant proteoglycan component of the basement membranes	(Friedrich et al., 1999)
Components of myelin lipid rafts	Myelin and lymphocyte protein (MAL)	A myelin membrane protein expressed in central and peripheral nerve, and found in rafts of the myelin; A T-cell differentiation protein	(Frank, 2000)
	GC and SGC	Major glycolipids of the myelin	(Boggs et al., 2000)

Intracellular chaperone	Heat shock proteins of the 70-kDa family (hsp70)	Molecular chaperones found on the surface of bacteria, male germ cells, and carcinoma cell lines	(Mamelak and Lingwood, 2001)
Growth factor	Midkine	A basic heparin-binding growth factor in the nervous system	(Kurosawa et al., 2000)
Anticoagulant	Annexin V	A calcium-dependent phospholipid-binding protein	(Ida et al., 2004)

* Contain the amino acid sequence homology , C-S/T-V-S/T-C-G-X-G-X-X-X-R/K-X-R/K (X = any amino acid) (Holt et al., 1989)

All these findings suggest that SGG may serve as an adhesion molecule in cell-cell/extracellular protein interactions during male germ cell development and fertilization process.

In fact, has been shown that SGG is involved in the binding between acrosome intact sperm and the ZP and between acrosome-reacted sperm and the egg plasma membrane (Ahnonkitpanit et al., 1999; White et al., 2000). Moreover, during the sperm transit in epididymis, SGG also serves as a ligand for adsorption of arylsulfatase A, a ZP binding molecule, onto the sperm surface (Weerachatyanukul et al., 2003). These results all together implicate SGG as an adhesion molecule in sperm maturation and sperm-egg interaction.

Moreover, it has been shown that 70% of SGG in capacitated sperm exists in lipid rafts isolated as Triton X-100 resistant membranes, along with cholesterol and saturated phospholipids (Bou et al., 2006). Therefore, all these results suggest the roles of SGG as a structural lipid contributing to the formation of mammalian sperm lipid rafts, which possess ZP-binding molecules needed for the gamete interaction. Isolated sperm lipid rafts, in fact, have direct ZP binding ability (Bou et al., 2006).

2. PROCESS OF FERTILIZATION

2.1 Fertilization

Fertilization is a complex process of molecular events that involved mature haploid male and female gametes and their mutual recognition and fusion to establish the genotype of a new individual. Fully matured oocytes and normally differentiated haploid spermatozoa are the prerequisites for the success for the fertilization process (Kupker et al., 1998).

A woman is usually fertile on about the 14th day of her menstrual cycle. Days before the woman ovulates, her cervix secretes mucus, which allows sperm to travel faster towards the uterus and into the fallopian tubes. During ovulation, a mature egg is released by the ovary to the fallopian tube and for about 12 to 24 hours, it is ready to be fertilized.

After sexual intercourse the sperm released inside the vagina travel towards the uterus to the fallopian tube to seek out the egg. Hundreds of thousands of sperm are released during ejaculation, but only one gets to penetrate the egg and starts the fertilization process. Sperm are capable of staying alive for 48 to 72 hours inside the female reproductive tract, and can fertilize the egg as soon as the ovulation takes place. When sperm and egg fuse, a zygote is formed.

The zygote then undergoes cell division and becomes an embryo. Within five to seven days, the embryo is implanted in the uterus. After implantation, the embryo will undergo many stages of development, which will be completed within about nine months inside the womb.

2.2 Male reproductive system

The male reproductive system consists of a set of organs involved in the production of sperm. These organs include visible bodies, such as the penis and scrotum, which contains the testicles, and internal organs, such as epididymis, seminal vesicles, bulbourethral glands and prostate gland (Fig. 3).
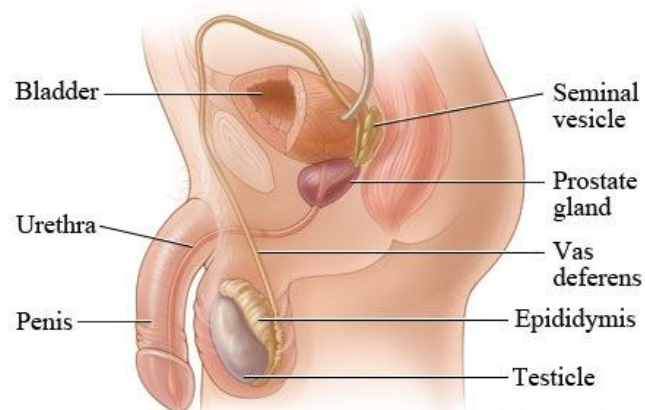

Fig. 3 Male reproductive system

The testicles are involved in the formation of sperm through the process called spermatogenesis (Fig. 4).
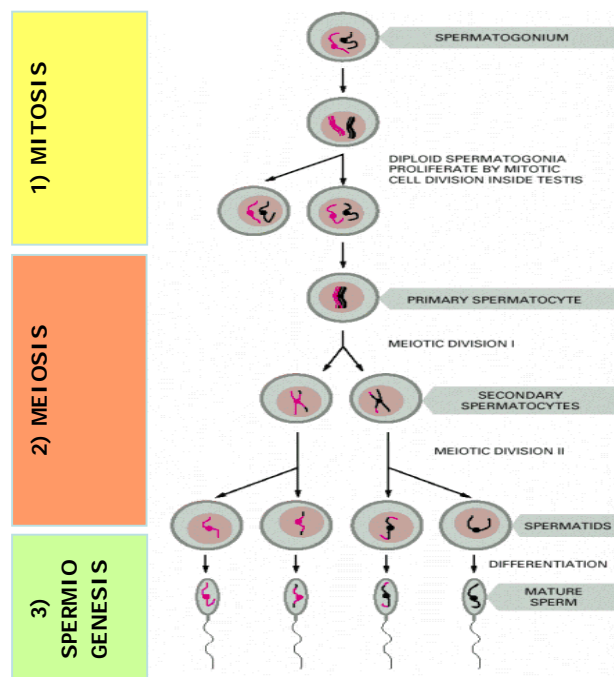

Fig. 4. Process of spermatogenesis

In mammals, spermatogenesis is composed of three phases: the proliferative phase during which the diploid spermatogonia undergo several mitotic divisions; the meiotic

phase during which primary spermatocytes give rise to secondary spermatocytes which themselves divide into haploid spermatids; and the final phase, corresponds to the metamorphosis of spermatids into spermatozoa (Alberts et al., 2002; de Kretser and Kerr, 1994).

2.3 Spermatozoa: structure and physiology

Highly differentiated and polarized spermatozoa are the final product of the spermatogenesis process. Each spermatozoon consists of two major parts: the head which is about 5-10 μm length and the tail which has the length of about 60 μm (Fig. 5).
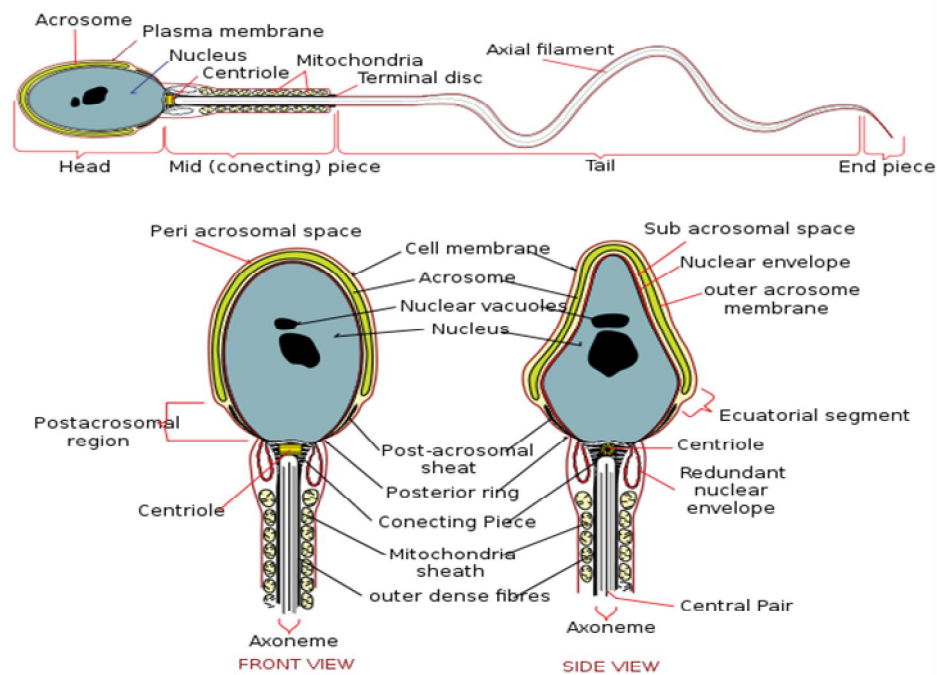

Fig. 5 Spermatozoa structure

The sperm head consists of a highly compact nucleus, containing the male genome, very little cytoplasm and the acrosome. The acrosome, located on the anterior portion of the sperm head, houses hydrolytic enzymes that will aid the spermatozoon to penetrate the zona pellucida (ZP), the extracellular glycoprotein matrix surrounding the oocyte. The sperm tail consists of the connecting piece, the midpiece, the principal piece, and the end piece. The connecting piece of the tail is a narrow segment containing the paired centrioles. The midpiece of the tail consists of the helically arranged mitochondrial sheath, the axoneme and the outer dense fibers of the

13

flagellum. The lower limit of midpiece is marked by the termination of the mitochondrial helix at the annulus. The principal piece, the longest segment of the tail, is composed of central axoneme surrounded by the outer dense fibers and the fibrous sheath. The end piece is a very short segment of the tail in which only the axoneme is present (de Kretser and Kerr, 1994; Eddy and O'Brien, 1994; Kierszenbaum, 2002; Yanagimachi, 1994).

2.4 Sperm maturation in male reproductive system

Once formed the spermatozoa begins their journey through the epididymis (Fig. 6). In the epididymis, sperm first is transported through the caput and corpus regions and they are stored in the proximal cauda epididymis until ejaculation. During epididymal transit and storage, sperm acquires its functional competence through a series of morphological, biochemical and physiological changes.
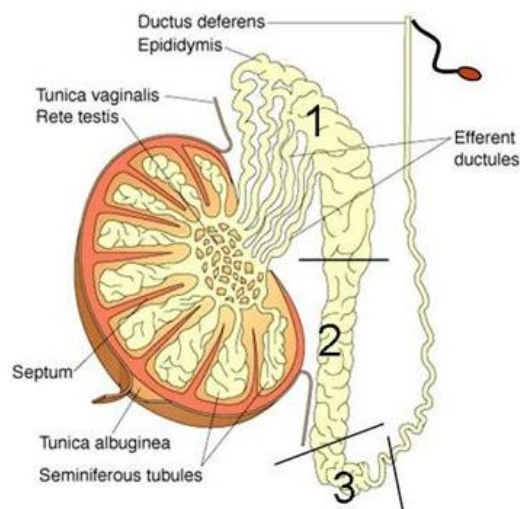

Fig. 6 Sperm maturation in epididymis: 1) Caput 2) Corpus 3) Cauda epididymis

Some of the pre-existing proteins on the sperm plasma membrane, such as fertilin alpha and beta, cyritestin, alpha-D-mannosidase are cleaved by proteolytic enzymes and released into the lumen, or redistributed in different plasma membrane domains (Evans, 1999; Gatti et al., 2000).

A large number of new components, present in the luminal fluid and presumably secreted from the epididymal epithelium, are also adsorbed onto the sperm surface during the epididymal maturation process (Dacheux et al., 2003). These new components include forward motility protein (FMP) involved in forward motility of

sperm (Acott et al., 1983), and proteins with ZP-binding ability, such as P26h (Berube et al., 1996), β-galactosidase (Sosa et al., 1996; Tulsiani et al., 1995), and arylsulfatase A (ASA) (Weerachatyanukul et al., 2001b). In addition, sperm membrane fluidity increases due to the enrichment of polyunsaturated fatty acid (PUFA)-containing phospholipids (Cooper and Yeung, 1997; Flesch and Gadella, 2000). This increased membrane fluidity contributes to the sperm capability to move forwardly, as well as to the sperm membrane fusion ability required during fertilization (Yanagimachi, 1994). Epididymal fluid may also play an important role in sperm maturation; it contains membranous vesicles, termed epididymosomes, which interact with sperm (Fornes et al., 1995; Frenette and Sullivan, 2001; Yeung et al., 1997). Proteins and cholesterol present in epididymosomes have been shown to be transferred onto the sperm surface (Frenette et al., 2002; Saez et al., 2003; Yanagimachi et al., 1985).

Also in the epididymis, chromatin condensation and stabilization of the spermatozoa occur, and the acrosome also acquires its final shape.

During ejaculation, the spermatozoa are transported from storage in the cauda epididymis and are mixed with the prostatic fluid and seminal vesicle fluid before passage along the penile urethra.

The semen ejaculate into the vagina will develop a second set of changes that will take place in the female reproductive system.

2.5 Composition and parameter of the human semen

The human semen is composed of two main components: sperm and seminal fluid. A grown man, with every ejaculation, emits about 1.5 ml to 6 ml of semen, an amount that is dependent on the long passes between one ejaculation to another, by the production of testosterone and on individual factors not fully studied. Variable is the number of sperm per milliliter of ejaculate, mainly related to the health of the subject; this number varies from 20 to 200 million per millilitre. The density of semen depends on several factors. In most cases a mass function, but its appearance can vary from a creamy eye-catching to a state almost completely liquid, but never transparent.

The semen of humans contains a complex range of organic and inorganic constituents which have protective nourishment for sperm during their journey through the female reproductive tract. The vaginal environment is in fact hostile to the sperm cell, it is a very acid environment (because of the microflora therein which produces lactic acid),

viscous and rich in immune cells. Many components present in the semen help in compensation with this hostile enviroment to enable sperm to survive long enough to reach and fertilize the egg.

2.6 Sperm maturation in the female reproductive system

The female reproductive system consists of a set of organs located in the lower portion of the abdomen called pelvi. These organs are mainly internal, such as ovaries, uterus and fallopian tube, and they are connected to the outside via the vagina.

The spermatozoa are deposited in the vagina, near the cervical os, during intercourse. Spermatozoa must swim trough the cervical mucus, traverse the uterus, enter the oviduct and reach the ampullary portion where fertilization occurs. The sperm motility patterns differ, associated with each of these regions, and the spermatozoa are also modified during the transport through the female reproductive tract.

As mention above, the mature sperm are stored in the caudal epididymis until ejaculation (Fig. 7).
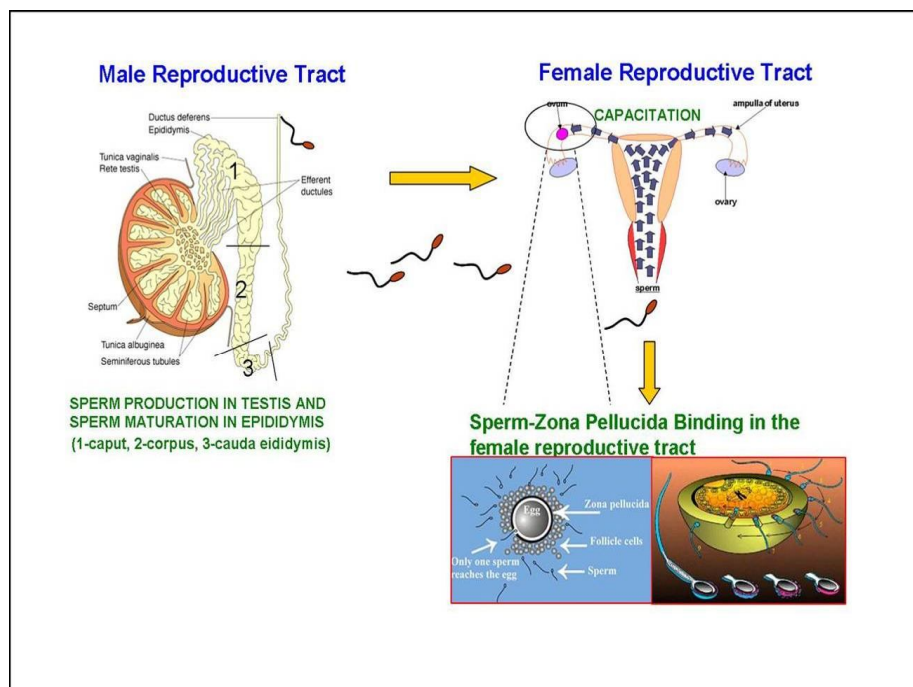

Fig. 7 Sperm maturation in female reproductive tract following the fertilization of the mature egg

The ejaculated sperm then undergo further surface modification in the female reproductive tract to gain full fertilizing ability through a process known as capacitation.

Several processes occur during capacitation: 1) **desorption processes** during which proteins and other macromolecules from epididymal and seminal fluids that mask key sites for ZP binding on the sperm surface or suppress sperm functional activity are removed; 2) **ionic changes** in particular those involving in bicarbonate influx and Ca^{2+} influx. Such changes trigger the activation of adenylyl cyclase, and subsequent increase in intracellular cAMP. As a result, protein kinase A (PKA) is activated, which induces downstream protein tyrosine phosphorylation; 3) **plasma membrane lipid changes**. The phospholipids are distributed asymmetrically between the lipid leaflets of plasma membrane. During capacitation, a similar asymmetric distribution occurs in sperm and apparently collapses. The collapse of phospholipid asymmetry facilitates a decrease on sperm membrane cholesterol (cholesterol efflux). The cholesterol efflux leads to a decreased ratio of cholesterol to phospholipids and an increase in fluidity of the sperm plasma membrane (Cross, 1998). The global increase in membrane fluidity in capacitated sperm is beneficial to the fusion-related events during sperm-egg interaction, i.e., acrosome reaction and the sperm-egg plasma membrane fusion (Primakoff and Myles, 2002). However, during the initial interaction between sperm and eggs, i.e., sperm-ZP binding, ordered domains on the sperm plasma membrane with clusters of ZP-binding molecules would be required for the stable interaction of gametes, withstanding the pulling force generated from ongoing sperm movement. Recently, results indicate that the levels of liquid-ordered microdomains or lipid rafts, which are enriched in cholesterol, saturated phospholipids, and SGG, are increased on the sperm plasma membrane following capacitation (Bou et al., 2006; Shadan et al., 2004).

This capacitation-related cholesterol efflux is accompanied by activation of lipid scramblase (Flesch et al., 2001), which catalyzes the movement of lipids. This may allow sperm lipids to regroup themselves according to their biochemical properties, leading to the formation of liquid-ordered microdomains, or lipid rafts.

Following capacitation, sperm acquire hyperactivated motility patterns and the ZP binding sites become exposed, resulting in sperm binding to the egg ZP and subsequent penetration through the ZP matrix (Florman and Ducibella, 2006).

Once the capacitated sperm bind to the ZP, the acrosome reaction is induced. This reaction results in the release of the acrosomal contents, composed mainly of hydrolases, which facilitate sperm penetration through the ZP matrix. Acrosome reacted sperm then enter the perivitelline space, bind to and fuse with the egg plasma

membrane, and finally one spermatozoon becomes incorporated into the egg proper, signifying that fertilization has occurred (Yanagimachi, 1994).

2.7 Sperm interaction to the zona pellucida(ZP)

The binding of sperm to ZP is the first step of gamete interaction, which leads to fertilization. The sperm-ZP binding occurs in two sequential steps, starting with the primary binding of the capacitated acrosome-intact sperm to the ZP, followed by the secondary ZP binding of the acrosome reacting/reacted sperm (Fig. 8).
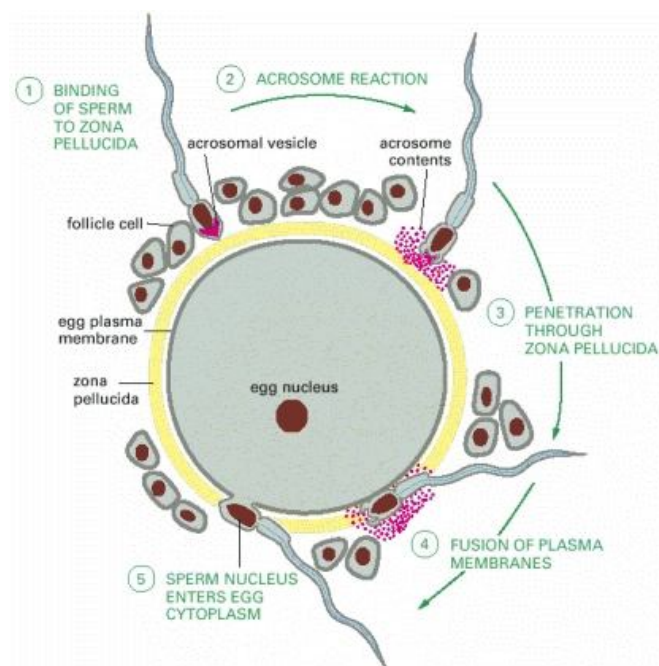

Fig. 8 Sperm interaction with zona pellucida (ZP)

The ZP consists of a few sulfoglycoproteins, and these glycoproteins are highly homologous among species (Wassarman, 2005). In the mouse, there are three ZP matrix glycoproteins: mZP3, mZP2, and mZP1. During the sperm-ZP binding, mZP3 serves as the receptor for the primary binding of sperm to ZP, whereas mZP2 is the secondary receptor and mZP1 is the cross-linker between mZP2 and mZP3.

Unlike the ZP, sperm have a number of ZP-binding molecules. Sperm molecules that are involved in the primary ZP binding are localized to the anterior plasma membrane of capacitated acrosome-intact sperm head. Some of these primary ZP binding molecules are synthesized in spermatogenic cells and localized to the plasma membrane, such as β-1,4-galactosyltransferase (GALT), sulfogalactosylglycerolipid

(SGG), mannosidase, and basigin. Other molecules, such as ASA, P26h, and β-galactosidase, are synthesized and secreted from the epididymal epithelium into the lumen, and adsorbed onto the sperm plasma membrane during the sperm transit trough the epididymis (as mentioned in the section of epididymal maturation). In contrast to sperm molecules involved in primary ZP binding, secondary ZP binding molecules, such as proacrosin, Sp38, zonadhesin, Sp17 and Sp56 are mostly synthesized in spermatogenic cells and they are directly targeted to the acrosome (Tanphaichitr et al., 2007).

The reasons for having many ZP-binding molecules on the sperm surface are unknown. One possibility that many scientists agree upon is that these molecules may act simultaneously/sequentially or serve as a backup for one another during sperm-ZP binding, an initial step that crucially leads to the complete fertilization (Tanphaichitr et al., 2007).

3. AIM OF WORK

Fertilization is the complex process by which haploids gametes, sperm and egg, unite to produce a genetically distinct individual. Focusing on the roles of sperm sulfogalactosylglycerolipid, it has been shown that SGG participates in sperm zona-pellucida (ZP)/egg-plasma membrane binding and also is selectively present at substantial amount (10 mole% of total lipids) in all mammals (Bou et al., 2006).

Besides ZP glycoproteins, SGG and its structural analogue sulfogalctosylceramide (SGC) have been shown to bind to many other proteins including gp120 of HIV-1 and CS6 of enterotoxigenic E. coli. Thus, SGG is considered a site on the sperm with which pathogens can interact.

As SGG plays a key role in the process of fertilization and also in the sexual transmitted disease it is believed important to identify a new ligand able to inhibit fertilization through the interaction with SGG and, at the same time, having an antimicrobial effect.

In the recent years a new class of cationic antimicrobial peptides (AMPs) has been identified. This family of peptide contains species, i.e. cathelicidin, with less than 100 amino acids, most of which are cationic and hydrophobic, that act as effector molecules of the innate immune system, and have a broad spectrum antimicrobial effects on Gram-positive and Gram-negative bacteria, and some fungi and enveloped virus.

4. ANTIMICROBIAL PEPTIDES

4.1 The family of antimicrobial peptides

The immune system of multi-cellular organisms comprises a vast arsenal of mechanisms to protect the host from constant interactions with infectious microorganisms (Boman et al., 2000).

Antimicrobial peptides (AMPs) are a small cationic peptide which protect their hosts against a vast array of microorganism. These peptides are produce by several species, including insect, plants and vertebrates, and they are known to be evolutionary conserved in several mammalian species (Lehrer et al., 1999).

The classification of AMPs is difficult owing to their considerable diversity. However, based on their amino acid composition, size and conformational structures, AMPs can be divided into several categories, such as peptides with α-helix structures, (i.e. cathelicidin in human), peptides with β-sheet structures stabilized by disulfide bridge, (i.e., defensin in human), peptides with extended structures, (i.e., bovine indolicins), and peptides with loop structures, (i.e., cyclic defensins found in rhesus macaques (Lai et al., 2009).

AMPs are expressed on primary barriers of the organism, such as skin, and mucosal epithelia, preventing the colonization of host tissues pathogens (Bulet et al., 2004).

Moreover, these peptides are stored in granules within phagocytes, where they assist in the killing of engulfed microorganisms (Zasloff et al., 2002; Ganz et al., 1999).

Beside antimicrobial activity, other biological effects of AMPs have been describe recently, including neutralization of endotoxins, chemokine-like activities, immunomodulating properties, antiviral action, and induction of both angiogenesis and wound repair (Yang et al., 2002; Zaiou et al., 2007).

Due to the board spectrum of their antibiotic properties, AMPs are attractive candidates for a novel therapeutic purposes.

4.2 Cathelicidins in human: biosynthesis, structure and gene expression

There are several AMPs described in mammals, but we will focus our attention on the family of cathelicidins, the most studied AMPs in humans.

Cathelicidins are synthesized as pre-pro-peptides (Fig. 9) and characterized by the conserved amino-terminal sequence of the peptide pro-piece. The carboxy-terminal domain of the peptide is variable amoung the AMPs, and its possesses the antimicrobial activities. The gene for the human cathelicidin is a compact gene located in the chromosome 3, and is composed of four exons. Exons 1 to 3 code for the signal sequence and the cathelin domain, while exon 4 codes for the antimicrobial peptide (Larrick et al., 1996; Gudmundsonn et al., 1996).
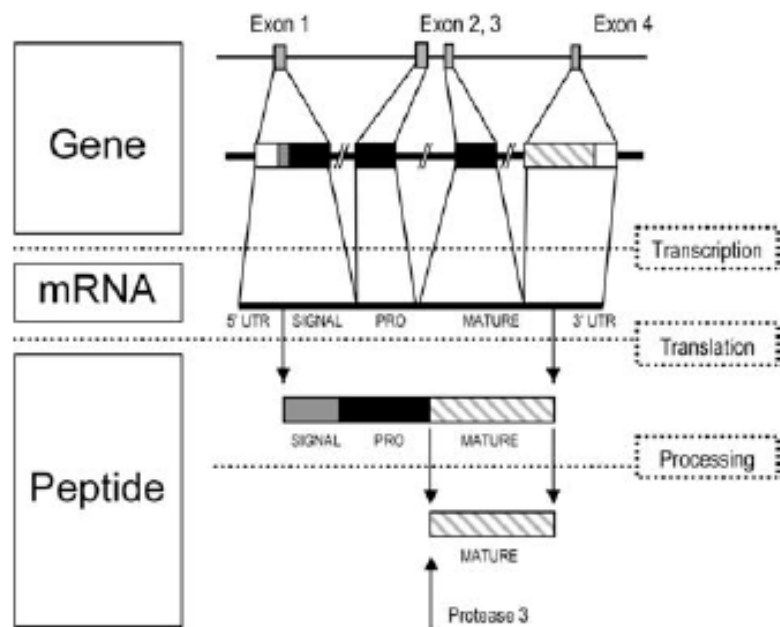

Fig. 9 Structure of the gene and peptide of hCAP18/LL37 as a prototypical example for the cathelicidin family. The gene is represented schematically with the following individual component: white box, 5' untranslated region (5'UTR); grey box, signal sequence; black box, pro-sequence; shaded box, mature peptide; white box, 3'UTR.

The pro-sequence is termed 'cathelin' after the function of this domain to inhibit the activity of cathepsin L (cathepsin L inhibitor) and is between 99 and 114 amino acids long (Zanetti et al., 1996). The 'cathelin' protein was initially identified from pig leukocytes (Ritonja et al., 1989). Molecules with a cathelin-like pro-peptide sequence have been isolated from multiple species including cow (Storici et al., 1994), pig (Storici and Zanetti, 1993a and 1993b), rabbit (Larrick et al., 1991), sheep (Bagella et al.,1995), human (Agerberth et al., 1995; Cowland et al., 1995; Larrick et al., 1995), mouse (Popsueva et al., 1996; Gallo et al., 1997), monkey (Bals et al., 2001; Zhao et al., 2001) and horse (Scocchi et al., 1999) (see more detail in table 2).

Table 2 : Amino acids sequence, animal source and structural features of cathelicidins from mammals

Peptide	Sequence	Origin	Class
LL-37	LLGDFFRKSKEKIGKEFKRIVQRIKDFLRNLVPRTES	Man	α-helical
RL-37	RLGNFFRKVKEKIGGGLKKVGQKIKDFLGNLVPRTAS	Rhesus monkey	α-helical
CAP18	GLRKRLRKFRNKIKEKLKKIGQKIQGLLPKLAPRTDY	Rabbit	α-helical
mCRAMP	GLLRKGGEKIGEKLKKIGQKIKNFFQKLVPQPE	Mouse	α-helical
rCRAMP	GLVRKGGEKFGEKLRKIGQKIKEFFQKLALEIEQ	Rat	α-helical
CAP11[a]	(GLRKKFRKTRKRIQKLGRKIGKTGRKVWKAWREYGQIPYPCRI) 2	Guinea pig	α-helical (dimeric)
Canine cath	KKIDRLKELITTGGQKIGEKIRRIGQRIKDFFKNLQPREEKS	Dog	α-helical (predicted)
Bac5[b]	RFRPPIRRPPIRPPFYPPFRPPIRPPIFPPIRPPFRPPLGPFP-NH$_2$	Cow	Linear, Pro-rich
Bac7	RRIRPRPPRLPRPRPRPLPFFPRPGPRPIPRPLPFFPRPGPRPIPRPLPFPRPGPRPIPRPL	Cow	Linear, Pro-rich
BMAP-27	GRFKRFRKKFKKLFKKLSPVIPLLHL-NH$_2$	Cow	α-helical
BMAP-28	GGLRSLGRKILRAWKKYGPIIVPIIRI-NH$_2$	Cow	α-helical
BMAP-34	GLFRRLRDSIRRGQQKILEKARRIGERIKDIFR-NH$_2$	Cow	α-helical
Indolicidin	ILPWKPWWPWRR-NH$_2$	Cow	Linear, Trp-rich
Dodecapeptide	RLCRIVVIRVCR	Cow	Disulfide bridged
OaDode	RICRIIFLRVCR	Sheep	Disulfide bridged
SMAP-29	RGLRRLGRKIAHGVKKYGPTVLRIIRIA-NH$_2$	Sheep	α-helical
SMAP-34	GLFGRLRDSLQRGGQKILEKAERIWCKIKDIFR-NH$_2$	Sheep	α-helical
OaBac5	RFRPPIRRPPIRPPFRPPFRPPVRPPIRPPFRPPFRPPIGPFP-NH$_2$	Sheep	Linear, Pro-rich
OaBac6	RRLRPRHQHFPSERPWPKPLPLPLPRPGPRPWPKPLPLPLPRPGLRPWPKPL	Sheep	Linear, Pro-rich
OaBac7.5	RRLRPRRPRLPRPRPRPRPRPRSLPLPRPQPRRIPRPILLPWRPPRPIPRPQIQPIPRWL	Sheep	Linear, Pro-rich
OaBac11	RRLRPRRPRLPRPRPRPRPRPRSLPLPRPKPRPIPRPLPLPRPRPKPIPRPLPLPRPRPRRIP RPLPLPRPRPRPIPRPLPLPQPQPSPIPRPL	Sheep	Linear, Pro-rich
ChBac5	RFRPPIRRPPIRPPFNPPFRPPVRPPFRPPFRPPFRPPIGPFP-NH$_2$	Goat	Linear, Pro-rich
eCATH-1	KRFGRLAKSFLRMRILLPRRKILLAS	Horse	α-helical
eCATH-2	KRRHWFPLSFQEFLEQLRRFRDQLPFP	Horse	α-helical
eCATH-3	KRFHSVGSLIQRHQQMIRDKSEATRHGIRIITRPKLLLAS	Horse	α-helical
PR-39	RRRPRPPYLPRPRPPPFFPPRLPPRIPPGFPPRFPPRFP-NH$_2$	Pig	Linear, Pro-rich
Prophenin-1	AFPPPNVPGPRFPPPNFPGPRFPPPNFPGPRFPPPNFPGPRFPPPNFPGPPFPPPIFPGPWFP PPPPFRPPPFGPPRFP-NH$_2$	Pig	Linear, Pro-rich
Prophenin-2	AFPPPNVPGPRFPPPNVPGPRFPPPNFPGPRFPPPNFPGPRFPPPNFPGPPFPPPIFPGPWFP PPPPFRPPPFGPPRFP-NH$_2$	Pig	Linear, Pro-rich
Protegrin-1	RGGRLCYCRRRFCVCVGR-NH$_2$	Pig	Two-disulfide bridged
Protegrin-2	RGGRLCYCRRRFCICV-NH$_2$	Pig	Two-disulfide bridged
Protegrin-3	RGGGLCYCRRRFCVCVGR-NH$_2$	Pig	Two-disulfide bridged
Protegrin-4	RGGRLCYCRGWICFCVGR-NH$_2$	Pig	Two-disulfide bridged
Protegrin-5	RGGRLCYCRPRFCVCVGR-NH$_2$	Pig	Two-disulfide bridged
PMAP-23	RIIDLLWRVRRPQKPKFVTVWVR	Pig	α-helical
PMAP-36	GRFRRLRKKTRKRLKKIGKVLKWIPPIVGSIPLGC-NH$_2$	Pig	α-helical
PMAP-37	GLLSRLRDFLSDRGRRLGEKIERIGQKIKDLSEFFQS	Pig	α-helical

[a] CAP11 is a homodimer *via* an intermolecular disulfide bond.
[b] -NH$_2$, C-terminal amidation.

The carboxy-terminal domain represents the antimicrobially active peptide that varies considerably between individual molecules in sequence, length (12–100 residues), and function (Table 2). Based on amino acid sequences, mature cathelicidin peptides can be organized into three groups:

- group I – linear, α-helical peptides without cysteines, i.e. LL37/hCAP-18 from human
- group II – peptides with an even number of cysteines linked by disulfide bridges, i.e. protegrins (porcine cathelicidin peptides).
- group III – peptides with an unusually high proportion of one or two amino acids, i.e. PR-39 from porcine leukocytes.

Several structural features have been identified as a relevant for the microbicidal function of antimicrobial peptide: size, sequence, charge, degree of structuring (helicity), overall hydrophobicity, amphipathicity and the angle subtended by hydrophobic and hydrophilic surface of the helical molecule (Giangaspero et al., 2001). High mean hydrophobicity has been correlated with increased cytotoxic activity against eukaryotic membranes (van't Hof et al., 2001).

There is no simple correlation between activity and charge. When the net charge becomes more positive, binding to negatively charged surface of microorganism is increased (Dathe et al., 1997 and 1999; Wieprecht et al., 1997). Since all these structural features are strongly interrelated, predicting the antimicrobial or cytotoxic activity from a given amino acids sequence is difficult.

In this scenario so it would be interesting to investigate whether this class of peptides, which has already been shown for its broad range of action against pathogens, can also be used in specific manner in biological processes. For these reason we want focusing our attention on hCAP18/LL37, the most studied antimicrobial peptide and the only member of cathelicidin family found in human.

4.3 Human hCAP18 is processed to LL37 or ALL38 (LL37 + Ala N-terminus)

The human cathelicidin LL37 is generated from the proprotein hCAP18 encoded by the CAMP gene (Gudmundsson et al., 1996). Following excision of the signal peptide, this proprotein is stored in neutrophil granules and epithelial cells until activated through cleavage by the serine protease, proteinase 3 (Soresen et al, 2001). The actual release of LL37 is proposed to occur at the cell surface as, on stimulation of the neutrophil, hCAP18 locates to the plasma membrane, potentially through an interaction with an hCAP18 specific receptors (Stie et al., 2007). In addition to that stored in neutrophils, significant quantities of hCAP18 are found in human plasma as complex with lipoproteins (Sorensen et al., 2005).

hCAP18 is also present in the epithelial cells (i.e. in various squamous epithelia) (Nilsson et al., 1999), in lungs (Bals et al., 1998; Agerberth et al., 1999), in sweat glands (Murakami et al., 2002), in salivary glands (Murakami et al., 2002), and in keratinocytes during inflammatory disorders (Frohm et al., 1997). The strongest epithelial expression of hCAP18 is found in the epididymis with a subsequent high concentration in seminal plasma (Malm et al., 2000; Hammami-Hamza et al., 2001) and is processed by gastricsin to generate the antimicrobial peptide ALL38 (LL37 + Ala at the N-terminus) at low pH in vagina (Sorensen et al., 2003).

As suggested by name, LL37 is a 37 residue peptide, positively charged (+6 at pH ~ 7.4) (Fig. 10), with high content of hydrophobic aminoacids that adopts an α-helical structure in the lipid membranes, micelles, and ions such as hydrocarbonate, sulphate and to lesser extent chloride, but is random coil in pure water (Nijnik and Hancock, 2009). Finally has been shown previously that LL37 has affinity for acidic lipid (Wang, 2008).

LL-37 LLGDFFRKSKEKIGKEFKRIVQRIKDFLRNLVPRTES   37 aa
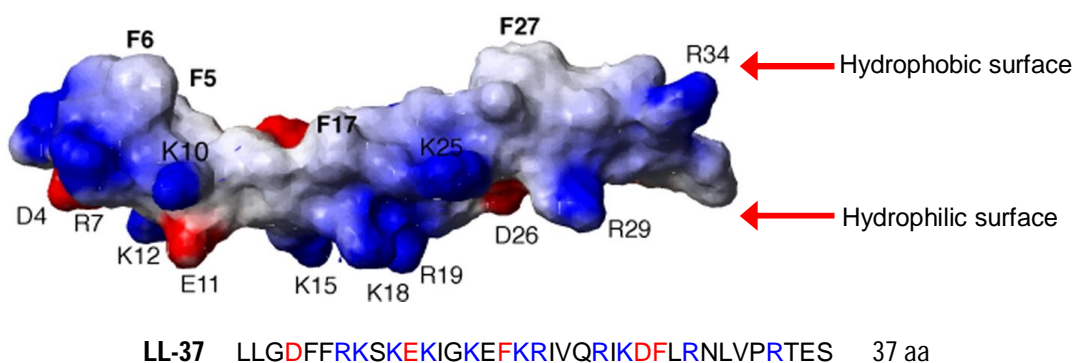
Fig 10 Structure of LL37 peptide

LL-37 as well as ALL-38 have shown a broad spectrum of activity against both Gram-negative and Gram-positive bacteria, various virus, and fungi (Sorensen et al., 2003).

This peptide exhibits potent activity against different bacterial strains, including *E.coli* (Smeianov et al., 2000), *Pseudomonas aeruginosa* (Travis et al., 2000), *Klebsiella pneumoniae* (Smeianov et al., 2000), *Staphylococcus aureus*, methicillin-resistant *S.aureus* (Travis et al. 2000), and *Neisseria gonorrae* (Bergman et al., 2005). LL37's bactericidal activity involves membrane disruption (pore formation, change of lipid packing and organization) following interaction with negatively charged bacterial molecules and insertion into the membrane (Bucki et al., 2010).

It was also recently proposed that cathelicidins produced by glia and other cells may play an important role in the innate immune response against pathogens in the central nervous system during bacterial infections (Brandenburg et al. 2008).

A potential antiviral effects of LL-37 is suggested by the finding that treatment of human leukocytes with neutralizing antibodies direct against LL37 significantly reduces the anti-cytomegalovirus (CMV) effect of LTB4, a potent mediator of inflammation that possess antiviral activities (Gaudreault and Grosselin, 2007).

HIV-1 replication in peripheral blood mononuclear cells (PBMCs), including primary CD4$^+$ T cells, was also compromised in the presence of LL37. This inhibition was subsequently reproduced using various HIV-1 isolates without detectable changes in the target cells expression of HIV-1 chemokine receptor. Accordingly, the HIV-1 inhibitory effect was shown to be independent of FPRL-1 signaling. Given the epithelial expression of LL37, this peptide may contribute to the local protection against HIV-1 (Bergman et al., 2007).

The antimicrobial spectrum of the human cathelicidin LL37 also includes fungicidal activity against *Candida albican* (den Hertog et al., 2006; Lopez-Garcia et al., 2005).

All together, these findings indicate a possible application of LL37 peptide in the treatment of sexual transmitted disease (STDs).

Based on the potential characteristics of this peptide reported in the literature, we believe that it can be used with a dual purpose. In fact, we believe that LL37 can interact with the molecules involved in the process of fertilization and especially we aspect that may interact with SGG and mask them to ZP-binding protein and also use to prevent by infection from the STDs.

Processing of hCAP18 to ALL-38 in the ejaculated seminal plasma occurs in the vagina by gastricsin, an aspartic enzyme with a pH optimum of 4 (Fig.11).
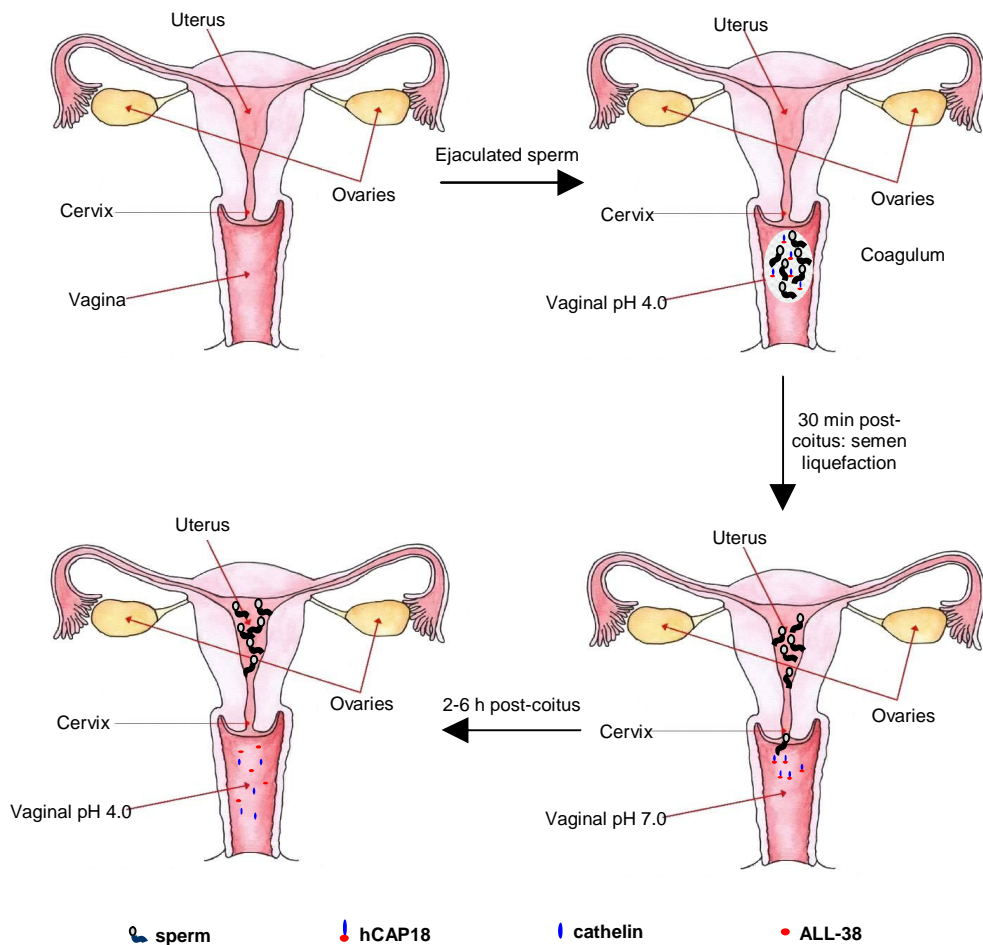
Fig 11 Processing of hCAP18 to LL37 in vagina

However, this processing event takes place 2-6 h post-coitus, the time frame needed for the vagina to resume its acidic milieu after the deposition of neutral pH seminal plasma. By this time, sperm have already entered the uterine cavity; therefore, ALL38 is most likely produced to protect the vagina from microbial/viral attacks. In the absence of ALL38-SGG interaction, SGG on the sperm surface is free to interact with the ZP. Furthermore, ALL38 and LL37 have indistinguishable antimicrobial activities (Sorensen et al., 2003).

For the all reasons listed above, we have considered promising to treat the sperm with the exogenous LL37, more easily available, to assess if it could be able to block the free SGG on the sperm. Should LL37 inhibit sperm fertilizing ability, it would be a great candidate as a non–hormonal vaginal contraceptive with antimicrobial/anti-HIV-1 activity.

5. MATERIALS AND METHODS

Lipids

SGG was prepared from pig testis as described previously (Franchini et al., 2008). Phosphatidylcholine (PC) and phosphatidylserine (PS) were purchased from Avanti Polar Lipids, Inc. (Alabaster, AL, USA). Sulfogalactosylceramide (SGC) and galactosylceramide (GC) were obtained from Sigma Chemical Co (St. Louis, MO).

Proteins

Synthetic antimicrobial peptide LL-37 and the rabbit polyclonal anti LL-37 antibody was generously given by Dr. Robert E.W. Hancock (University of British Columbia, Canada)

Animals

CD-1 male and CF-1 female mice (8- to 12-week-old) were purchased from Charles River Canada (St-Constant, QC, Canada). All mice were kept in a temperature-controlled room (22 °C) with a 14:10 dark/light cycle. The boarding and handling of these mice, as well as all subsequent experimental procedures with them, were approved by Animal Care Committee, Ottawa Hospital Research Institute (OHRI).

Human sperm sample

With approval from the Human Ethics Committee, Ottawa Health Research Institute, Ottawa Hospital Civic Campus the sperm sample were obtained from Ottawa Fertility Center (Ottawa, ON, Canada).

6. EXPERIMENTAL SECTION

Mouse sperm preparation

The caudal epididymides of CD-1 male were longitudinally scored once with a surgical blade and the dense sperm masses squeezed out from this incision and from the vas deferens were placed at the bottom of a 1.5 ml microcentrifuge tube containing 1ml of KRB-Hepes pre-warmed at 37°C. To prepare Percoll-gradient centrifuged (PGC) sperm, the sperm suspension was diluted up to 2 ml with HEPES-buffered Krebs Ringers bicarbonate (KRB-HEPES) medium (KRB-HEPES: 119.4 mM NaCl, 4.8 mM KCl, 1.7 mM $CaCl_2$, 1.2 mM KH_2PO_4, 1.2 mM Mg_2SO_4, 21 mM HEPES, 5 mM $NaHCO_3$, 25 mM sodium lactate, 1 mM sodium pyruvate, 5.6 mM glucose, 2.8 µM phenol red, pH 7.4), and loaded onto a two-step Percoll gradient (45% and 90% Percoll (Amersham Biosciences, Uppsala, Sweden) in KRB-HEPES) (Tanphaichitr et al., 1990). The gradient was centrifuged (650 x *g,* 25°C for 30 min), allowing motile sperm to sediment as a pellet and immotile sperm to interface between the two Percoll layers. After removing the interfaced immotile sperm and most of the Percoll solution, the pelleted motile sperm were washed once in KRB-HEPES (350 x *g,* 30°C for 10 min), and then were re-suspended and capacitated in the Krebs Ringers bicarbonate (KRB) supplemented with 0.3% BSA (KRB-BSA) (KRB: 119.4 mM NaCl, 4.8 mM KCl, 1.7 mM $CaCl_2$, 1.2 mM KH_2PO_4, 1.2 mM Mg_2SO_4, 25 mM $NaHCO_3$, 25 mM sodium lactate, 1 mM sodium pyruvate, 5.6 mM glucose, 2.8 µM phenol red, pH 7.4) at a concentration of approximately 10 x 10^6 sperm/ml (37°C, 5% CO_2 for 30 min). An aliquot of appropriately diluted (10-20 X) sperm suspension was placed onto a hemocytometer, and the numbers of total motile sperm were immediately counted under a Nikon inverted microscope (DIAPHOT-TMD, Nikon Canada, Mississauga, ON) at 200 X magnification. The capacitated sperm were used for *in vitro* fertilization assay (IVF), indirect immunofluorescence (IIF), flow cytometry, and immunoblotting after appropriate treatment with different concentrations of LL-37 (0.162, 1.62, 3.24, 16.2 and 81 µg/ml). These LL-37 concentrations were corresponding to 0.01, 0.1, 0.2, 1, and 5 times molar ratio of SGG amount in 1 million sperm, which is 0.36 nmole (Bou et al., 1990). For IVF, after

treatment, the capacitated sperm were washed once (350 x g, 30°C for 10 min) with KRB-0.3%BSA and re-suspended in the same medium at concentration of 1 million/ml. For IIF and flow cytometry, the sperm were washed twice with PBS containing 0.1% polyvinylpyrrolidone (PVP) and were reconstituted in the same buffer. For immunoblotting, the sperm were washed 5 times with PBS-0.1%PVP and the sperm pellet was used for LL-37 detection by this analysis.

Human sperm preparation

With approval from the Human Ethics Committee, Ottawa Health Research Institute, Ottawa Hospital Civic Campus, frozen ejaculated semen sample were obtained from frozen sample of fertile donor with normal semen parameter (volume 2-6 ml, concentration > 20 x 10^6 sperm/ml, motility $> 50\%$ normal morphology $> 30\%$, WHO criteria, 2009). The sperm were washed once in Hepes buffered Human Tubal Fluid (HTF) medium (HTF-Hepes: 101 mM NaCl, 4.96 mM KCl, 2.04 mM $CaCl_2$, 0.37 mM KH_2PO_4, 0.2 mM Mg_2SO_4, 25 mM $NaHCO_3$, 4 mM sodium lactate, 0.24 mM sodium pyruvate, 2.78 mM glucose, 20 mM HEPES, penicillin G 100 U/ml, streptomycin sulfate 50 µg/ml and 2.8 µM phenol red, pH 7.4).

To select motile sperm, sperm were centrifuged through a discontinuous Percoll-gradient. The sperm suspension (~0.5 ml) was diluted up to 2 ml with Human Tubal Fluid (HTF) medium (HTF: 101 mM NaCl, 4.96 mM KCl, 2.04 mM $CaCl_2$, 0.37 mM KH_2PO_4, 0.2 mM Mg_2SO_4, 25 mM $NaHCO_3$, 21.4 mM sodium lactate, 0.24 mM sodium pyruvate, 2.78 mM glucose, penicillin G 100 U/ml, streptomycin sulfate 50 µg/ml and 2.8 µM phenol red, pH 7.4), and loaded onto a two-step Percoll gradient (45% and 90% Percoll (Amersham Biosciences, Uppsala, Sweden) in HTF) (Tanphaichitr et al., 1990). The gradient was centrifuged (650 x g, 25°C for 30 min), allowing motile sperm to sediment as a pellet and immotile sperm to interface between the two Percoll layers. After removing the interfaced immotile sperm and most of the Percoll solution, the pelleted motile sperm were washed once in HTF (350 x g, 30°C for 10 min), and then were re-suspended and capacitated in the HTF supplemented with 0.3% BSA (HTF-0.3%BSA) at a concentration of approximately 10 x 10^6 sperm/ml (37°C, 5% CO_2 for 30 min). An aliquot of appropriately diluted (10-20 X) sperm suspension was placed onto a hemocytometer, and the numbers of total motile sperm were immediately counted under a Nikon inverted microscope (DIAPHOT-TMD, Nikon Canada, Mississauga, ON) at 200 X magnification. The capacitated sperm was used for immunoblotting after appropriate treatment with different concentrations of LL-37 (3.24, 16.2 and 81 µg/ml). The sperm were washed 5 times with PBS and the sperm pellet was used for LL-37 detection by this analysis.

Mouse *In Vitro* Fertilization (IVF)

To determine whether LL-37 can inhibit sperm fertilizing ability, IVF was carried out as previously described (Tantibhedhyangkul et al., 2002; Wu et al., 2007). CF-1 females were superovulated by sequential intraperitoneal injection of PMSG (5 IU) and hCG (5 IU) (Sigma Chemical Co., St. Louis, MO) with a 48 h interval. Ovulated cumulus masses containing mature eggs were retrieved from the females 14 h after hCG injection and placed in KRB-Hepes containing 0.3% BSA. Cumulus layers were dissociated by treating the cumulus masses with 0.1% hyaluronidase in KRB-0.3% BSA for 1-2 min (Hogan et al., 1994); this freed up the eggs which were then washed with KRB-0.3% BSA and stored at 37°C under 5% CO_2 until insemination.

Caudal epididymal and vas deferens sperm of CD-1 male were collected and capacitated as describe above. Non-treated and treated capacitated sperm (0.5 million in 0.5 ml KRB-0.3%BSA) were then co-incubated with approximately 20 cumulus free eggs in KRB-0.3%BSA under mineral oil for two hours, then the eggs were transferred to KSOM containing 0.3%BSA. The KSOM medium consisted of 95 mM NaCl, 2.5 mM KCl, 1.7 mM $CaCl_2$, 0.35 mM KH_2PO_4, 0.2 mM Mg_2SO_4, 25 mM $NaHCO_3$, 0.2 mM sodium pyruvate, 10 mM sodium lactate, 0.01 mM sodium EDTA, 1 mM L-glutamine, 1 U/ml of penicillin G, 1 µg/ml of streptomycin sulfate, and 28 µM phenol red at pH 7.4. Six hours afterwards, the eggs were scored under an inverted microscope for evidence of two-pronuclei formation. Fertilization rate was defined as percentage of total eggs fertilized in each sample. This *in vitro* fertilization experiment was performed in collaboration with Hongbin Xu and Nopparat Srakaew, Ph.D. students in Dr. Tanphaichitr's laboratory.

Indirect immunofluorescence and flow cytometry for LL-37 treated mouse sperm

Capacitated mouse sperm (treated with different concentrations of LL-37 or without the treatment) prepared as described above were incubated in 5% normal goat serum (37°C, 30 min), and centrifuged (350 x *g,* 30°C for 10 min) to pellet the sperm. The sperm pellet was re-suspended and incubated with affinity purified anti LL-37 polyclonal rabbit IgG antibody (1:500 dilution in PBS) (37°C, 30 min). The incubation of sperm with this primary antibody was omitted for the control group. After the incubation, the sperm were washed twice with PBS and further incubated (37°C, 30 min) with the secondary antibody, Alexa-488-conjugated goat anti-rabbit IgG (Molecular Probes) at the dilution of 1:200 in PBS. The sperm were then washed twice with PBS and the sperm pellet was re-suspended in 20-50 µl in PBS/glycerol (1:1, v/v). A 8-µl aliquot of sperm suspension was mounted onto a slide and topped with a cover slip. The slide was viewed under a Olympus fluorescent IX50/IX70 inverted system microscope (Olympus America Inc., Melville, N.Y, USA). Phase contrast and fluorescent images of sperm were recorded by Infinity Capture software (Lumenera Corporation, Ottawa, ON, Canada) and processed through Image J software (http://rbs.info.nih.gov/ij/).

The remaining sperm suspension of each treatment was diluted in PBS to 0.5 ml and subjected to flow cytometric analysis by a Coulter Epics Profile II Flow Cytometer (Beckman Coulter, Fullerton, CA). Samples were excited by an argon ion laser at 488 nm, and the emission fluorescence was monitored at 525 ± 20 nm band pass. Sperm cells were gated from debris using their unique properties of forward and side light scattering. Data from at least 10000 events were collected, and relative LL-37 staining intensity was determined using FCS Express Software (De Novo Software, Orangeville, ON, Canada).

Immunoblotting for LL-37 treated mouse and human sperm

Pellet of capacitated sperm treated with LL-37 as described above was solubilized in 1X Laemmli SDS sample buffer (Laemmli, 1970) containing 4M urea and 0.2 M DTT (20 µl of this buffer was used for 1 million sperm from each treatment). The sperm suspension was sonicated (10 sec for 20 cycle, boiled for 5 min and centrifuged (14000 g for 10 min). The supernatant of each sample was subjected to 16.5% Gel Tris-Tricine SDS-PAGE (Schägger and Von Jagow 1987, Schägger, 2006), followed by electroblotting onto a nitrocellulose membrane (Towbin and Gordon, 1984). The nitrocellulose was blocked for 1 hour with 5% fat free milk in Tris-buffered saline (TBS: 137 mM NaCl in 20 mM Tris-HCl, pH 7.6) containing 0.05% Tween 20. Immunoblotting was performed using affinity purified anti-LL-37 polyclonal rabbit IgG (1:1000 dilution) as primary antibody, and goat anti-rabbit IgG conjugated with horseradish peroxidase (Bio-Rad Laboratories) (1:10000 dilution) as secondary antibody. The primary and secondary antibodies were prepared in the blocking medium. After incubation with each antibody, the membrane was washed 5 times (5 min each time) with TBS-0.05% Tween20. The reactivity of antibody-antigen was detected by enhanced chemiluminescence (ECL) using an ECL kit (Pierce, Rockford, IL).

Enzyme linked immunosorbent assay (ELISA)

The binding of LL37 to different types of lipids (SGG, SGC, GC, PS and PC) was quantitated using ELISA. Lipids (100 µl in EtOH, containing 1 µg) was coated onto a polypropylene 96-well plate (Greiner Bio-one) and dried overnight at room temperature (RT) in a dessicator. The plates were then blocked with a blocking buffer (TBS at pH 7.4) containing 2% (w/v) BSA and 0.05% (v/v) TWEEN-20 (100 µl/well) for 1 hour at RT. After removing the blocking solution, 100 µl of protein solution prepared in a TBS buffer containing 0.05% (v/v) TWEEN-20 at different concentrations (0, 0.1, 0.25, 0.5, 0.75, 1.5, 3, 4.5 ng/µl) was added to the wells and incubated with the lipids for 1 h. Following the incubation, the plates were washed three times with the washing buffer (TBS at pH 7.4) containing 0.2% (w/v) BSA and 0.05% (v/v) TWEEN-20 to remove unbound proteins. The primary antibody, 100 µl of affinity purified anti-LL-37 rabbit polyclonal IgG (1:5000 dilution), was added and incubated for 1 h, RT. The plates were washed as above and then incubated for 1 h, RT with 100 µl of the secondary antibody goat anti-rabbit IgG conjugated with horseradish peroxidase (H+L) at 1:3000 dilution (Bio-Rad Laboratories). After washing as described above, 100 µl of developer solution, containing 0.4 mg/ml of o-Phenylenediamine dihydrochloride (OPD) and 0.01% H_2O_2 in citrate buffer at pH 5.0, was added to each well and incubated in the dark until the color was developed. The quenched solution (30% sulphuric acid) was then added and the optical density was determined at 490 nm.

Assessment of acrosome integrity of LL37 treated mouse sperm

To determine whether LL37 binding to the sperm could lead to premature acrosome reaction, the acrosomal status of capacitated sperm was assessed after LL37 treatment. Capacitated sperm (1 million sperm) prepared as described above were treated with different concentrations of LL-37 (1.62, 3.24 and 16.2 µg/ml in PBS) for 30 min at 37°C, 5% CO_2. Capacitated sperm without treatment and those treated with 10 µM of A23187 were used as negative and positive control, respectively. After treatment, the sperm were washed twice with PBS and fixed with 4% paraformaldehyde in PBS for 15 min, RT. Following the fixation, the sperm were washed twice with 0.1 M ammonium acetate buffer (pH 9.0) and re-suspended in the same buffer at the concentration of 5 million sperm/ml. An aliquot of sperm suspension (10 µl) was spread onto a 0.25% gelatin-coated glass slide. The sperm were stained with 0.22% Coomassie blue G-250 in 50% methanol, 10% glacial acetic acid. The excess dye was removed by washing with distilled water. Two-hundred sperm from each sample were evaluated for their acrosomal status based on the Coomassie blue staining patterns using a Zeiss Axioskop light microscope at x400 magnification.

7. RESULTS

Binding Assay (ELISA test)

LL-37 is a cationic peptide previously shown to bind to acidic lipids, such as phosphatidylglycerol (PG), and acidic detergents, such as sodiumdodecylsulfate (SDS) (Wang, 2008). Based on this property, LL-37 may also bind to SGG and SGC, which are the major sulfoglycolipids in mammalian germ cells and myelin sheath, respectively. These anionic lipids may serve as receptor for LL37 in the biological process. To first test whether LL37 has affinity for SGG and/or SGC, ELISA test was used.

Using the procedure described in the Material and Methods section we obtained the following results:

LL37 (nM)	OD SGG			OD SGC			OD PS		
0	0	0	0	0	0	0	0	0	0
22.5	0,029	0,008	0,011	0,069	0,046	0,074	0,439	0,421	0,390
55	0,096	0,124	0,071	0,137	0,133	0,199	0,760	0,699	0,615
111	0,243	0,226	0,196	0,301	0,305	0,360	1,049	0,942	0,905
167	0,334	0,326	0,251	0,357	0,360	0,432	1,142	1,331	1,032
333	0,479	0,503	0,434	0,527	0,494	0,440	1,353	1,315	1,248
667	0,698	0,764	0,664	0,716	0,648	0,547	1,530	1,487	1,446
1000	0,705	0,809	0,706	0,702	0,553	0,480	1,497	1,489	1,321

LL37 (nM)	OD GC	OD PC
0	0	0
22.22	0.017	0.049
55.55	0.017	0.064
111.11	0.012	0.081
166.66	0.006	0.081
333.33	0.006	0.085
666.66	0.002	0.096
1000.00	-0.002	0.096

The data were obtained in triplicate only for the lipids that showed the affinity for the peptide. (SGG, SGC and PS)

The absorbance value of each sample show above were already subtracted from the background values, obtained at 490 nm. All these data were then analyzed using graph Pad Prism 5.0.

ELISA test of SGG/SGC/GC/PS and PC binding to LL37 at pH 7.4
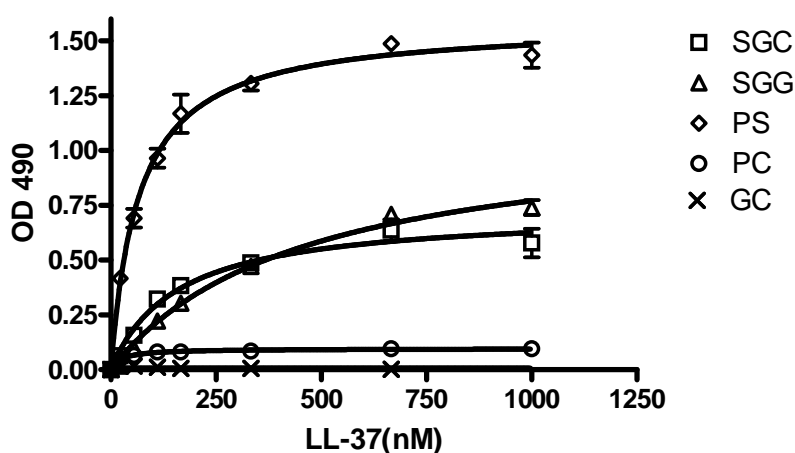
ACIDIC LIPIDS	K_d value (nM)
Sulfogalactosylceramide (SGC)	157.0 ± 27.8
Sulfogalactosylglycerolipid (SGG)	455.7 ± 59.1
Galactosylceramide(GC)	n.d.
Phosphatidylcholine (PC)	n.d.
Phosphatidylserine (PS)	66.7 ± 6.1

Our preliminary data reveled that LL37 indeed has affinity to acidic lipids, and in particular for those containing charged structures, i.e., SGC, SGG and PS; however, the data suggest that the lipophilic tails of these lipids may also play a role in terms of interaction with the peptide.

In fact, PC, which has a charged structure, and on the other hand, GC, which has the same structural features of SGC but it is not charged, do not present any affinity for the peptide.

These data suggest that this peptide most likely presents a specific binding task for acid lipids and therefore this it appropriate for our biochemical studies.

In this context we decided to evaluate the potential role of LL37 in the inhibition of sperm fertilizing ability. So we began studies of interaction with sperm, probably via SGG, through several techniques like immunoblotting, immunofluorescence, flow cytometry and in vitro fertilization. Furthermore we intended to look on the ability of LL37 to interfere with the sperm function and

for these reason we planned to investigate the integrity of the acrosome membrane.

Estimating LL37 concentration for sperm treatment

The LL-37 concentration for sperm treatment was estimated on the basis of the amount of SGG on sperm and assuming that SGG is the site for LL37 binding to the sperm. One million sperm contain 0.36 nmole of SGG (Bou et al., 2006); therefore, 1.62 µg of LL-37 (4.5 kDa) is needed for treatment of one million sperm at 1 molar ratio of SGG (1X). Usually, sperm treatment is carried out in a 100-µl sperm suspension at a concentration of sperm of 10 million/ml. In this study, different concentrations of LL-37, based on different molar ratios of SGG, were used for the sperm treatment (see details in the table below).

Concentration of LL-37 (µg/ml)	Molar ratios to SGG
0.162	0.01X
1.62	0.1X
3.24	0.2X
16.2	1X
81	5X

Immunoblotting of capacitated cauda mouse sperm treated with LL37

To investigate whether exogenous LL37 can bind to the sperm in a dose dependent manner, the amounts of LL37 on treated sperm were determined by immunoblotting.
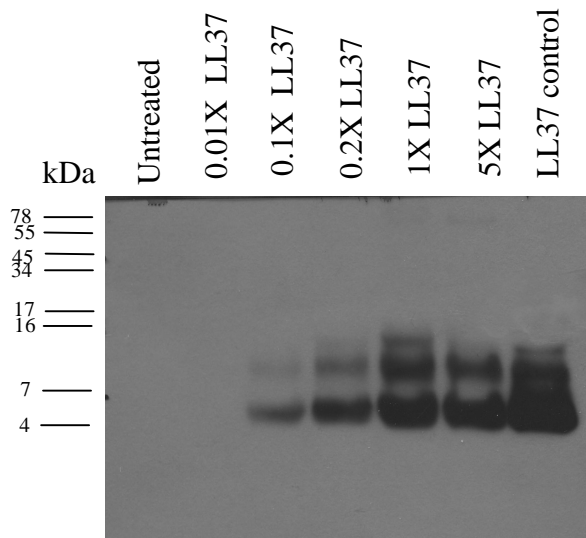
Conditions for gel running and immunoblotting:

Sample loading; 1 million sperm for each treatment

Gel used and sample preparation 16.5% polyacrylamide Gel (Tris-Tricine SDS-PAGE), Samples were prepared in a reducing sample loading buffer containing, DTT and 4M urea and boiled for 5 minute prior to use.

Primary antibody
Affinity purified anti-LL-37 polyclonal rabbit IgG (1:5000)
Secondary antibody
goat anti-rabbit IgG HRP conjugate (H+L) (1:3000)
Exposure time
5 minute

The result obtained showed that exogenous LL37 can bind to the capacitated mouse sperm in a dose-dependent manner. We then desidered to investigate the site where LL37 binds to sperm, especially on the sperm head where the SGG is localized.

Indirect immunofluorescence of capacitated mouse sperm treated with LL37

Dr. Tanphaichitr group has shown that SGG is present on the anterior head surface of the mammalian sperm plasma membrane and is involved in sperm-zona pellucida (ZP) binding (White *et al.*, 2002; Weerachatyanukul *et al.*, 2001) They have also demonstrated that SGG exists at a substantial amount on the sperm surface, namely at 10% mole of the total sperm lipids, and is a main component of capacitated sperm lipid rafts, which have affinity for the ZP (Bou Khalil *et al.*, 2006).

Indirect immunofluorescence was used for localization of LL37 on the sperm after the treatment.

Untreated sperm
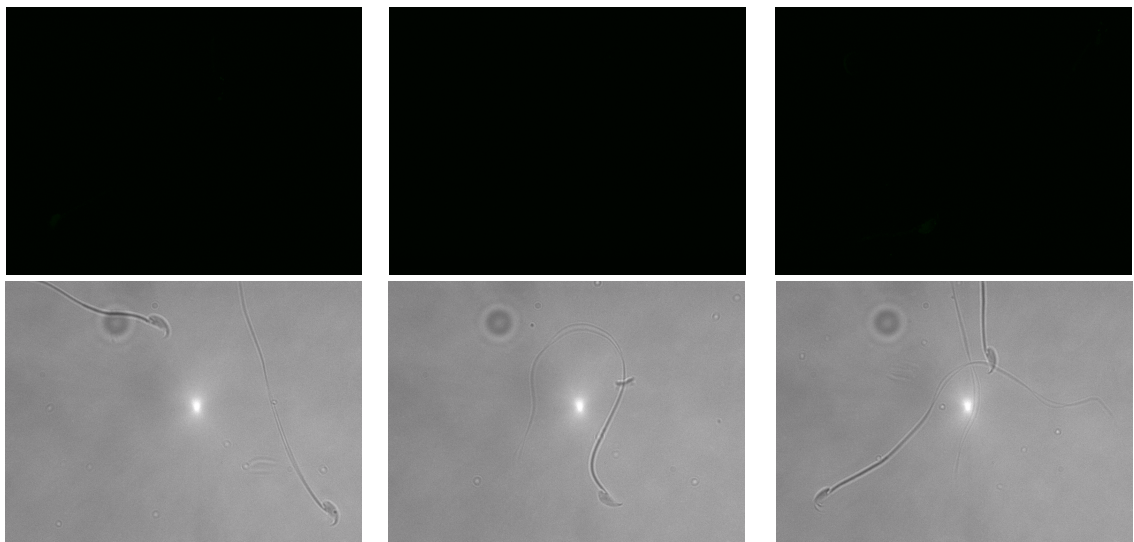
LL37 treated sperm (without 1° Ab)
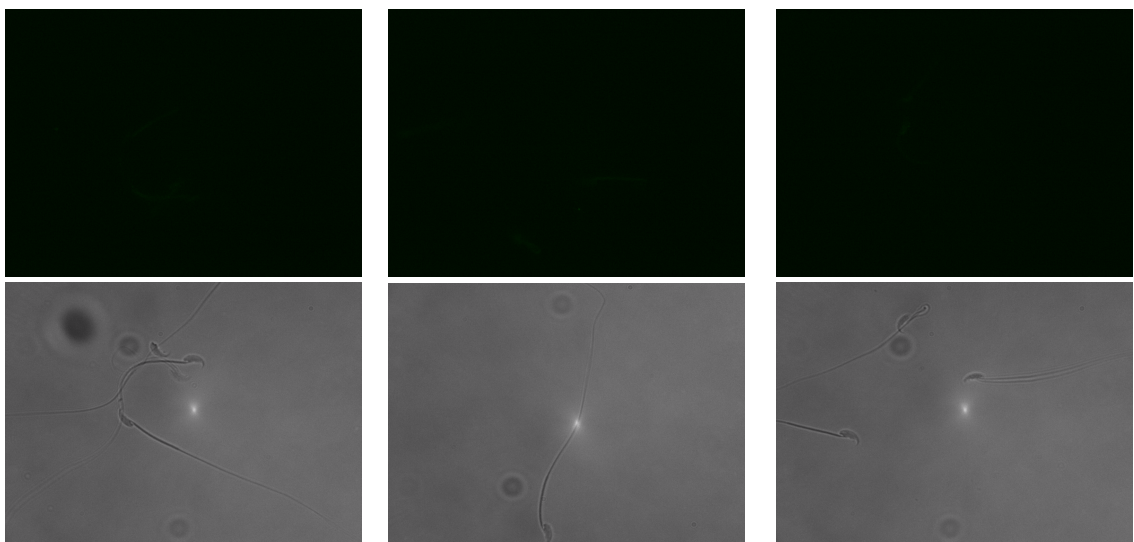
Sperm treated with 0.2 X LL37
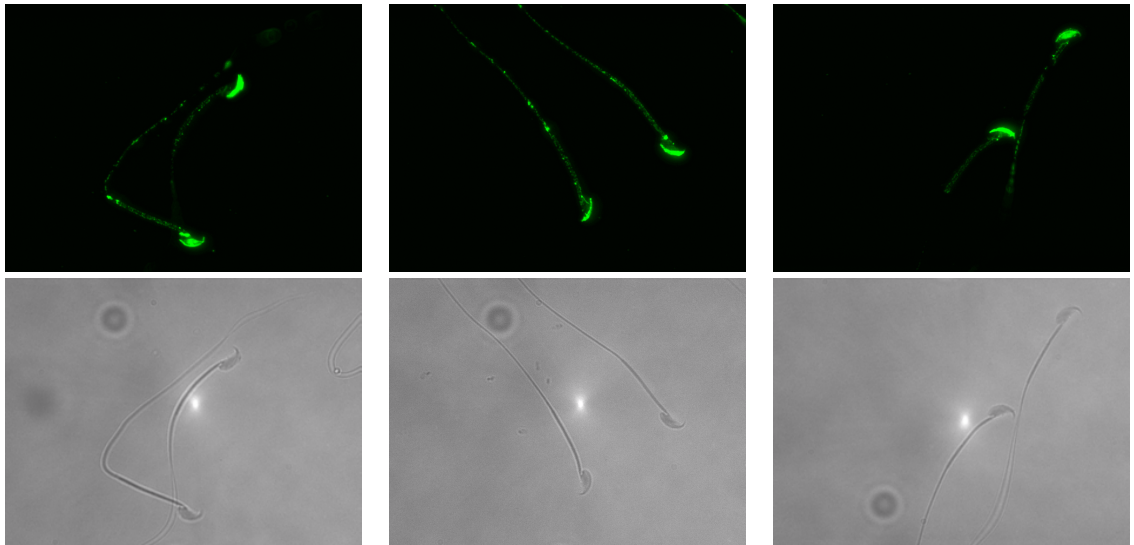
Sperm treated with 1X LL37
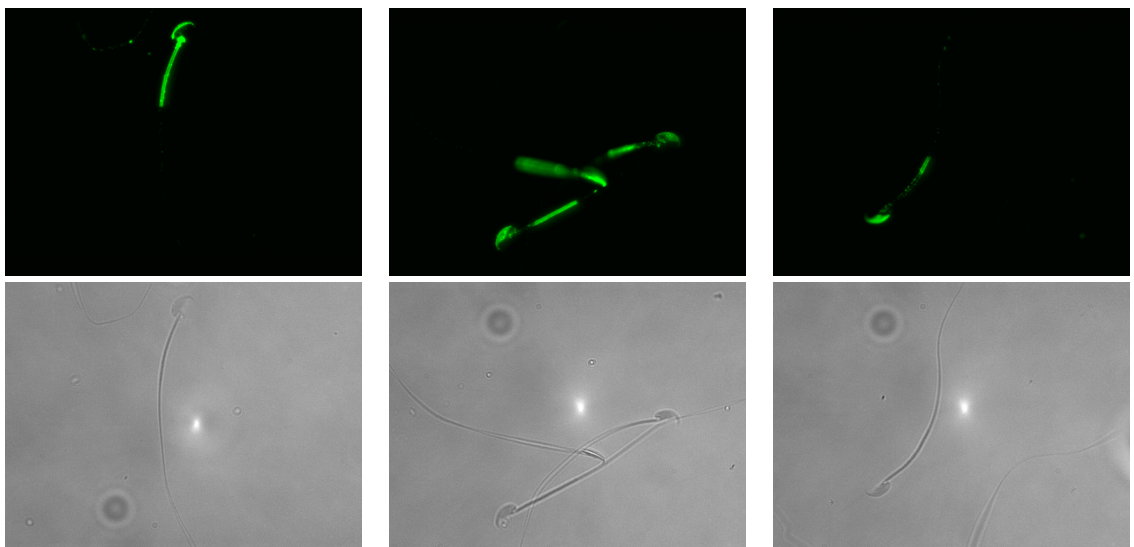
After treating sperm with LL37 at the concentration of 0.2X molar ratio of SGG, we found that LL37 bound principally on the sperm head surface where SGG is localized; however, when the concentration of LL37 was increased to 1X of SGG molar ratio, staining at the midpiece of sperm was also observed. These findings suggest that LL37 may inhibit sperm functions by masking SGG on the sperm head surface and it may also bind to other unknown ligands on the midpiece and interfere with other sperm functions.

Flow cytometry on the capacitated mouse sperm treated with LL37

To confirm the results on the LL37 binding to sperm obtained from indirect immunofluorescence, flow cytometry was performed as previously described in the Methods section.
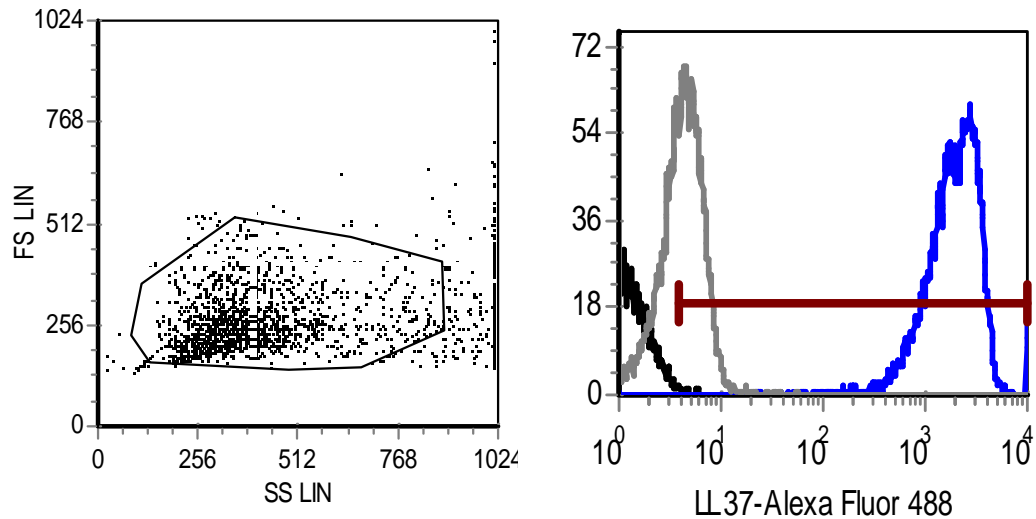
	Line color	# Events	% of gated cells	Geometric mean
Untreated	black	38	0.0	8.0
1° Ab (omitted)	gray	9993	55.0	6.0
Treated with 1X LL37	blue	5463	100.0	1776.0

The high geometric mean obtained from the sperm sample treated with 1X concentration of LL37 indicated that all the mouse sperm population analyzed showed the binding with the peptide.

This data not only support the results from indirect fluorescence but also confirm that LL37 at 1X molar ratio of SGG is sufficient for masking all SGG molecules present on the sperm head surface. This concentration of LL37 can then be used in the *in vitro* fertilization experiments to assess sperm fertility.

In Vitro Fertilization

To determine whether LL-37 can inhibit sperm fertilizing ability, *in vitro* fertilization (IVF) was carried out as previously described.

Fertility-related changes on sperm, such as motility and viability, were also investigated. After treatment with different concentration of LL37, sperm motility and viability were assessed by microscopic analysis and calcein fluorescent staining, respectively. This part of experiment was done in collaboration with Dr. Hongbin Xu, a former postdoctoral fellow in Dr. Tanphaichitr's laboratory.

	Control	0.162 μg/ml	1.62 μg/ml	3.24 μg/ml	16.2 μg/ml	81 μg/ml
Sperm motility	90%	90%	40-50%	10-20%	10%	0%
Sperm viability	90%	88%	82%	76%	26%	24%
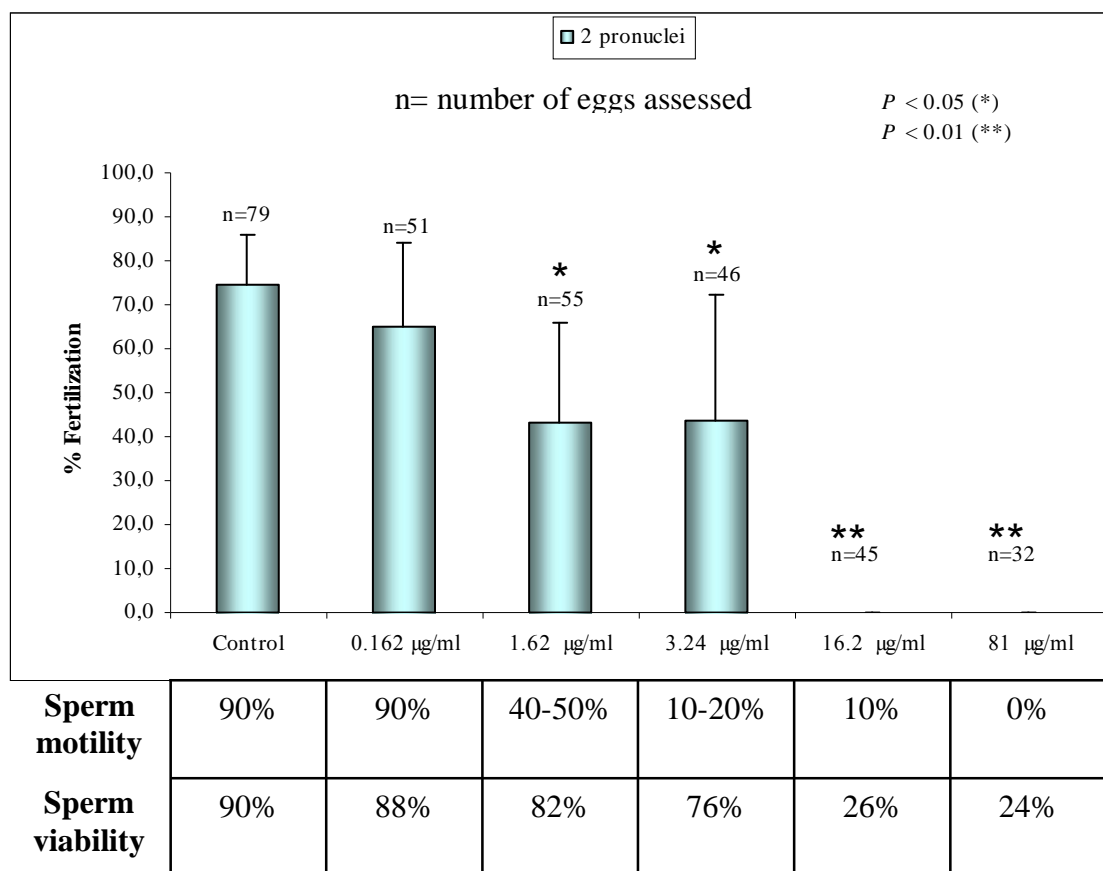
Data presented are the average of three experiments

These results showed that sperm motility and viability were reduced in a concentration-dependent manner upon treatment with LL37. Significantly, the sperm fertilizing ability was abolished when the sperm were treated with LL37 at the concentration of 16.2 μg/ml, equivalent to 1X molar ratio of SGG amount on sperm. This result suggested that LL37 at this concentration was able to completely mask SGG on the sperm head and drastically reduce sperm motility and viability.

Acrosome Reaction

Another important sperm function that is involved in the sperm fertilizing ability is the acrosome reaction, a process resulting in the release of hydrolytic enzymes for sperm penetration to the ZP layer prior to fertilize the egg. In fact sperm that undergo acrosome reaction prematurely lost their ability to fertilize the egg.

To investigate whether LL37 can induce premature acrosome reaction, the assessment of acrosomal status was carried out as previously described.

Comassie blue staining patterns of mouse sperm heads show different acrosomal status:
(a) = acrosome intact, (b) = acrosome reacting, and (c) acrosome reacted
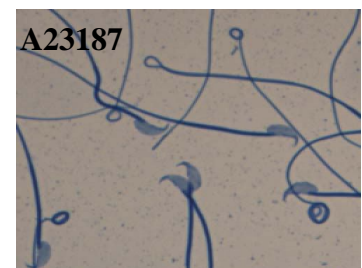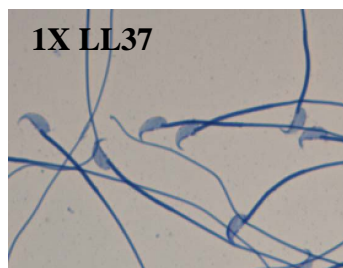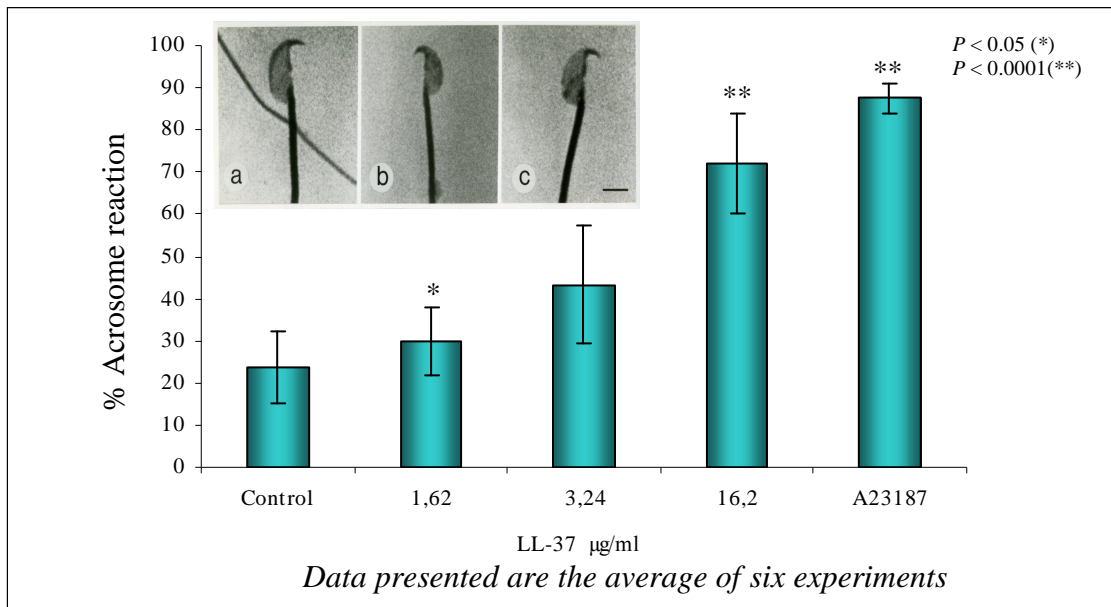
The results revealed that LL37 was able to induce premature acrosome reaction and when the sperm were treated with 16.2 µg/ml of LL37, 72% of the total treated mouse sperm showed acrosome reacted patterns.

8. CONCLUSION

LL37, a broad spectrum antimicrobial peptide (AMP) belonging to the cathelicidin family, is a multifunctional host defense peptide that has been shown to act against infectious pathogens. The main goal of our study is to develop LL37 as a non-hormonal vaginal contraceptive with dual functions. These functions include 1) inhibiting the fertilization by masking the binding of SGG present on the sperm head during sperm-egg interaction and 2) preventing sexually transmitted infections (STI) by attacking the pathogens.

The results presented in this thesis strongly support the potential of LL37 as an effective non-hormonal vaginal contraceptive with antimicrobial properties. Firstly, LL-37 has high affinity for SGG (K_d = 455.7 $\pm$ 59.1). Secondly, exogenous LL-37 binds tightly on live mouse sperm head, where SGG is abundantly expressed, suggesting that LL37 can inhibit sperm function by interaction with SGG. Thirdly, the binding of exogenous LL-37 to sperm decreases the sperm motility and viability. The reduction of sperm motility may be related to the observed additional binding of LL37 to the midpiece region where mitochondria are localized. Treatment of sperm with 1X molar ratio of LL-37 to SGG completely abolishes the sperm's fertilizing ability. The impairment in sperm functions is likely due to premature acrosome reaction induced by LL-37 treatment, given that 72% of sperm undergo acrosome reaction after treating with 1X molar ratio of LL-37 to SGG.

9. FUTURE AND PROSPECTIVE

Based on the effects of LL37 on the mouse sperm fertilizing ability, we would like to expand our study to investigate the role of LL37 on human sperm. Preliminary results shown here were obtained from treatment of frozen capacitated human sperm with exogenous LL37 following by immunoblotting analysis.

The experiment was carried out as precendently described.

Conditions for running gel and immunoblotting:

Sample loading 1 million sperm for each treatment
Gel used and sample preparation;
16.5% polyacrylammide Gel (Tris-Tricine SDS-PAGE), sample were prepared in reducing sample loading buffer containing, DTT and 4M urea and boiled for 5 minutes prior to use
Primary antibody
Affinity purified anti-LL-37 polyclonal rabbit IgG 1: 1,000
Secondary antibody
Goat anti-rabbit IgG HRP 1: 10,000
Exposure time 4 minute

The result shown a specific protein band around 18-kDa correlated to hCAP18 and other two protein band at 4-kDa and 8-kDa corresponding to the monomer and dimer of LL37. Furthermore these data suggest a specific binding of exogenous LL37 in a dose-dependent manner to the human sperm.

These preliminary results prompt us to further investigate the effects of LL37 on human sperm fertilizing ability, which will fulfill our goal in developing LL37 as a non hormonal contraceptive.

SECTION II

10. INTRODUCTION

Sponges (*Porifera*) are metazoans that have developed for 600 million years, and today are found in many different marine habitats and also in freshwater lakes and streams (Brusca and Brusca, 1990). It is well know that marine sponges are a rich source of bioactive compounds that play an important role of protection against predator, overgrowing space competitor and invading microorganisms (Pawlik et al., 1993).

Over the past three decades, several biologically secondary metabolities have been isolated from marine sponges and used as new therapeutic agents (Towle et al., 2001).

More recently, it has been shown that some metabolites in sponges are actually biosynthesized by microorganisms, mostly bacteria, living as a symbionts in the sponge (Piel et al., 2004). This is not surprising, if one considers that in some species, such as *Plakortis Simplex*, bacterial symbionts constitute 50% of the mass of the organism, an there are 80 times more bacterial cells than sponge cells (Laroche et al., 2007).

Sponges of the genera *Agelas* and *Axinella* were shown to contain a unique class of glycosphingolipids with an α-galactose as the first sugar of the saccharide chain (Costantino et al., 1995). Such glycolipids are immunostimulating if the OH group at position 2 of the inner galactose is not glycosylated (Costantino et al. 1996). Due to their immunostimulating activity, agelasphins (α-galactosylceramides) and their synthetic analogue KRN-7000 (Kobayashi, 1995) (Fig. 12) show a remarkable *in vivo* antitumor activity (Motoki et al., 1995); the latter compound is being currently tested as a candidate anti-cancer drug.
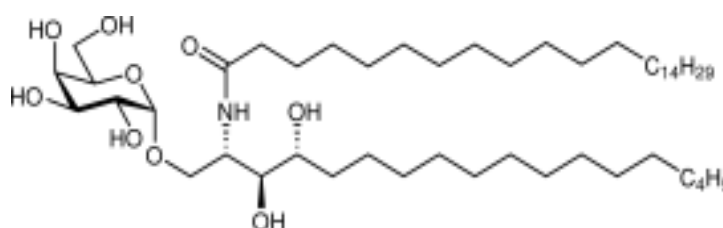
Fig. 12 KRN7000 structure

More recently, it has been shown that other two molecule, plakoside A (Fig. 13 (a)) and B (Fig. 13 (b)) two prenylated glycosphingolipids, show potent immunosuppressive properties.
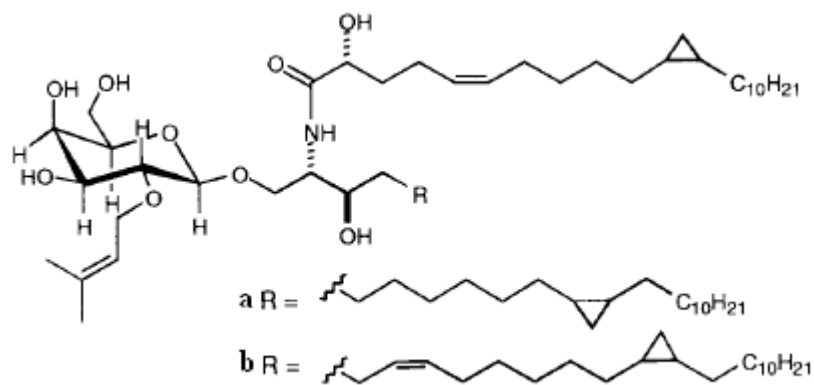
Fig.13 Plakoside structure

These unique glycolipids were isolated from the Caribbean sponge Plakortis simplex.
In the context of molecule that exhibits immunomodulating activities we will focuse
our attention on a new class of atypical glycolipids, i.e simplexide, which is product
from a symbionts bacteria present in the *Plakortis Simplex* sponge, and had been shown
as a potent stimulator for the production of unique profile of cytokine from human
peripheral blood mononuclear cells (PBMC) (Loffredo et al., 2010 in press).

11. SIMPLEXIDE

Simplexide is a unique glycolipid which is found in the sponge *Plakortis Simplex* (Fig. 14), but is produced by the bacterial simbionts of the sponge.

Fig. 14 Caribbean sponge *Plakortis Simplex*

It is a diglycosylated very long chain secondary alcohol, with the OH group at about the middle of alkyl chain. The OH group is glycosylated by a β-galactopyranose, which in turn is glycosylated at position 4 by an α-glucopyranose.

Glycosylated long-chain secondary alcohols have never been reported as natural compounds, so that simplexide can be considered the first member of a new class of glycolipids (Fig. 15).
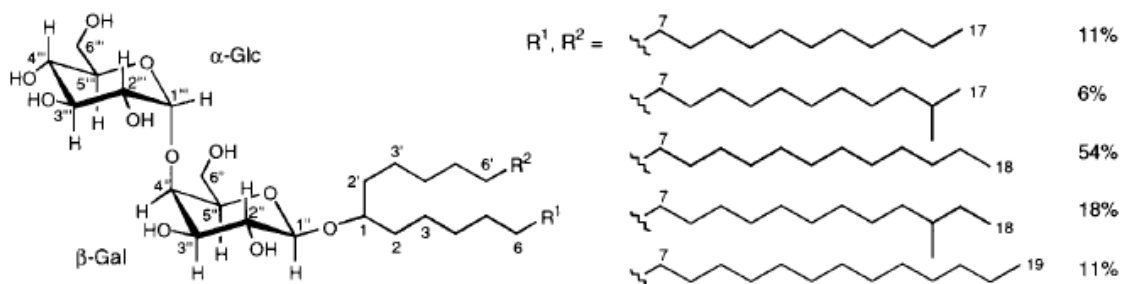
Fig. 15 Simplexide structure

Another unusual feature of simplexide is the very long chains of the lipid part, which presents heterogenicity and is composed of 34-37 carbon atoms with the hydroxyl

group nearly in the middle, although the species more represented is the one with 35 carbon atoms.

This suggests that the lipid part of simplexides could be biosynthesized from the coupling of two molecules of fatty acid. A reasonable biogenetic hypothesis is sketched in Scheme 1.
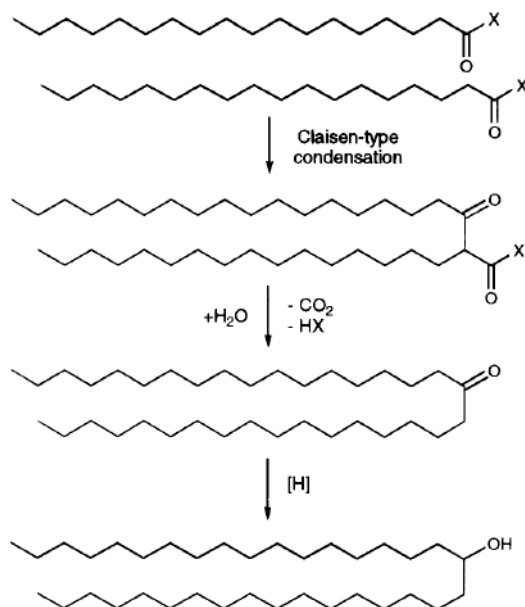
Scheme 1. Proposed biosynthesis of the lipid part of simplexides 1 (X = SCoA or any other acyl carrier).

At the time of its first isolation, simplexide had shown immunosuppressive activity in a preliminary assay on a pure population of murine T cells. Micromolar concentration of simplexide were able to inhibit concanavalin-A induced proliferation of lymph-node cells (Ianaro et al., 1995). The activity of simplexide has been recently tested measuring the effect on cytokine and chemokine production from PBMC (Fig. 16) (Loffredo et al., 2010 in press).
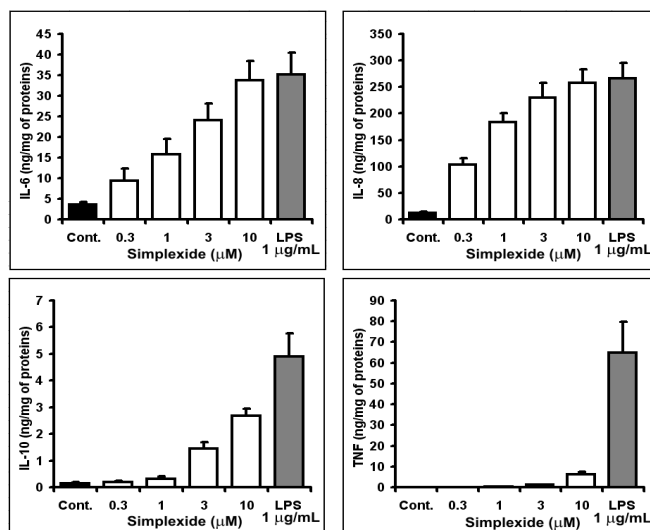
Fig. 16 Activities of simplexide on PBMC

The result of these experiments were particularly interesting, because the simplexide turned out to be a potent stimulus for the production of IL-6, IL-8 and IL-10 from human PBMC. In contrast, simplexide has no effect on TNF-α release. The cytokine profile induced by simplexide appears quite unique, because classic activation of PBMC (i.e. by LPS or immunocomplexes) always result in the production of TNF-α (Loffredo, 2010 in press).

Interestingly, simplexide is very potent in stimulating human PBMC, and the highest concentration tested (10 µM) its effect on the synthesis of IL-6 and IL-8 is comparable to that of LPS, the most potent stimulus know for human PBMC activation. Preliminary investigation to identify the receptor activated by simplexide showed the Toll-like receptor-2 and 4 (TRL-2 and 4), the receptors engaged by LPS, are not involved in the effect of simplexide (Fig.17).
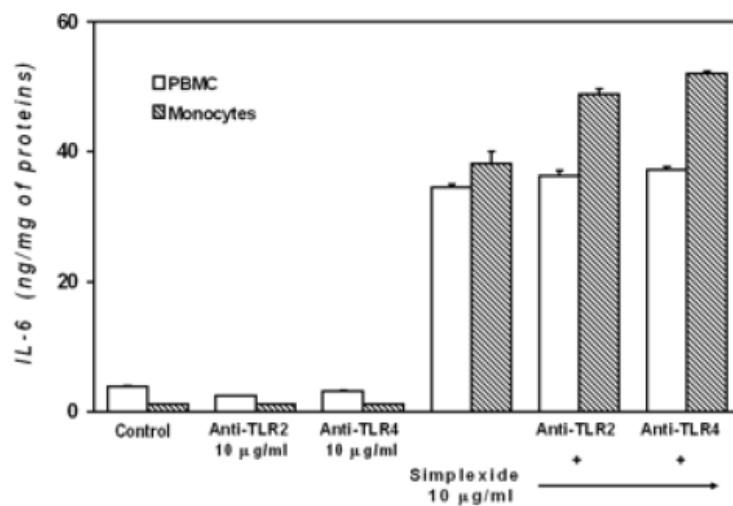
Fig. 17 Binding receptor

Among the possible receptors for simplexide, it has been considered CD1d, a protein expressed on the surface of antigen presenting cell (APC), which can bind lipid or glycolipid antigens and activate cytokine release from monocytes and NK cells (Exley et al., 2000). The anti-CD1d antibody induced a cytokine profile which is quite similar to that induced by simplexide (IL-6, IL-8, IL-10 but not TNF-α). The data shown suggest that the effects of simplexide may be mediated by CD1d. This hypothesis is further supported by the observation that α-GalCer, the reference ligand for CD1d (Koch et al., 2005), is capable for inducing a cytokine profile similar to that simplexide, although at a 100-fold higher concentration.

Overall, these results show that simplexide is a potent inducer of a unique cytokine and chemokine profile and its able to modulate lymphocyte and monocyte functions. Therefore, it is conceivable that simplexide may have immunoregulatory properties that may be potentially useful for treatment of neoplastic and autoimmune disease.

12. AIM OF WORK

Simplexide, a long chain secondary alcohol glycosylated by a disaccharide (Fig. 18) is a glycolipid isolated from the marine Caribbean sponge *Plakortis Simplex* (Costantino et al., 1999).
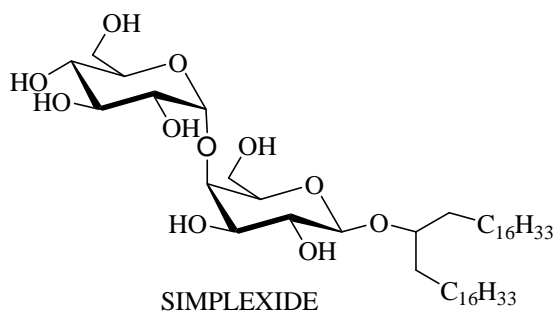
SIMPLEXIDE

Fig. 18

Simplexide shows immunosuppressive activity and strongly inhibits proliferation of activated T cells without cytotoxic activity (Costantino et al., 1999). More recently, a very interesting and unique pattern of cytokines release from PBMC (*Peripheral Blood Mononuclear Cells)* was observed after stimulation with simplexide (Loffredo et al., 2010 in press). This unprecedented profile makes simplexide a potential lead for the treatment of autoimmune diseases. Nevertheless, more detailed studies are needed in order to understand the biochemical mechanism of action and for a better comprehension of the structural requirements for activity.

In this context a synthetic approach towards the preparation of a simplexide fluorescent probe (Hoang et al., 2003; Im et al., 2004) has been developed. This compound will be functional to evaluate the subcellular distribution of the glycolipid and to clarify its mechanism of action.In particular, the analogue **(1)** (Fig.19), with a fluorescent group (i.e dansyl), attached to the position 6 of glucose through a spacer arm, has been designed and prepared during my Ph.D period.

(1)
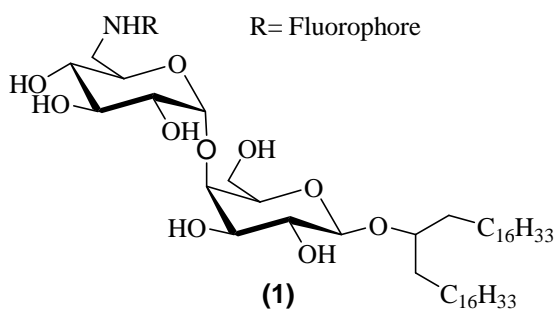
Fig. 19 Fluorescent analogue of simplexide

In order to minimize inaccurate results it is important that the addition of the fluorescent probe does not interfere in the association of the ligand with its host. The choice of position 6 of glucose should meet these requirements, since preliminary results revealed that the biological receptor of simplexide should be the CD1d protein, which recognizes glycolipids by docking their lipid part in the hydrophobic binding region while leaving the polar head group protruding from the surface of the protein binding groove for T cell recognition (Koch et al., 2005; Borg et al., 2007).

13. RESULTS

13.1 Synthetic approach

We have designed a retrosynthetic strategy (Fig. 20) and planned to obtain fluorescent simplexide **(1)** through glycosylation between the preformed activated disaccharide **(14)** (LG = leaving group) and the lipid moiety. In turn disaccharide could be obtained through glycosylation between a glucosyl donor **(9)** selectively functionalized with an azido group at position 6 and galactoside **(13)**. The hydroxyl protecting group in both saccharides have been chosen in order to guarantee the correct stereochemistry in the formation of the glycosydic bonds. The lipid acceptor is commercial available.
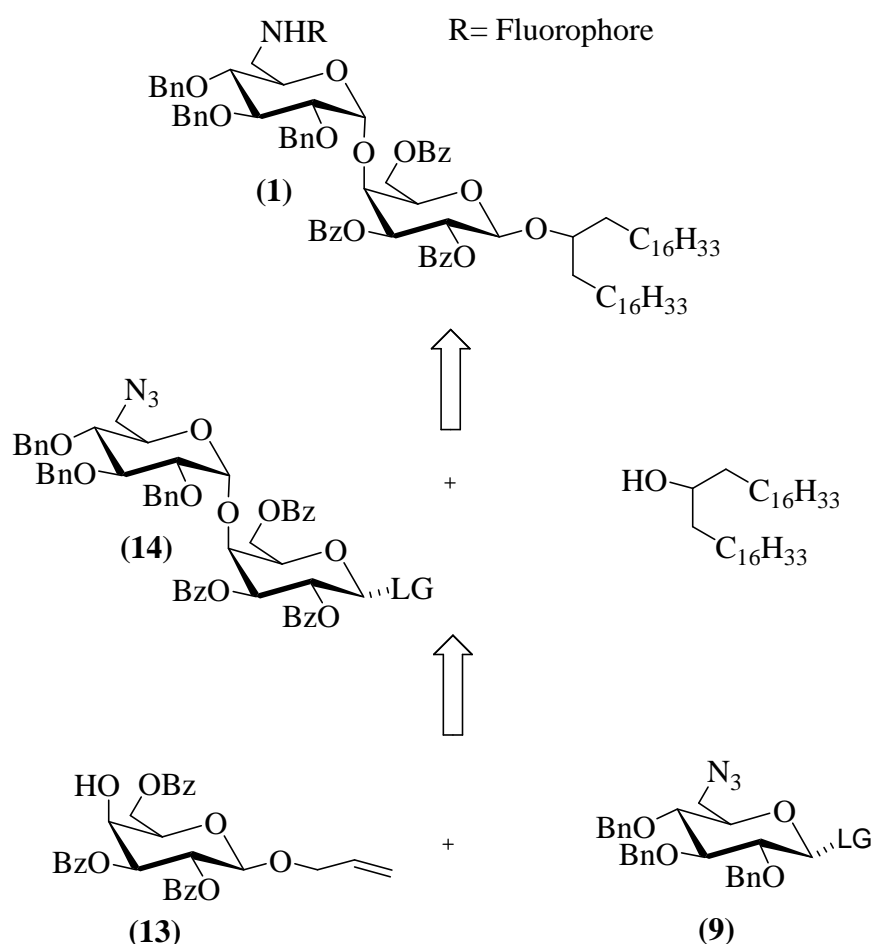
Fig 20 Retrosynthetic scheme of fluorescent simplexide

Following this retrosynthetic scheme we have planned the synthesis of the single sugar moiety necessary to obtain the fluorescent simplexide.

13.2 Synthesis of glucosyl donor
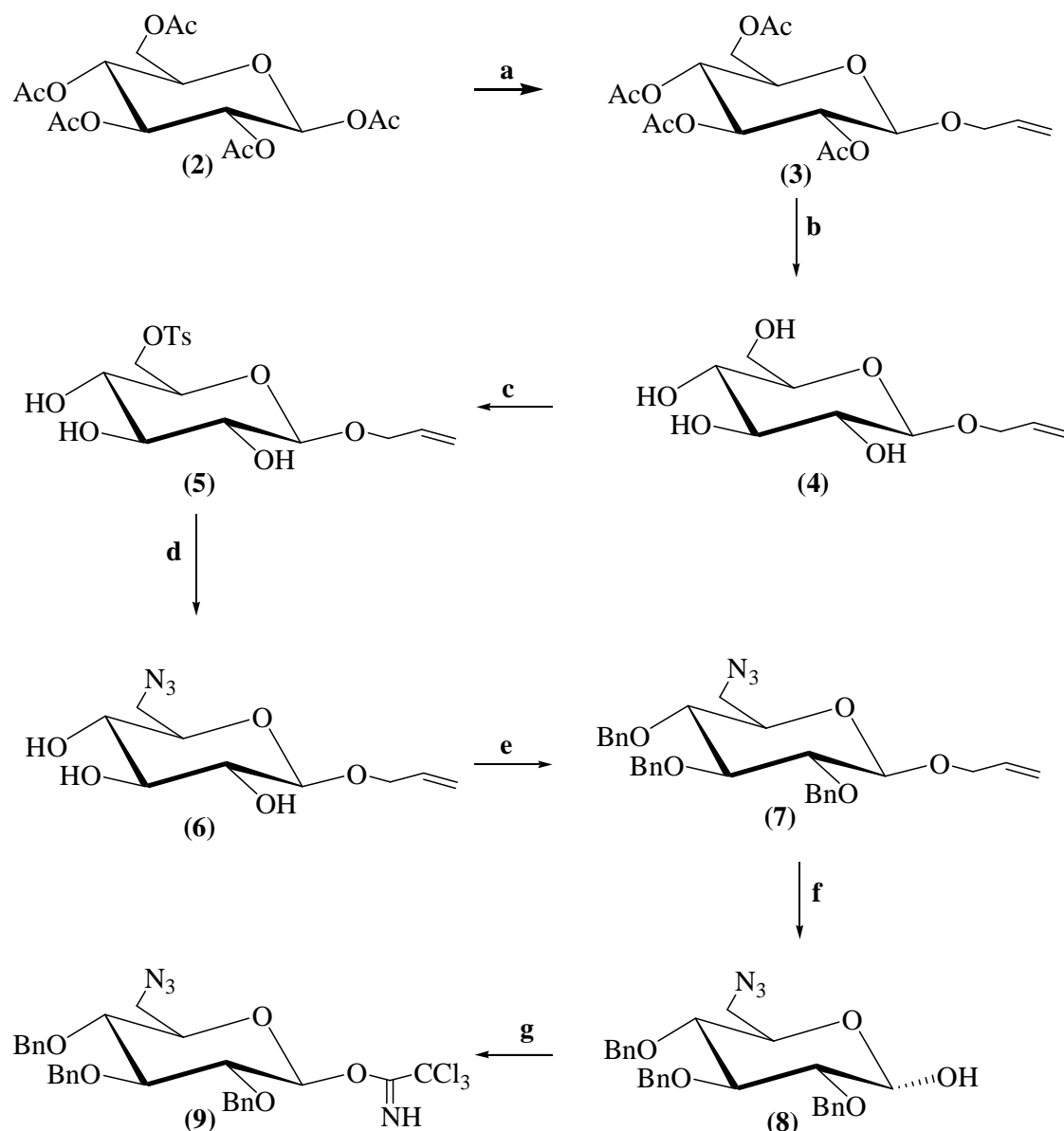
Scheme 2. **a**. Allyl alcohol, BF$_3$Et$_2$O, DCM, RT, 3 h (60%). **b**. MeONa, MeOH, RT, overnight (99%). **c**. Tosyl chloride, Py, 0 °C, overnight (80%). **d**. Sodium azide, TBAI, DMF, 80 °C, 6 h (90%). **e**. Benzyl bromide, NaH, DMF, 55 °C, 1,30 h (90%). **f**. Ir catalyst, THF, then NBS, H$_2$O, 3 h (70%). **g**. Cl$_3$CCN, K$_2$CO$_3$, DCM, RT, 20 h (77%).

The synthesis of the glucosyl donor was performed as described above.

Compound **(3)** was obtained by reaction of commerciable available β-D-glucose pentaacetate with allyl alcohol in dichloromethane and boron trifluoride di-ethyl etherate as the catalyst (yield 60%). Then, the protecting groups were removed in a quantitative yield by methanolysis and the product **(4)** was used without purification and functionalized in position 6 through reaction with tosyl chloride in pyridine to give compound **(5)** (yield 80%).

The tosyl group was subsequently replaced with an azido functionality in order to obtain compound **(6)** by reaction with sodium azide in DMF catalyzed by tert-butyl ammonium iodide (yield 90%) .

Compound **(7)** was obtained by reaction of the hydroxyl group of compound **(6)** with sodium hydride in *N,N*-dimethylformamide and subsequent treatment with benzyl bromide (90%). Finally compound **(9)** was achieved via the intermediate **(8)** by treatment with trichloroacetonitrile and potassium carbonate in dichloromethane (yield 77%).

Compound **(9)** was then used for the glycosylation with galactosyl acceptor.

13.3 Synthesis of galactosyl acceptor
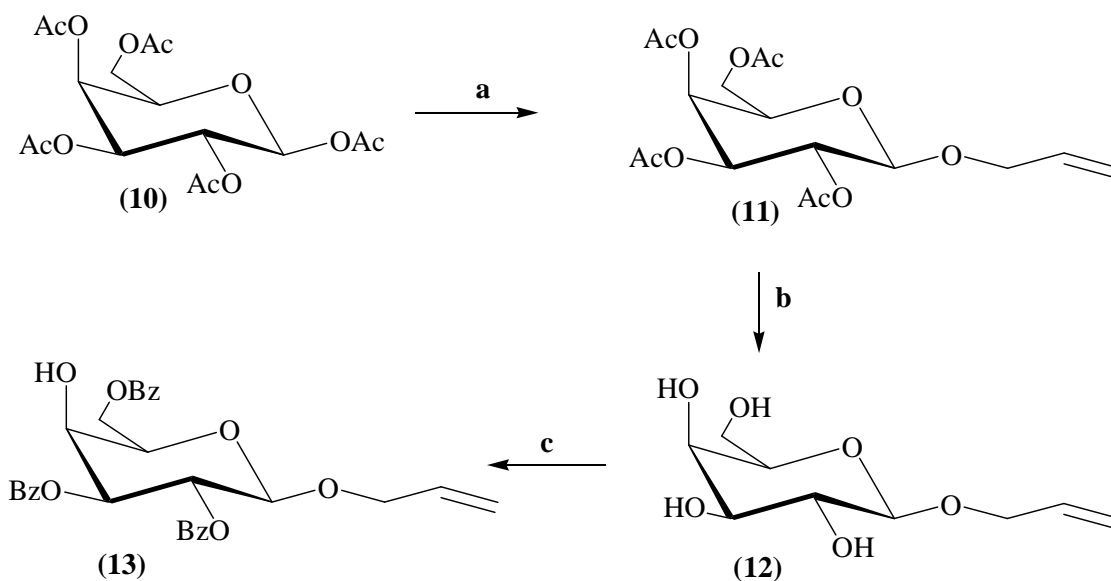
Scheme 3. **a**. Allyl alcohol, BF$_3$Et$_2$O, DCM, RT, 3 h (70%). **b**. MeONa, MeOH, RT, overnight (99%). **c**. Benzoyl chloride, Py, -30 °C, 1 h (50%).

The synthesis of the galactosyl acceptor **(13)** was performed as described above.

Compound **(11)** was obtained for reaction of commercial available β-D-galactose pentaacetate **(10)** with allyl alcohol in dichloromethane and boron trifluoride di-ethyl etherate as the catalyst (yield 70%). Then, the protecting groups were removed in a quantitative yield by methanolysis and the product **(12)** was used without purification to obtain the compound **(13)** by selectively benzoylation through reaction with benzoyl chloride in pyridine at low temperature (yield 50%).

Compound **(13)** was used for the glycosylation with the glucosyl donor.

13.4 Synthesis of fluorescent simplexide
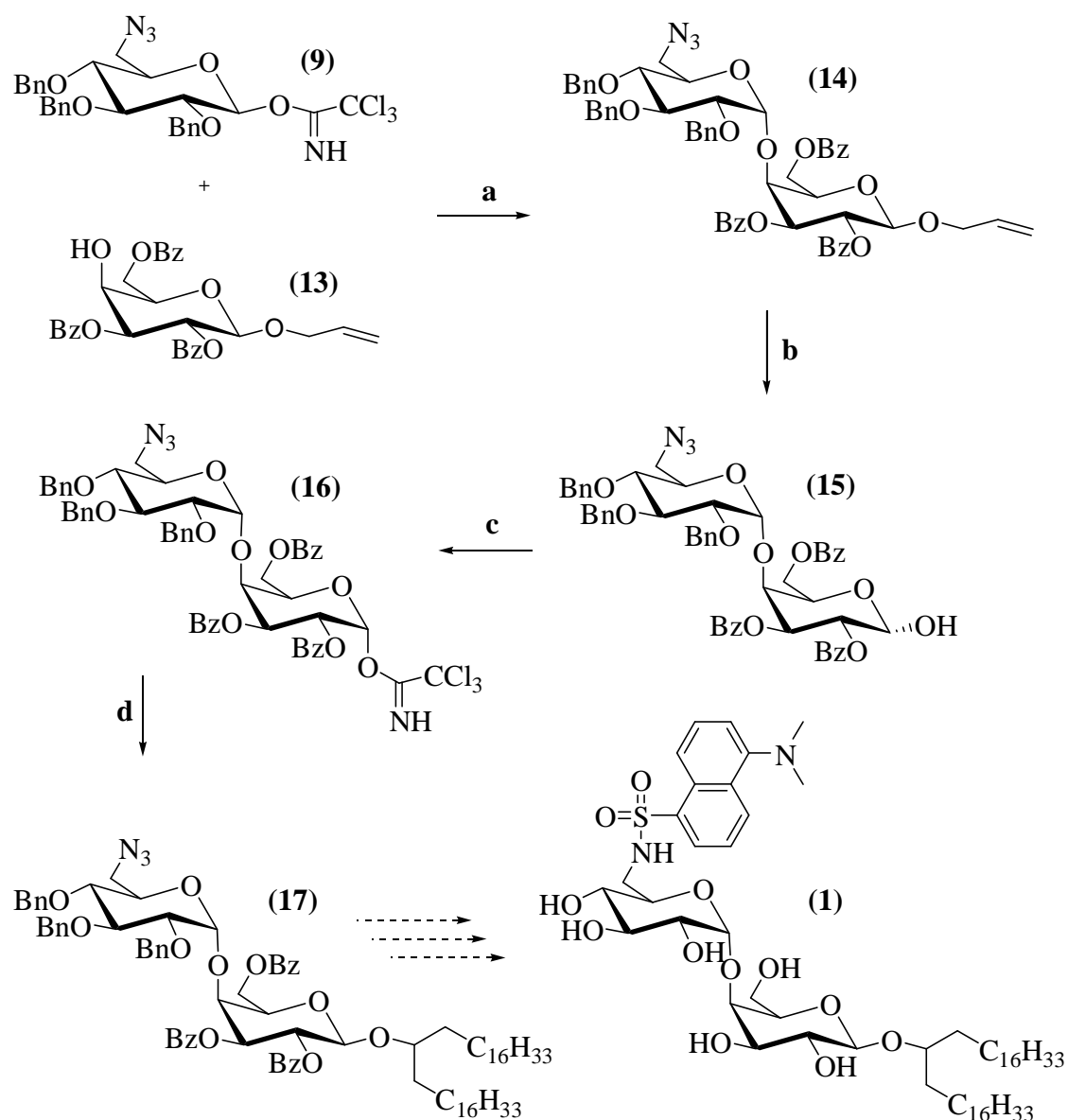
Scheme 4. **a** TMSOTf, Et$_2$O dry, MS 4 Å, -40 °C, 0.5 h (53%). **b**. Ir catalyst, THF, then NBS, H$_2$O, 3 h (71%). **c**. Cl$_3$CCN, DBU, DCM, RT, 20 h (80%). **d**. 18 pentatria-contanol, MS AW300, CHCl$_3$ dry, 0 °C, 0.5 h, then TMSOTf, RT, 0.5 h (83%).

The synthesis of fluorescent simplexide was achivied by the scheme describe above. Compound (**14**) was obtained through glycosylation between the glucosyl donor (**9**) and galactosyl acceptor (**13**) catalyzed with trimethylsilyl trifluoromethansulfonate in dichloromethane (yield 53%). Then, compound (**16**) was achieved by initial formation of intermediate (**15**), obtained through deprotection of the anomeric position of compound (**14**), followed by treatment with trichloroacetonitrile and 1,8-diazabiciclo[5.4.0]undec-ene in dichloromethane (yield 80%). Finally compound (**17**) was obtained by pretreatment of a solution of compound (**16**) and long chain alcohol,

18-pentatria-contanol, in dry chloroform with acidic MS AW300, followed by treatment with a solution of trimethylsilyl trifluoromethansulfonate (yield 83%).

14. EXPERIMENTAL SECTION

General Methods

- Optical rotations were determined on a Perkin-Elmer 241 polarimeter at 20°C.

- All NMR spectra were recorded at 298 K with a Bruker FT-NMR Avance DRX500 spectrometer in CDCl$_3$ or CD$_3$OD solutions with TMS as internal standard.

- The mass spectrometric analyses were performed in electron impact (EI-MS) ionization at an electron energy of 70 eV with a source temperature of 250°C and in negative or positive electrospray (ESI-MS). MS spectra were recorded on a Hewlett-Packard HP-5988-A or a Thermo Quest Finnigan LCQ™deca ion trap mass spectrometer; the mass spectrometer was equipped with a Finnigan ESI interface; data were processed by Finnigan Xcalibur software system.

- All reactions were monitored by TLC on Silica Gel 60 F-254 plates (Merck) with detection by spraying with 50% H$_2$SO$_4$ in MeOH/H$_2$O (1/1) solution or with phosphomolybdate-based reagent and heating to 110 °C. Flash column chromatography was performed on Silica Gel 60 (230-400 mesh, Merck).

- Dry solvents and liquid reagents were distilled prior to use: THF was distilled from sodium; dichloromethane and pyridine were distilled from calcium hydride; DMF, methanol were dried on 4 Å molecular sieves; CHCl$_3$ was put under stirring on calcium chloride, then was filtred and trhough on allumina column (neutr., Typ 507C, 150 mesh, Sigma-Aldrich) and finally were dried on 4 Å molecular sieves.

- All reagents were purchased from Sigma-Aldrich.

Synthesis of Allyl 2,3,4,6-tetra-*O*-acetyl-β-D-glucopyranoside (3)
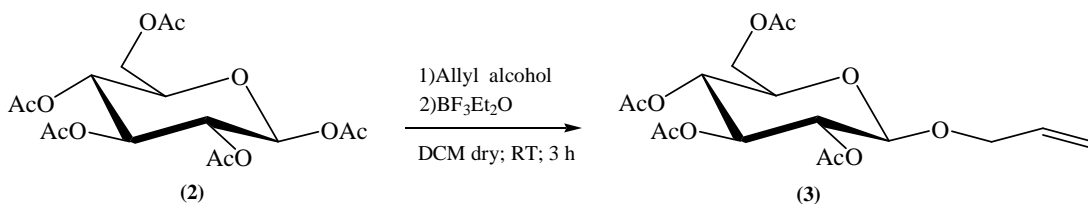
Compound	P(g)	V(ml)	d(g/ml)	M.W.	mmol	Eq
(2)	6			390.27	15.37	1
Allyl alcohol		2.51	0.852	58.08	36.90	2.4
BF$_3$Et$_2$O		5.79	1.13	141.93	46.11	3
CH$_2$Cl$_2$ dry		39				
Theoretical **(3)**	5.96			388.1	15.37	

Boron trifluoride di-ethyl etherate (5.79 ml, 46.11 mmol) was added dropwise to a solution of compound **(2)** (6 g, 15.37 mmol) and allyl alcohol in dry dichloromethane at 0 °C. The ice bath was removed after 0.5 h, and the reaction was allowed to warm to room temperature and kept under stirring until the starting material had been consumed (monitored by TLC). The reaction mixture was quenched with a aqueous saturated sodium bicarbonate solution (200 ml), then was extracted with dichloromethane (3*50 ml). The organic layers were washed with Brine(2*100 ml), drying (Na$_2$SO$_4$) and evaporated under vacuum. The crude residue was chromatographed on silica column with ethyl acetate/petroleum ether 4/6 to afford 3.57 g of compound **(3).** Yield: 60%.

TLC AcOEt/ETP 5/5 Rf **(3)** = 0.52
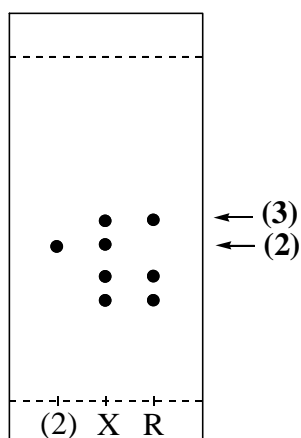
Allyl 2,3,4,6-tetra-*O*-acetyl-β-D-glucopyranoside (3)
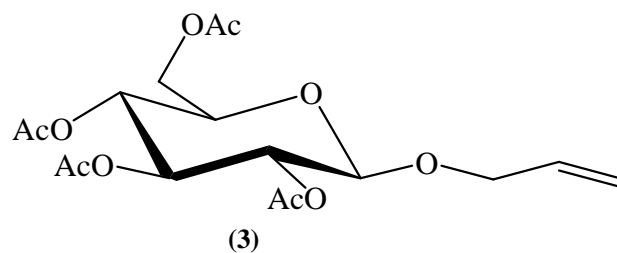
OAc

AcO

AcO

AcO

O

O

(3)

- Amorphous solid

- Mol. Wt. = 388.4

- Exact mass = 388.1

- $C_{17}H_{24}O_{10}$

- This product has been characterised by comparison of its physical data ($[α]_D$, ^{1}H NMR, ^{13}C NMR) with that reported (Kishida et al., 2005).

Synthesis of Allyl-β-D-glucopyranoside (4)
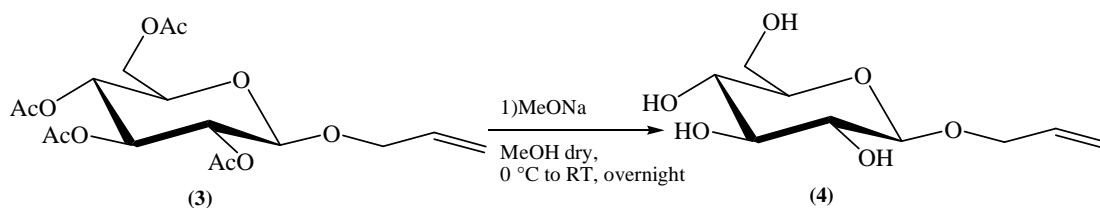
Compound	P(g)	V(ml)	d(g/ml)	M.W.	mmol	Eq
(3)	3.57			388.1	9.19	1
Sol. MeONa 1 M		18.38			18.38	2
MeOH dry		16.0				
Theoretical **(4)**	2.02			220	9.19	

An ice-cold solution of compound **(3)** (3.57 g, 9.19 mmol) in dry MeOH (16 ml) was treated with a freshly prepared solution of sodium methoxide in methanol (18.3 ml sol 1M). The ice bath was removed after 0.5 h, and the reaction was allowed to warm to room temperature and stirred overnight. The reaction mixture was quenched with an ion exchange resin (Dowex Marathon C - H$^+$ form activated). The resin was filtered off and the filtrate was concentrated under vacuum to obtain 2.01 g of compound **(4)**, Yield 99%. Compound **(4)** was used in the next step without further purification.

TLC AcOEt/ETP 5/5 Rf **(4)** = 0   TLC AcOEt/MeOH 9/1 Rf **(4)** = 0.25
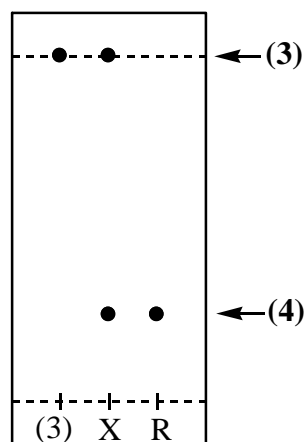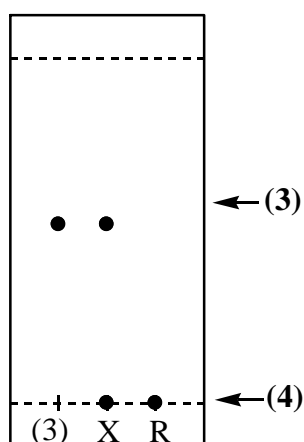
Allyl-β-D-glucopyranoside (4)
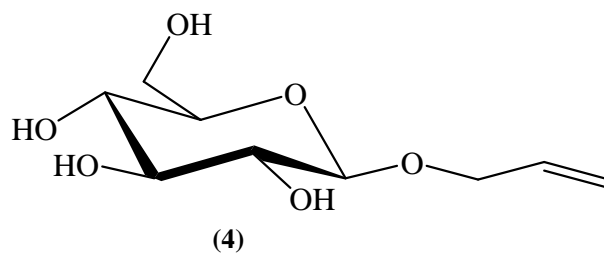
(4)

- Amorphous solid

- Mol. Wt. = 220.2

- Exact mass = 220.1

- $C_9H_{16}O_6$

- This product has been characterised by comparison of its physical data ($[\alpha]_D$, ^1H NMR, ^{13}C NMR) with that reported in (Kishida et al., 2005).

Synthesis of Allyl 6-*O*-tosyl-β-D-glucopyranoside (5)
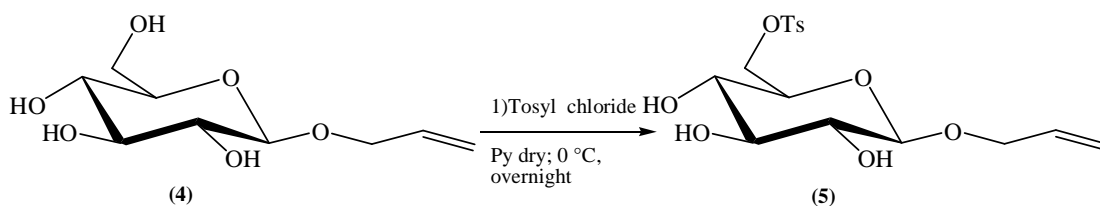
Compound	P(g)	V(ml)	d(g/ml)	M.W.	mmol	Eq
(4)	1,96			220	8.91	1
Tosyl chloride	2,89			190.65	15.15	1.7
Pyridine dry		61				
Theoretical **(5)**	3.33			374.1	8.91	

To a solution of compound **(4)** (1,96 g, 8.91 mmol) in dry pyridine (61 ml) was added 4-toluensulfonyl chloride (2.89 g, 15.15 mmol) at 0 °C. The reaction was stirred at 0 °C overnight. The reaction mixture was quenched with MeOH and pyridine was remove under vacuum. The residue was purified by chromatography with ethyl acetate/methanol 9/1 to afford 2,66 g of compound **(5).** Yield: 80%.

TLC AcOEt/MeOH 9/1 Rf **(5)** = 0.60

Allyl-6-*O*-tosyl-β-D-glucopyranoside (5)

(5)
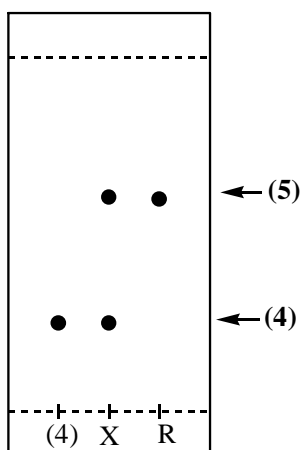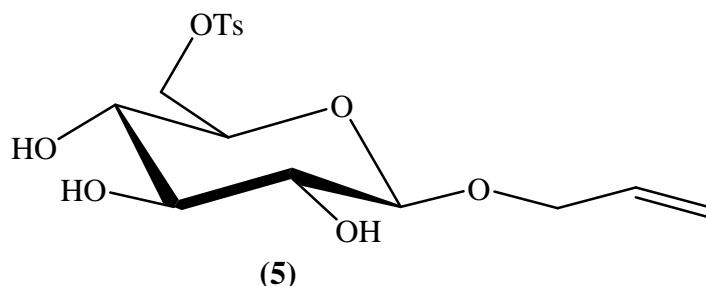
- Amorphous solid

- Mol. Wt. = 374.4

- Exact mass = 374.1

- $C_{16}H_{22}O_8S$

- ^{1}H NMR (500MHz, CDCl$_3$): δ = 2.47 (s, 3 H, CH$_3$), 3.16 (dd, 1 H, J$_{1,2}$ = 8.1, J$_{2,3}$ = 9.2 Hz, H-2), 3.22 (t, 1 H, J$_{3,4}$ = J$_{4,5}$ = 9.2 Hz, H-4), 3.31 (t, 1 H, J$_{2,3}$ = J$_{3,4}$ = 9.2 Hz, H-3), 3.39 – 3.45 (m, 1 H, H-5), 4.01 – 4.10 (m, 1 H, OC*H$_a$*H$_b$CH=CH$_2$), 4,17 (dd, 1 H, J$_{5,6a}$ = 6.1 Hz, J$_{6a,6b}$ = 10.8 Hz, H-6a), 4.18-4.28 (m, 2 H, H-1 and OCH$_a$*H$_b$*CH=CH$_2$), 4.36 (dd, 1 H, J$_{5,6a}$ = 1.7 Hz, J$_{6a,6b}$ = 10.8 Hz, H-6b), 5.14-5.21 (m, 1 H, CH=C*H$_a$*H$_b$), 5.30-5.36 (m, 1 H, CH=CH$_a$*H$_b$*), 5.88-5.99 (m, 1 H, C*H*=CH$_2$), 7.42 -7. 50 (m, 2 H, arom), 7.79 -7.85 (m, 2 H, arom) ppm.

- ^{13}C NMR (CD$_3$OD): δ = 20.2, 69.4, 69.7, 69.8, 73.4, 73.6, 76.5, 101.9, 116.2, 127.7 (2 C), 129.6 (2 C), 133.0, 134.4, 145.1 ppm.

- $[\alpha]_D^{20}$ = - 21,0 (*c* = 1 in methanol)

- ESI-MS (positive-ion mode) : m/z =397.1 (100) [M + Na]$^+$, 770.7 (40) [2M + Na]$^+$

Synthesis of Allyl 6-Azido-6-deoxy-β-D-glucopyranoside (6)
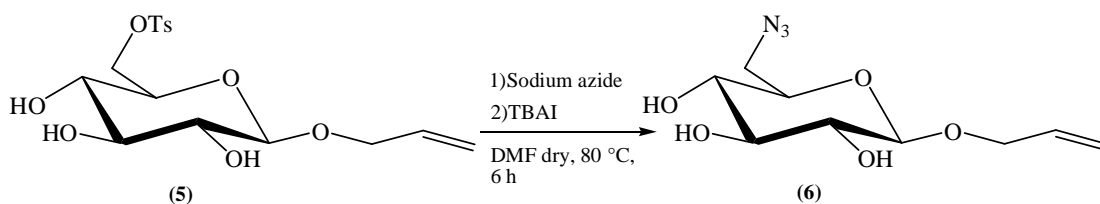
Compound	P(g)	V(ml)	d(g/ml)	M.W.	mmol	Eq
(5)	2.66			374	7,11	1
Sodium azide	1,38			65,01	21.33	3
TBAI	0,52			369,37	0,14	0,02
DMF dry		50				
Theoretical **(6)**	1.74			245.2	7.11	

A mixture of compound **(5)** (2.66 g, 7.11 mmol), sodium azide (1.38 g, 21.33 mmol) and a catalytic amount of tetra-n-butyl-ammonium iodide (0.52 g, 0.14 mmol) in dry DMF (50 ml) was put under stirring at 80 °C. After the reaction was complete (6 h approx.), DMF was removed under high vacuum and the residue was purified through flash column chromatography with dichloromethane/methanol 9/1 to afford 1,57 g of compound **(6).** Yield: 90%.

TLC CH$_2$Cl$_2$/MeOH 9/1 Rf **(6)** = 0.26
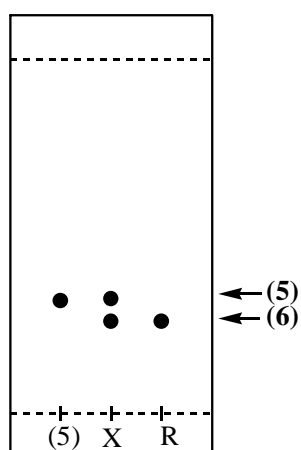
Allyl-6-Azido-6-deoxy-β-D-glucopyranoside (6)

(6)
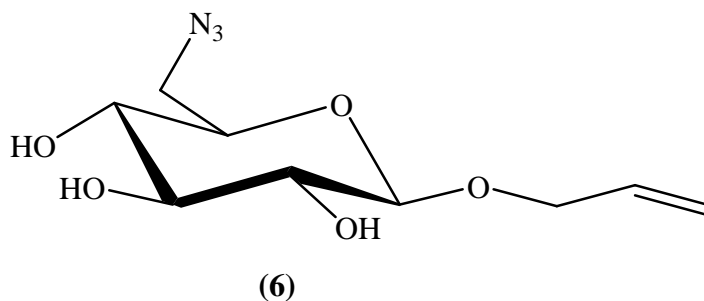
- Amorphous solid

- Mol. Wt. = 245.2

- Exact mass = 245.2

- $C_9H_{15}O_5N_3$

- ^{1}H NMR (500MHz, CD$_3$OD) : δ = 3.19-3.54 (m, 6 H, H-2, H-3, H-4, H-5 and 2 H-6), 4.14–4.21 (m, 1 H, OCH_aH$_b$CH=CH$_2$), 4.31-4.39 (m, 2 H, H-1 and OCH$_a$$H_b$CH=CH$_2$), 5.16-5.23 (m, 1 H, CH=CH_aH$_b$), 5.30-5.38 (m, 1 H, CH=CH$_a$$H_b$), 5.92-6.01 (m, 1 H, C$H$=CH$_2$) ppm.

- ^{13}C NMR (CD$_3$OD): δ = 51.4, 69.7, 71.2, 73.7, 75.7, 76.5, 101.9, 116.2, 134.2 ppm.

- $[\alpha]_D^{20}$ = - 81.5 (c = 1 in methanol)

- ESI-MS (negative-ion mode) : m/z = 243.9 (30) [M - 1]$^-$, 498.0 (100) [2M - 1]$^-$

Synthesis of Allyl 6-azido-6-deoxy-2,3,4-tri-*O*-benzyl-β-D-glucopyranoside (**7**)
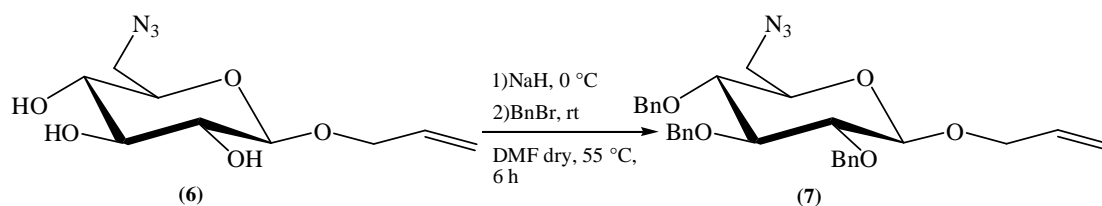
Compound	P(g)	V(ml)	d(g/ml)	M.W.	mmol	Eq
(**6**)	1,5			245	6,12	1
NaH 60%	1,64			23	42,8	7
BnBr	9,42	6,55	1,44	171,04	55,08	9
DMF dry		50				
Theoretical (**7**)	3.15			515.2	6.12	

Sodium hydride (60% in mineral oil, 1,64 g, 42.8 mmol, previously washed three times with n-hexane) was added under anhydrous condition at 0 °C to a solution of compound (**6**) (1.5 g, 6.12 mmol) in dry DMF (50 ml), and the foaming gray reaction was then allowed to warm to room temperature. Benzyl bromide (6.55 ml, 55.08 mmol) was slowly added, and the slurry was then heated at 55 °C and vigorously stirred at this temperature for 6 h. After MeOH had been added to destroy the excess of NaH, the mixture was concentrated under high vacuum, and then diluted with ethyl acetate (100 ml) and washed with water (200 ml). The aqueous layer was further extracted with ethyl acetate (2* 50 ml). The combined organic extract were dried (Na₂SO₄) and concentrated. The residue was purified on flash column chromatography with petroleum ether/ethyl acetate 9/1 to afford 2.84 g of compound (**7**). Yield: 90%.

TLC ETP/AcOEt 9/1 Rf (**7**) = 0.32
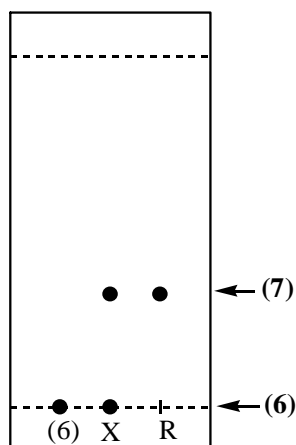
Allyl 6-azido-6-deoxy-2,3,4-tri-*O*-benzyl-β-D-glucopyranoside (7)

(7)
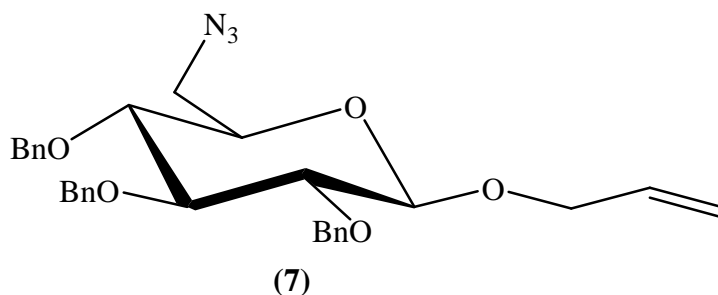
- Amorphous solid

- Mol. Wt. = 515.6

- Exact mass = 515.2

- $C_{30}H_{33}O_5N_3$

- ^{1}H NMR (500MHz, CDCl$_3$) : δ = 3.31-3.73 (m, 6H, H-2, H-3, H-4, H-5 and 2H-6), 4.16 – 4.21 (m, 1 H; OC*H$_a$*H$_b$CH=CH$_2$), 4.43 - 4.48 (m, 1 H, OCH$_a$*H$_b$*CH=CH$_2$), 4.52 (d, 1 H, J$_{1,2}$ = 7.81 Hz, H-1), 4.56 – 5.03 (3 d, 6 H, J = 10.8 Hz, CH$_2$Ph) 5.22-5.28 (m, 1 H, CH=C*H$_a$*H$_b$), 5.35-5.41 (m, 1 H, CH=CH$_a$*H$_b$*), 5.93-6.03 (m, 1 H, C*H*=CH$_2$), 7.24-7,41 (m, 15 H arom.) ppm.

- ^{13}C NMR (CDCl$_3$): δ = 51.5, 70.3, 74.7, 74.9, 75.0, 75.7, 78.4, 82.3, 84.5, 102.5, 117.6, 127.7-128.5 (15 C), 133.8, 137.7, 138.3, 138.4 ppm.

- $[\alpha]_D^{20}$ = + 7,1 (*c* = 1 in chloroform)

- ESI-MS (positive-ion mode) : m/z = 538,1 (100) [M + Na]$^+$

Synthesis of 6-azido-6-deoxy-2,3,4 tri-*O*-benzyl-β-D-glucopyranoside (8)
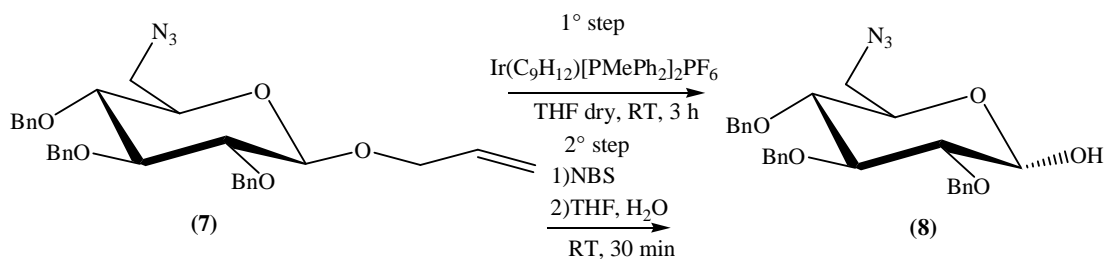
Compound	P(g)	V(ml)	d(g/ml)	M.W.	mmol	Eq
(7)	1			515	1.94	1
Ir(C$_9$H$_{12}$)[PMePh$_2$]$_2$PF$_6$	0.05	10.8 di THF dry		845.79	0.058	0.03
THF dry		23.5				
NBS	0.52			177.99	2.91	1.5
H$_2$O		6.5				
THF		100				
Theoretical **(8)**	0.92			475	1.94	

To a solution of compound **(7)** (1 g, 1,94 mmol) in THF dry (23.5 ml) was added dropwise a solution of Ir catalyst (49 mg, 0.058 mmol in 10.8 ml THF dry), previously activated with hydrogen for 0.5 h, under anhydrous condition at RT, then the reaction mixture was stirred for 3 h at RT. After this time NBS (0.52 g, 2.91 mmol), water (6.5ml) and THF (100 ml) were added and the reaction mixture was stirred for 0.5 h, then the THF was removed under vacuum. The residue was diluted with ethyl acetate, washed with a aqueous saturated sodium bicarbonate solution (200 ml) and Brine (2*100 ml). Drying (Na$_2$SO$_4$) and evaporation of the ethyl acetate layer gave a crude residue that was chromatographed on silica column with ethyl acetate/petroleum ether

4/6 to afford 0.64 g of compound **(8).** Yield: 70%. The identity of the compound was assessed through MS experiment. Compound **(8)** was used in the next step without further characterization.
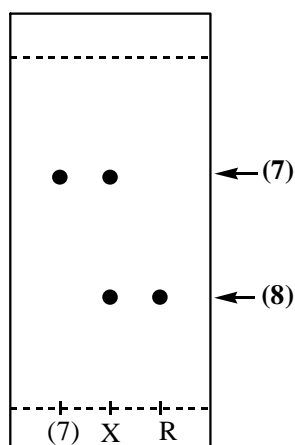
TLC ETP/AcOEt 8/2 Rf **(8)** = 0.32

6-azido-6-deoxy-2,3,4 tri-*O*-benzyl-β-D-glucopyranoside (8)

(8)
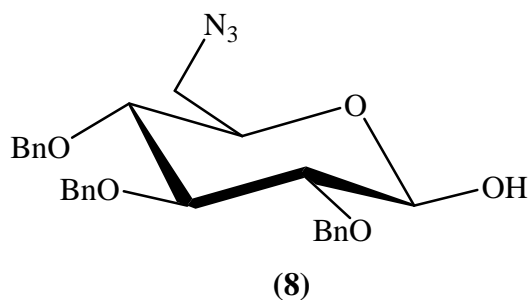
- Amorphous solid

- Mol. Wt. = 475.5

- Exact mass = 475.2

- $C_{27}H_{29}O_5N_3$

- ESI-MS (positive-ion mode) : m/z = 498.2 (100) [M + Na]$^+$, 972.8 (33) [2M + Na]$^+$

Synthesis of 6-azido-6-deoxy-2,3,4-tri-*O*-benzyl β-D-glucopyranosyl trichloroacetimidate (9)
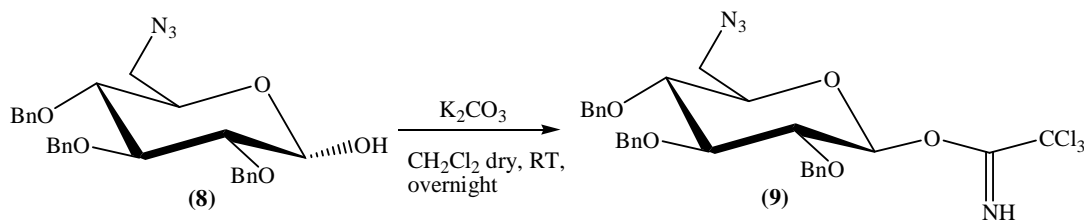
Compound	P(g)	V(ml)	d(g/ml)	PM	mmol	Eq
(8)	0.20			475	0.42	1
Trichloroacetonitrile	0.58	404 µl	1.44	144.39	4.03	9.6
K_2CO_3	0.17			138.21	1.26	3
CH_2Cl_2 dry		3.6				
Theoretical **(9)**	0.26			618	0.42	

Compound **(8)** (0.200 g, 0.42 mmol) was dissolved in dichloromethane dry (3.6 ml). Trichloroacetonitrile (404 µl, 4.03 mmol) and potassium carbonate (0.17 g, 1.26 mmol) were added and the reaction mixture was stirred under argon overnight before being filtered through celite and concentrated. The residue was chromatographed on silica column with ethyl acetate/petroleum ether 1/9 with 1% TEA to afford 0.2 g of compound **(9).** Yield: 77%.

TLC ETP/AcOEt 8/2 Rf **(9)** = 0.54
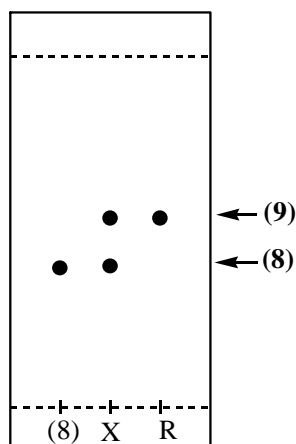
6-azido-6-deoxy-2,3,4-tri-*O*-benzyl β-D-glucopyranosyl trichloroacetimidate (9)

(9)
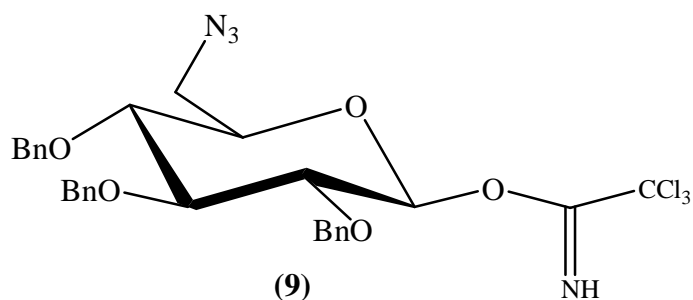
- Colourless oil

- Mol. Wt. = 619.9

- Exact mass = 618.1

- $C_{29}H_{29}O_5N_4Cl_3$

- ^1H NMR (500MHz, CDCl$_3$) : δ = 3.31-3.82 (m, 6H, H-2, H-3, H-4, H-5 and 2H-6), 4.59 – 5.02 (3 d, 6 H, J = 10.8 Hz, CH$_2$Ph) 5.88 (d, 1 H, J$_{1,2}$ = 7.4 Hz, H-1), 7.25-7,39 (m, 15 H arom.), 8.78 (s, 1H, NH) ppm.

- ^{13}C NMR (CD$_3$OD): δ = 50.88, 74.91, 75.13, 75.30, 75.60, 77.2, 77.57, 80.85, 84.37, 97.81,127 -129 (15 C), 137.65, 137.80, 138.24, 160.95 ppm.

- ESI-MS (positive-ion mode) : m/z = 641.0 (100) [M + Na]$^+$, 1260.7 (17) [2M + Na]$^+$

Synthesis of Allyl 2,3,4,6-tetra-*O*-acetyl-β-D-galactopyranoside (11)
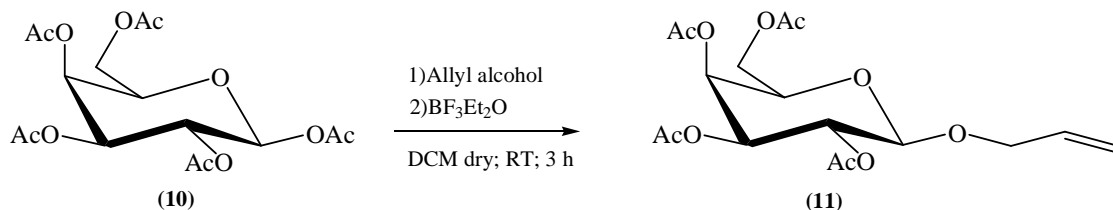
Compound	P(g)	V(ml)	d(g/ml)	M.W.	mmol	Eq
(10)	6			390.27	15.37	1
Allyl alcohol		2.51	0.852	58.08	36.91	2.4
BF$_3$Et$_2$O		5.79	1.13	141.93	46.11	3
CH$_2$Cl$_2$ dry		39				
Theoretical **(11)**	5.96			388	15,37	

Boron trifluoride di-ethyl etherate (5.79 ml, 46,12 mol) was added dropwise to a solution of compound **(10)** (6 g, 15.37 mol) and allyl alcohol (2.51 ml, 36.90 mol) in dry dichloromethane (39 ml) at 0 °C. The ice bath was removed after 0.5 h, and the reaction was allowed to warm to room temperature until the starting material had been consumed (monitored by TLC). The reaction mixture was quenched with a aqueous saturated sodium bicarbonate solution (200 ml), extracted with dichloromethane (3*50 ml), and the combined organic layer were washed with Brine(2*100 ml). Drying (Na$_2$SO$_4$) and evaporation of the solvent gave a crude residue that was purified on flash column chromatography with ethyl acetate/petroleum ether 4/6 to afford 4.17 g of compound **(11).** Yield : 70%.

TLC AcOEt/ETP 5/5 Rf **(11)** = 0.52
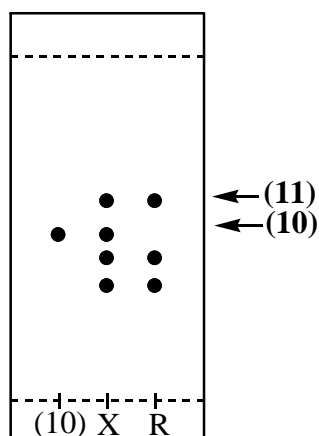
Allyl 2,3,4,6-tetra-*O*-acetyl-β-D-galactopyranoside (11)
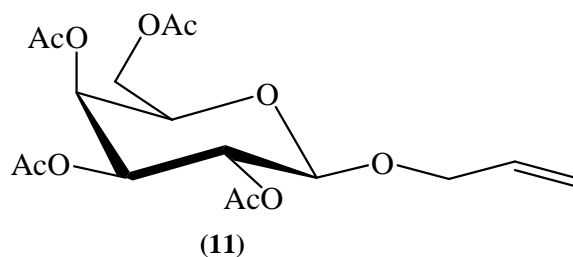
(11)

- Amorphous solid
- Mol. Wt. = 388.4
- Exact mass 388.1
- $C_{17}H_{24}O_{10}$
- This product has been characterised by comparison of its physical data ($[\alpha]_D$, ^{1}H NMR, ^{13}C NMR) with that reported in (Kishida et al., 2005)

Synthesis of Allyl -β-D-galactopyranoside (12)
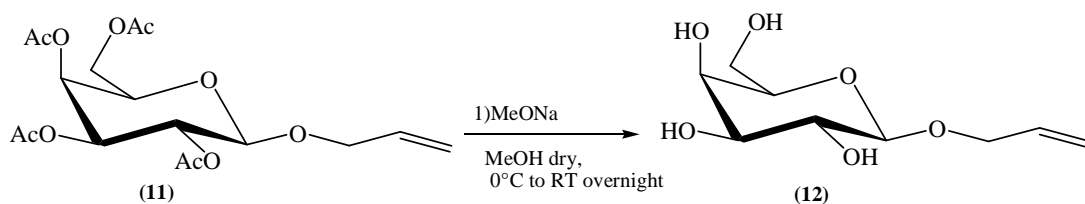
Compound	P(g)	V(ml)	d(g/ml)	M.W.	mmol	Eq
(11)	3.82			388	9.84	1
MeONa sol 1 M		19.6			19.69	2
MeOH dry		78.8				
Theoretical **(12)**	2.16			220	9.84	

An ice-cold solution of compound **(11)** (3.82 g, 9.84 mmol) in dry MeOH (78.8 ml) was treated with a freshly prepared solution of sodium methoxide in methanol (19.6 ml sol 1M). The ice bath was removed after 0.5 h, and the reaction was allowed to warm to room temperature and stirred overnight. The reaction mixture was quenched with an ion exchange resin (Dowex Marathon C – H$^+$ form). The resin was filtered off and the filtrate was concentrated under vacuum to obtain 2.15 g of compound **(12)**, Yield 99%. Compound **(12)** was used in the next step without further purification.

TLC AcOEt/ETP 5/5 Rf **(12)** = 0   TLC AcOEt/MeOH 9/1 Rf **(12)** = 0.25
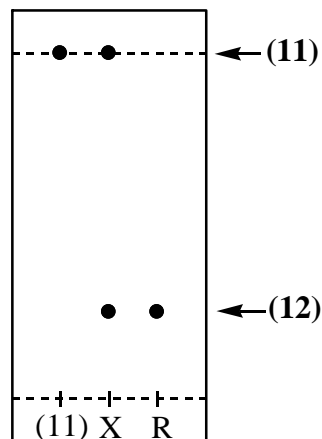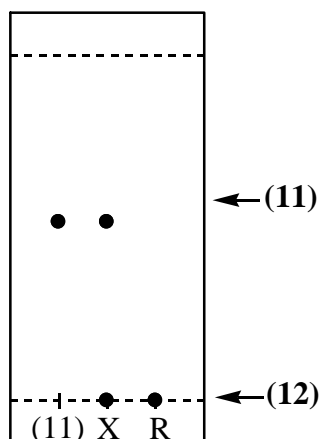
Allyl-β-D-galattopyranoside (12)
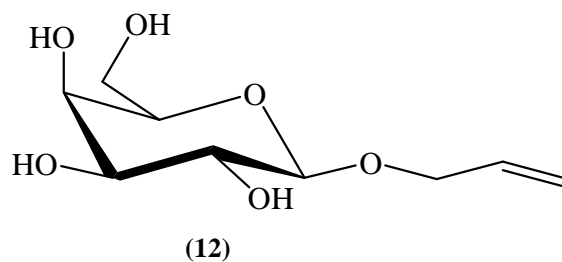
(12)

- Amorphous solid
- Mol. Wt. = 220.2
- Exact mass 220.1
- $C_9H_{16}O_6$
- This product has been characterised by comparison of its physical data ($[\alpha]_D$, ^{1}H NMR, ^{13}C NMR) with that reported (Dasgupta et al., 1994).

Synthesis of Allyl 2,3,6-tri-*O*-benzoyl-β-D-galactopyranoside (13)
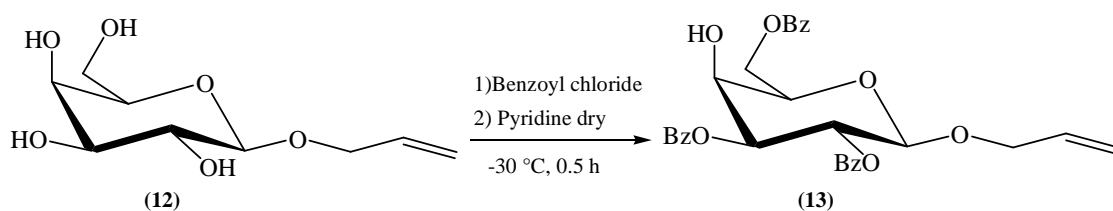
Compound	P(g)	V(ml)	d(g/ml)	M.W.	mmol	Eq
(12)	0.15			220	0.68	1
Benzoyl chloride		0.356 in 5 ml of Py dry	1.21	140.57	3.07	4.5
Py dry		5				
Theoretical **(13)**	0.36			532	0.68	

A solution of benzoyl chloride in pyridine (356 μl, 3.07 mmol) was added dropwise to a solution of compound **(12)** (0.15 g, 0.68 mmol) in dry Pyridine (5 ml) at -30 °C. After 0.5 h the reaction mixture was quenched with an aqueous saturated sodium bicarbonate solution (200 ml), extracted with dichloromethane (3*50 ml), and the combined organics were washed with Brine (2*100 ml). Drying (Na$_2$SO$_4$) and evaporation of dichloromethane gave a crude residue that was chromatographed first with toluene/ethyl acetate 8/2, to remove the allyl 2,3,4,6-tetra-*O*-benzoyl-β-D-galattopyranoside, and then with hexane/ethyl acetate 75/25 to afford 0.181 g of compound **(13)**. Yield : 50%.

TLC toluene/ethyl acetate 8/2 Rf **(13)** = 0.51
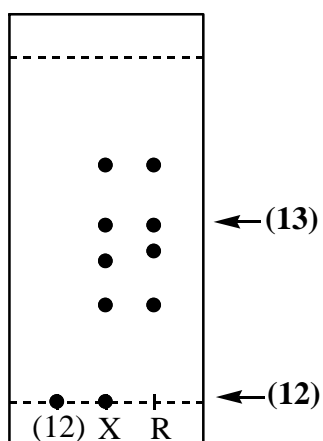
Allyl 2,3,6-tri-*O*-benzoyl-β-D-galactopyranoside (13)

(13)
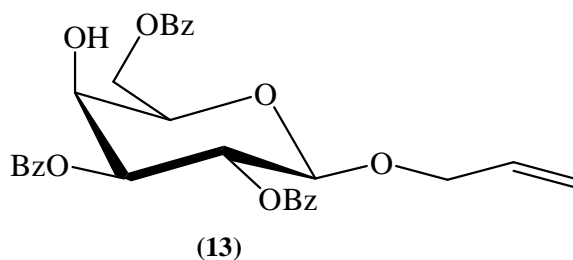
- Amorphous solid
- Mol. Wt. = 532.5
- Exact mass = 532.2
- $C_{30}H_{28}O_9$
- ^{1}H NMR (500MHz, CDCl$_3$): δ = 2.60 (d, 1 H, J = 5.4 Hz, OH), 4.09 (dd, 1 H, $J_{4,5}$ = $J_{5,6}$ = 6.5 Hz, H-5), 4.16–4.23 (m, 1 H, OCH_aH$_b$CH=CH$_2$), 4.34-4.43 (m, 2 H, OCH$_a$$H_b$CH=CH$_2$ and H-4), 4.65 (dd, 1 H, $J_{5,6a}$ = 6.5, $J_{6a,6b}$ = 11.4 Hz, H-6a), 4.72 (dd, 1 H, $J_{5,6b}$ = 6.5, $J_{6a,6b}$ = 11.4 Hz, H-6b), 4.81 (d, 1 H, $J_{1,2}$ = 7.9 Hz, H-1), 5.11-5.17 (m, 1 H, CH=CH_aH$_b$), 5.21-5.27 (m, 1 H, CH=CH$_a$$H_b$), 5.38 (dd, 1 H, $J_{2,3}$ = 10.3, $J_{3,4}$ = 3.2 Hz, H-3), 5.77–5.89 (m, 2 H, CH=CH$_2$ and H-2), 7.36–7.64 (m, 10 H, arom.), 7.96–8.12 (m, 5 H, arom.) ppm.
- ^{13}C NMR (CD$_3$OD): δ = 62.7, 67.3, 69.6, 69.9, 72.3, 74.2, 100.1, 117.7, 128.3 – 133.5 (19 C), 165.3, 165. 9, 166.4.
- $[\alpha]_D^{20}$ = + 56.5 (*c* = 1 in chloroform)
- ESI-MS (positive-ion mode) : m/z = 555.1 (52) [M + Na]$^+$, 1087.0 (100) [2M + Na]$^+$

Syntesis of Allyl 6-azido-6-deoxy-2,3,4-tri-*O*-benzyl-α-D-glucopyranosyl-(1→4)-2,3,6-tri-*O*-benzoyl-β-D-galactopyranoside (14)
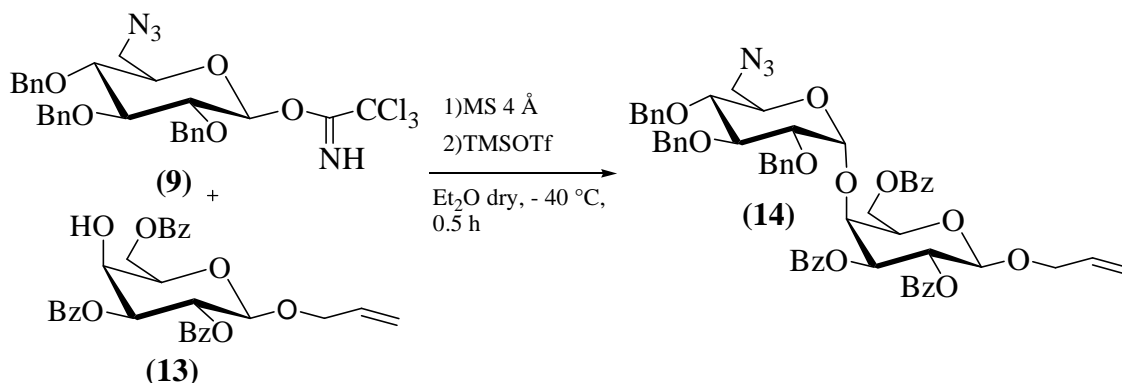
Compound	P(g)	V(ml)	d(g/ml)	P.M.	mmol	Eq
(9)	1,63			618.1	2.64	2
(13)	0.70			532.1	1.32	1
Sol. 0.1 M TMSOTf		2.56			0.26	0.2
MS 4 Å	1.63					
Et₂O dry		40				
Theoretical (14)	1.30			989.1	1.32	

Trimethylsilyl trifluoromethansulfonate (2.56 ml, sol 0.1M) was added dropwise to a cooled solution of compound **(9)** (1.63 g, 2.64 mmol), compound **(13)** (0.70 g, 1.32 mmol) and molecular sevies 4 Å (1.63 g) in dry diethyl ether (40 ml). The reaction mixture was quenched after 0.5 h with a solid sodium bicarbonate before being filtered through celite and concentrated. The residue was chromatographed on silica column with ethyl acetate/hexane 15/85 to afford 0.69 g of compound **(14).** Yield: 53%.

TLC AcOEt/Hex 15/85 Rf **(14)** = 0.36
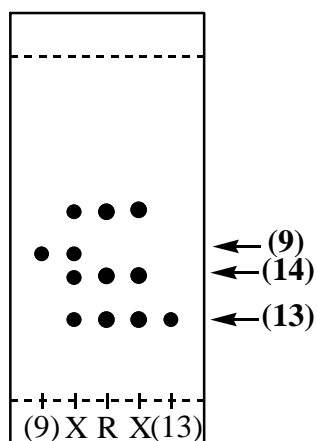
Allyl 6-azido-6-deoxy-2,3,4-tri-*O*-benzyl-α-D-glucopyranosyl-(1→4)-2,3,6-tri-*O*-benzoyl-β-D-galactopyranoside (14)
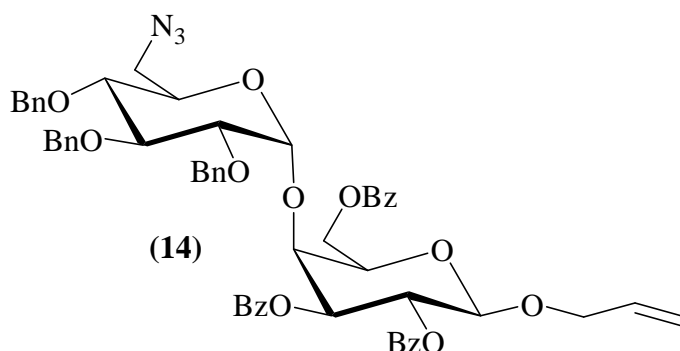
- Amorphous solid

- Mol. Wt. = 990.1

- Exact mass = 989.4

- $C_{57}H_{55}O_{13}N_3$

- ^1H NMR (500MHz, CDCl$_3$): δ = 3.14–3.25 (m, 2 H, 2 H-6$^'$), 3.52 (dd, 1 H, $J_{1',2'}$ = 3.4, $J_{2',3'}$ = 9.8 Hz, H-2$^'$), 3.61 (dd, 1 H, $J_{3',4'}$ = $J_{4',5'}$ = 9.6 Hz, H-4$^'$), 4.05 (t, 1 H, $J_{4',5'}$ = $J_{5',6'}$ = 6.6, H-5$^'$), 4.13–4.25 (m, 3 H, H-3$^'$, H-5$^'$ and OCH_aH$_b$CH=CH$_2$), 4.36–4.43 (m, 2 H, H-4 and OCH$_a$$H_b$CH=CH$_2$), 4.58–4.78 (m, 6 H, 2 H-6, H-1, 3 CH$_2$Ph), 4.88 (d, 1 H, $J_{1',2'}$ = 3.4 Hz, H-1$^'$), 4.92-5.06 (m, 3 H, 3 CH$_2$Ph), 5.10–5.15 (m, 1 H, CH=CH_aH$_b$), 5.20-5.27 (m, 1 H, CH=CH$_a$$H_b$), 5.29 (dd, 1 H, $J_{2,3}$ = 10.6, $J_{3,4}$ = 2.9 Hz, H-3), 5.73 (dd, 1 H, $J_{1,2}$ = 7.8, $J_{2,3}$ = 10.6 Hz, H-2), 5.78-5.88 (m, 1 H, CH=CH$_2$), 7.11–7.65 (m, 24 H, arom), 7.93–8.09 (m, 6 H, arom) ppm.

- ^{13}C NMR (CDCl$_3$): δ = 50.68, 63.0, 69.7, 70.0, 71.1, 72.8, 73.8, 74.0, 75.1, 75.6, 76.0, 77.9, 80.2, 80.2, 81.4, 99.9, 100.1, 117.8, 127.6–133.6 (33 C), 137.9, 138.3, 138.7, 165.4, 166.1, 166.2 ppm.

- $[\alpha]_D^{20}$ = + 94.3 (*c* = 1 in chloroform)

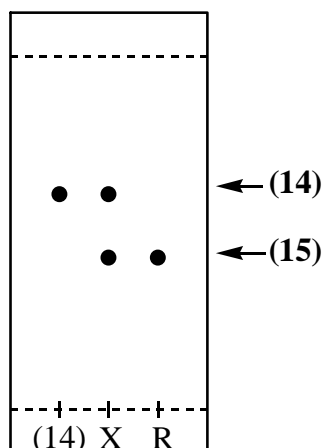- ESI-MS (positive-ion mode) : m/z = 1012.3 (100) [M + Na]$^+$

Synthesis of 6-azido-6-deoxy-2,3,4-tri-*O*-benzyl-α-D-glucopyranosyl-(1→4)-2,3,6-tri-*O*-benzoyl-D-galactopyranoside (15)
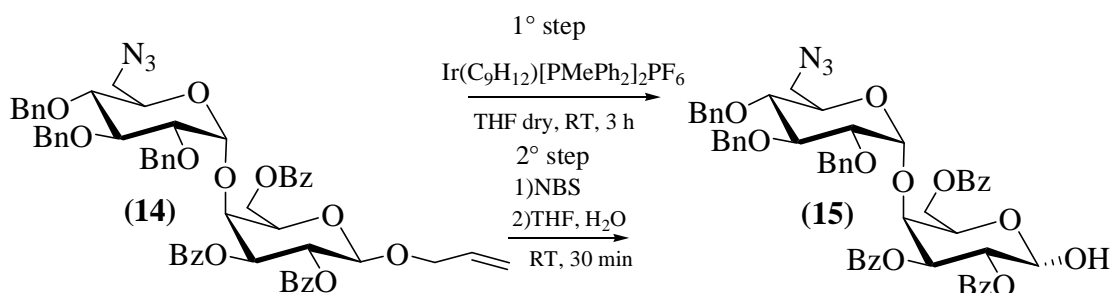
Compound	P(g)	V(ml)	d(g/ml)	P.M.	mmol	Eq
(14)	0.67			989.4	0.68	1
$Ir(C_9H_{12})[PMePh_2]_2PF_6$	0.017	3.7 di THF dry		845.79	0.02	0.03
THF dry		15.7				
NBS	0.18			177.99	1.02	1.5
H_2O		2.27				
THF		34.9				
Theoretical **(15)**	0.645			949	0.68	

To a solution of compound **(14)** (0.67 g, 0.68 mmol) in THF dry (15.7 ml) was added dropwise under anhydrous condition at RT a solution of Ir catalyst (17 mg, 0.0203 mmol in 3.7 ml THF dry), previously activated with hydrogen for 0.5 h, under anhydrous condition at RT, then the reaction mixture was stirred for 3 h at RT. After this time NBS (0.18 g, 1.02 mmol), water (2.27 ml) and THF (34.9 ml) were added and the reaction mixture was stirring for 0.5 h, then the THF was removed under vacuum. The residue was diluted with ethyl acetate (100 ml), washed with a aqueous saturated sodium bicarbonate solution (100 ml) and Brine(2*100 ml). Drying (Na_2SO_4) and

evaporation of the ethyl acetate layer gave a crude residue that was chromatographed on silica column with ethyl acetate/petroleum ether 2/8 to afford 0.445 g of compound **(15).** Yield: 71%. The identity of the compound was assessed through MS experiment. Compound **(15)** was used in the next step without further characterization.
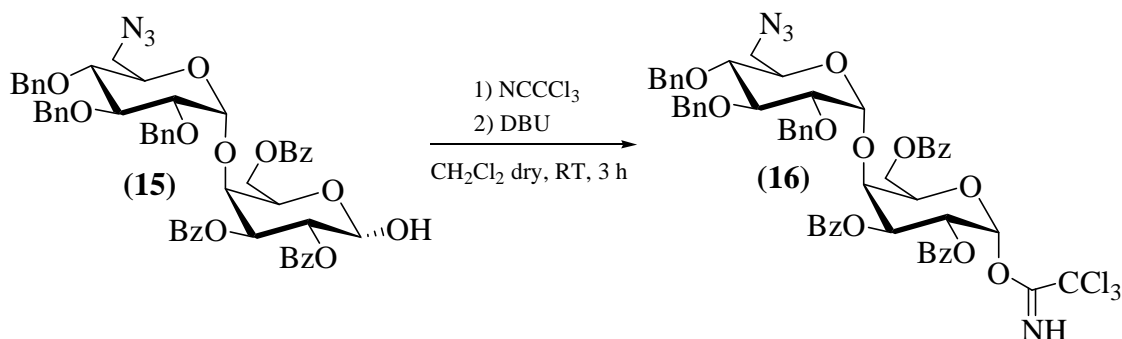
TLC AcOEt/ETP 5/5 Rf **(15)** = 0.4

6-azido-6-deoxy-2,3,4-tri-*O*-benzyl-α-D-glucopyranosyl-(1→4)-2,3,6-tri-*O*-benzoyl-D-galactopyranoside (15)
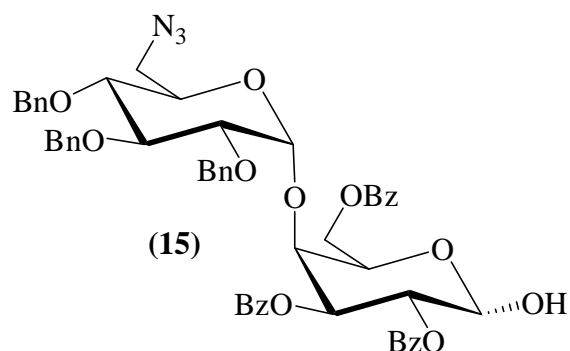
- Amorphous solid

- Mol. Wt. = 950

- Exact mass = 949.3

- $C_{54}H_{51}O_{13}N_3$

- ESI-MS (positive-ion mode) : m/z = 972.3 (100) $[M + Na]^+$, 1921.3 (12) $[2M + Na]^+$

Synthesis 6-azido-6-deoxy-2,3,4-tri-*O*-benzyl-α-D-glucopyranosyl-(1→4)-2,3,6-tri-*O*-benzoyl-α-D-galactopyranosyl trichloroacetimidate (16)

Compound	P(g)	V(ml)	d(g/ml)	PM	mmol	Eq
(15)	0.445			949.3	0.468	1
Trichloroacetonitrile	0.649	450 µl	1.44	144.39	4.500	9.6
DBU		5 µl				
CH$_2$Cl$_2$ dry		5				
Theoretical **(16)**	0.511			1092	0.468	

Compound **(15)** (0.445 g, 0.468 mmol) was dissolved in CH$_2$Cl$_2$ dry (5 ml). Trichloroacetonitrile (0.450 ml, 4.500 mmol) and DBU (5µl) were added and the reaction mixture was stirred under argon for 3 h before being filtered through celite and concentrated. The residue was chromatographed on silica column with ethyl acetate/petroleum ether 2/8 with 1% TEA to afford 0.408 g of compound **(16).** Yield: 80%.

TLC AcOEt/ETP 5/5 Rf **(16)** = 0.46
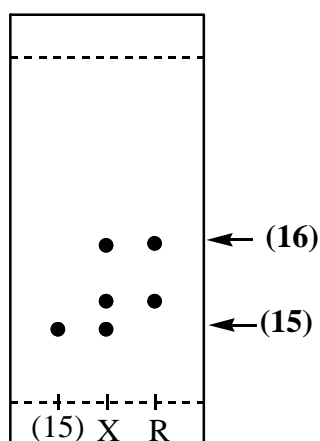
6-azido-6-deoxy-2,3,4-tri-*O*-benzyl-α-D-glucopyranosyl-(1→4)-2,3,6-tri-*O*-benzoyl-α-D-galactopyranosyl trichloroacetimidate (16)
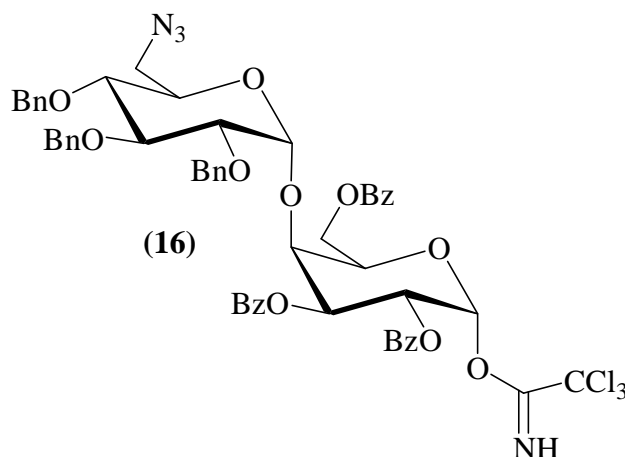
- Colourless oil

- Mol. Wt. = 1094.2

- Exact mass = 1092.3

- $C_{56}H_{51}O_{13}N_3Cl_3$

- ^{1}H NMR (500MHz, CDCl$_3$): δ = 3.07 – 3.17 (m, 2 H, 2 H-6$^{'}$), 3.55 (dd, 1 H, $J_{1',2'}$ = 3.3, $J_{2',3'}$ = 9.8 Hz, H-2$^{'}$), 3.61 (dd, 1 H, $J_{3',4'}$ = $J_{4',5'}$ = 9.5 Hz, H-4$^{'}$), 4.11–4.23 (m, 2 H, H-3$^{'}$ and H-5$^{'}$), 4.56 (d, 1 H, $J_{3,4}$ = 2.6 Hz), 4.58–4.83 (m, 6 H, H-5, 2 H-6, 3 CH$_2$Ph), 4.89 (d, 1 H, $J_{1',2'}$ = 3.4 Hz, H-1$^{'}$), 4.92–5.11 (m, 3 H, 3 CH$_2$Ph), 5.82 (dd, 1 H, $J_{2,3}$ = 10.9, $J_{3,4}$ = 2.6 Hz, H-3), 5.94 (dd, 1 H, $J_{1,2}$ = 3.7, $J_{2,3}$ = 10.9 Hz, H-2), 6.80 (d, 1 H, $J_{1,2}$ = 3.7 Hz, H-1), 7.10–7.65 (m, 24 H, arom), 7.92–8.06 (m, 6 H, arom), 8.59 (s, 1 H, NH) ppm

- ^{13}C NMR (CDCl$_3$): δ = 50.7, 63.1, 67.5, 70.5, 71.2, 71.6, 74.3, 75.2, 75.6, 76.2, 77.2, 78.0, 80.1, 81.4, 94.0, 99.7, 127.6-130.0 (30 C), 133.2, 133.4, 133.6, 137.7, 138.1, 138.5, 160.6, 165.5, 165.9, 166.0.

- $[\alpha]_D^{20}$ = + 121.1 (*c* = 1 in chloroform)

- ESI-MS (positive-ion mode) : m/z = 1115.0 (100) and 1116.9 (96) [M + Na]$^+$

Synthesis of 18-Pentatriacontanyl 6-azido-6-deoxy-2,3,4-tri-*O*-benzyl-α-D-glucopyranosyl-(1→4)-2,3,6-tri-*O*-benzoyl-β-D-galactopyranoside (17)
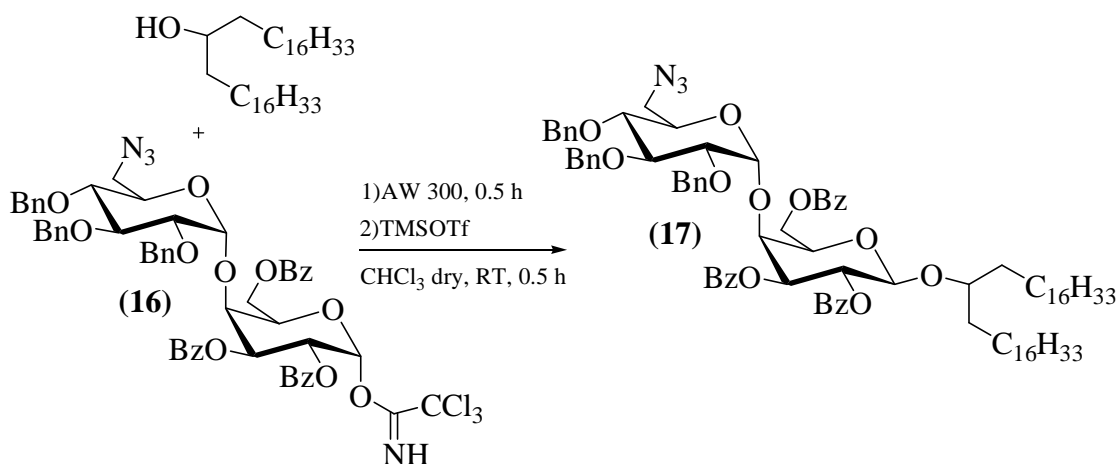

Compound	P(g)	V(ml)	d(g/ml)	PM	mmol	Eq
(16)	0.330			1092.3	0.302	1
18-Pentatriacontanol	0.230			508.6	0.453	1.5
MS AW-300	2.44					
CHCl$_3$ dry*		13.5				
Sol. 0.1 M TMSOTf		0.6			0.060	0.2
Theoretical **(17)**	0.434			1439.9	0.302	

* Chloroform was treated with calcium chloride under argon overnight to remove the presence of ethanol, then was filtered and through on alumina column, to remove the presence of acidity, and finally dried on MS 4 Å.

A solution of compound **(16)** (0.330 g, 0.302 mmol), 18-pentatriacontanol (0.230 g, 0.453 mmol) and MS AW300 (2.44 g) in chloroform dry (13.5 ml) was stirred for 0.5 h a RT under argon, and than cooled to 0 °C. Trimethylsilyl trifluoromethansulfonate (0.6 ml) was added and the stirring was continued for 0.5 h at RT. The reaction mixture was quenched with TEA and solid were filtred off with celite and washed with chloroform. The organic layer was concentrated, the excess of alcohol was cristallized with Et$_2$O and separated by filtration.The organic layer was concentrated and the crude was chromatographed on silica column with n-hexan/dichloromethane/ethyl acetate 8.5/1/0.5 to afford 0.364 g of compound **(17)**. Yield: 83 %.
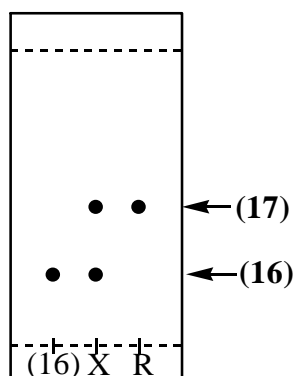
TLC Hex/CH$_2$Cl$_2$/AcOEt 8.5/1/0.5 Rf **(17)** = 0.47

18-Pentatriacontanyl 6-azido-6-deoxy-2,3,4-tri-*O*-benzyl-α-D-glucopyranosyl-(1→4)-2,3,6-tri-*O*-benzoyl-β-D-galactopyranoside (17)
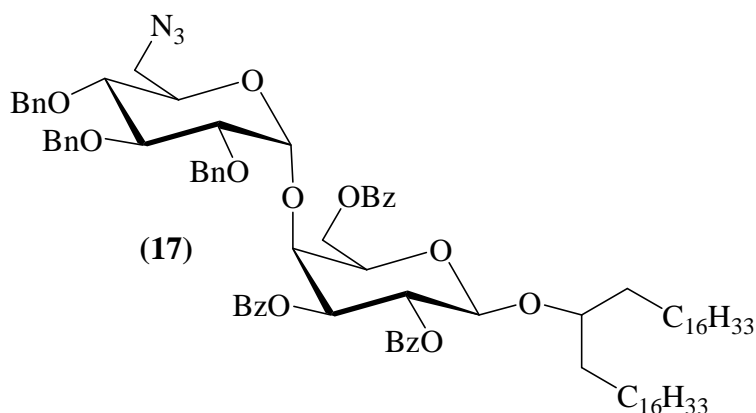
- Colourless oil

- Mol. Wt. = 1440.9

- Exact mass = 1439.9

- $C_{89}H_{121}O_{13}N_3$

- ^{1}H NMR (500MHz, CDCl$_3$) : δ = 0.73–1.76 (m, 70 H, aliphatic), 3.12–3.26 (m, 2 H, 2 H-6$^'$), 3.47–3.66 (m, 3 H, H-2$^'$, H-4$^'$ and OCH), 4.03 (t, 1H, $J_{4,5} = J_{5,6} = 6.3$ Hz, H-5), 4.14-4.26 (m, 2 H, H-3$^'$, H-5$^'$), 4.37 (d, 1 H, $J_{3,4} = 2.6$ Hz, H-4), 4.57 – 4.82 (m, 6 H, H-1, 2 H-6 and 3 CH$_2$Ph), 4.87 (d, 1 H, $J_{1',2'} = 3.4$ Hz, H-1$^'$), 4.90 – 5.07 (m, 3 H, 3 CH$_2$Ph), 5.29 (dd, 1 H, $J_{2,3} = 10.7$, $J_{3,4} = 2.6$ Hz, H-3), 5.67 (dd, 1 H, $J_{2,3} = 10.7$, $J_{1,2} = 7.8$ Hz, H-2), 7.10-7.64 (m, 24 H, arom), 7.91-8.09 (m, 6 H, arom) ppm.

- ^{13}C NMR (CD$_3$OD): δ = 14.1, 22.7 – 35.0 (33 C), 50.7, 63.3, 70.0, 71.0, 72.7, 73.9, 74.0, 75.1, 75.6, 76.2, 78.0, 80.3, 81.4, 82.4, 99.9, 101.7, 127.6 – 129.9 (30 C), 133.0, 133.1, 133.5, 138.0, 138.3, 138.7, 165.2, 166.1, 166.2.

- $[\alpha]_D^{20} = + 79.1$ (*c* = 1 in chloroform)

- ESI-MS (positive-ion mode) : m/z = 1463.7 (100) [M + Na]$^+$, 1478,7 (33) [M + K]$^+$

15. CONCLUSION

The aim of this work was to prepare a fluorescent analogue of simplexide to evaluate the subcellular distribution of the glycolipid and to clarify its mechanism of action.

The synthetic approach has been develop in order to obtain fluorescent simplexide through glycosylation between the preformed activated disaccharide (14) and the lipid moiety. The disaccharide in turn was obtained by glycosylation between a glucosyl donor (9) selectively functionalized with an azido group at position 6 and a galactoside acceptor(13).

The galactoside acceptor was achieved in a few steps for the reason that we used a protocol for selective benzoylation, at low temperature, that allowed us to avoid tedians step of protection and deprotection of the hydroxyl group to obtain the final product.

Furthermore, several studies have been conducted on the reaction of glycosylation between the two sugar moieties as reported in the table 3.

Table 3 . Study of glycosilation between the glucosyl donor and galactosyl acceptor.

GLUCOSYL DONOR	GALACTOSYL ACCEPTOR	CONDITION (1 h)	YELD OF (14) (%)
(9)	(13)	TMSOTf / DCM / -40 °C	25
		TMSOTf / DCM / -40 °C / MS 4 Å	25
		TMSOTf / DCM / 0°C	15
		TMSOTf / THF / -40 °C	< 5
		TMSOTf / THF / 0 °C	< 5
		TMSOTf / Et$_2$O / -40 °C / MS 4 Å	55
		BF3Et2O / Et$_2$O / -40 °C / MS 4 Å	< 10
		BF$_3$Et$_2$O / DCM / -40 °C	< 10
		TESOTf / DCM / -40 °C	20

We tried different conditions and finally we were able to select a protocol that has allowed us to obtain, using dry diethyl ether as the solvent and a solution of trimethylsilyl trifluoromethansulfonate as the catalyst, disaccharide (14) in good yields and high selectivities.

In addition, the dissaccaride (14), after activation of anomeric position, was glycosylated with a long chain alcohol to obtain the intermediate (17) in very satisfactory yield if compared to the few examples described in the literature.

16. FUTURE AND PROSPECTIVE

Starting from compound **(17)** the synthesis of final product **(1)** will be carried out using standard deprotection procedures, to remove the protective groups, then will be reduced the azido group, through Staudinger reaction, to obtain the corresponding amine which finally will be combined with the flourescent probe.

This compound will be used for study of subcellular distribution and also to clarify the mechanism of action of simplexide.

17. LIST OF ABBREVIATIONS

AAG   1-*O*-alkyl-2-*O*-acyl-*sn*-glycerol

AcOEt   Ethyl Acetate

AMPs   Antimicrobial peptides

APC   Antigen presenting cell

APM   Anterior plasma membrane

AR   Acrosome reaction

ASA   Arylsulfatase A

BF_3Et_2O Boron trifluoride di-ethyl etherate

BSA   Bovine serum albumin

CAD   Collisionally activated dissociation

CAMP   Cathelicidin antimicrobial peptide gene

cAMP   Cyclic adenosine monophosphate

CGT   Ceramide galactosyltransferase

CHO   Chinese hamster ovary cells

CMV   Ciïytomegalovirus

CST   Cerebroside sulfotransferase

DCM   Dichloromethane

DBU   1,8-diazabiciclo[5.4.0]undec-ene

DMF   *N*,*N*-dimethylformamide

ECL   Enhanced chemiluminescence

EDTA   Ethylenediaminetetraacetic acid

ELISA   Enzyme-linked immunosorbent assay

ER   Endoplasmic reticuli

ESI   Electrospray ionization

ETP   Petroleum Ether

FMP	Forward motility protein
FRLP-1	Formyl peptide receptor-1
GC	galactosylceramide
GG	galactosylglycerolipid
hCG	Human chorionic gonadrotropin
HIV	Human immunodeficiency virus
HPTLC	High performance thin layer chromatography
HTF	Human tubal fluid
HTF-HEPES	HEPES-buffered Human tubal fluid
HRP	Horseradish peroxidase
HSP	Heat shock protein
IB	Immunoblotting
IgG	Immunoglobulin G
IIF	Indirect immunofluorescence
IL	Interleukine
KRB	Krebs Ringers bicarbonate
KRB-HEPES	HEPES-buffered Krebs Ringers bicarbonate
LTB4	Leukotriene B4
LPS	Lipopolysaccharide
MeOH	Methanol
MeONa	Sodium Methoxyde
MLD	Metachromatic leukodystrophy
MS	Mass spectrometry
MS	Molecular sevies
NBS	*N*-bromosuccinimide
mZP	mouse zona(e) pellucida(e)

NMR	Nuclear magnetic resonance
NK	Natural killer cells
OPD	*o*-phenylenediamine dihydrochloride
PAP	3'-phosphoadenosine-5'-phosphate
PAPS	3'-phosphoadenosine-5'-phosphosulfate
PBMC	Peripheral blood mononuclear cell
PBS	Phosphate-buffered saline
PC	3-*sn*-glycerophosphorylcholine
PGC	Percoll gradient centrifuged
PKA	Protein kinase A
PMSG	Pregnant Mare Serum Gonadrotropin
PS	3-*sn*-glycerophosphorylserine
PUFA	Polyunsaturated fatty acid
Py	Pyridine
PVP	Polyvinylpyrrolidone
RT	Room temperature
SDS	Sodium dodecyl sulfate
SDS-PAGE	Sodium dodecyl sulfate-polyacrylamide gel electrophoresis
SGC	sulfogalactosylceramide
SGG	seminolipid
STD	Sexual transmitted disease
STI	Sexual transmitted infectious
TBAI	Tetra-n-butylammoniun iodide
TBS	Tris-buffered saline
TEA	Triethylammine
TLC	Thin layer chromatography

TMSOTf	Trimethylsilyl trifluoromethansulfonate
TNF-α	Tumor necrosis factor-alpha
UDP	Uridine diphosphate
UDP-Gal	Uridine diphosphate galactose
X	Molar ratio
WHO	Word Healt Organizzation
ZP	Zona(e) pellucida(e)

18. REFERENCES

Acott,T.S. et al., **1983**, *Biol. Reprod.*, 29:389-399.

Agerberth,B. et al., **1995**, *Prot. Natl. Acad. Sci. U.S.A.*, 92:195-199.

Agerberth,B. et al., **1999**, *Am. J. Respir. Crist. Care Med.*, 160:283-290.

Ahnonkitpanit,V. et al., **1999**, *Biology of Reproduction*, 61:749-756.

Alberts,B. et al., **2002**, *Molecular Biology of the Cell.* (New York: Garland).

Bajorath,J. et al., **1994**, *Biochemistry*, 33:1332-1339.

Bals,R. et al., **1998**, *Proc. Natl. Acad. Sci. U.S.A.*, 95:9541-9546.

Bals.R, et al., **2001**, *Clin. Diagn. Lab. Immunol.*, 8:370-375.

Bals,R. and Wilson,J.M., **2003**, *Cell. Mol. Life Sci.*, 60:711-720.

Berube,B. et al., **1996**, *Journal of Andrology*,17:104-110.

Bergman,P. et al., **2005**, *Cell. Microbiol.*, 7:1009-1017.

Bergman,P. et al., **2007**, *Curr. HIV Res.*, 5:410-415.

Brandenburg,L.O. et al., **2008**, *J. Neuropathol. Exp. Neurol.*, 67:1041-1054.

Boggs,J.M. et al., **2000**, *Biophysical Journal*, 78:874-885.

Boman,H.G. et al., **2000**, *Immunol. Rev.*, 173:5-16.

Borg,N.A. et al., **2007**, *Nature*, 448:44-49.

Bou,K.M. et al., **2006**, *Dev. Biol.*, 290:220-235.

Brogi,A. et al., **1999**, *J. Submicrosc. Cytol. Pathol.*, 27:565-571.

Brogi,A. et al., **1996**, *AIDS Res. Hum. Retroviruses*, 12:483-489.

Brusca,R.C. et al., **1990**, *Sinuar Press, MA, USA*, pp 181-210.

Bucki,R. et al., **2010**, *Arch. Immunol. Ther. Exp.*, 58:15-25.

Bulet,P. et al., **2004**, *Immunol. Rev.*, 198:169-184.

Chen,S. and Cardullo,R., **1994**, *Molecular Biology of the Cell*, 5:224a.

Coetzee,T. et al., **1996a**, *Cell*, 86:209-219.

Cooper,T.G. et al., **1997**, *Physiology of sperm maturation and fertilization.* In Andrology: Male Reproductive Health and Dysfunction, E.Nieschlag, ed. (Berlin Heidelberg: Springer-Verlag), pp. 61-78.

Costantino,V. et al., **1995**, *Liebigs Ann.*, 2133.

Costantino, V. et al., **1996**, *Tetrahedron*, 52:1573-1578.

Costantino,V. et al., *Bioorg. Med. Chem. Lett.,* **1999**, 9:271.

Cowland,J.B. et al., **1995**, *FEBS Lett.*, 368:173-176.

Cross,N.L., **1998**, *Biology of Reproduction*, 59:7-11.

Crossin,K.L. and Edelman,G.M., **1992**, *Journal of Neuroscience Research*, 33:631-638.

Dacheux,J.L. et al., **2003**, *Microsc. Res. Tech.*, 61:7-17.

Dathe,M. et al., **1999**, *Biochim. Biophys. Acta*, 1462:71-78.

Dathe,M. et al., **1997**, *FEBS Lett.*, 403:208-212.

Dasgupta,F. et al., **1994**, *Carbohydr. Res.*, 264:155-160.

de Kretser,D.M.et al., **1994**, *In The Physiology of Reproduction*, E.Knobil and J.D.Neill, eds. (New York: Raven press), pp. 1177-1290.

De Libero,G. and Mori, L., **2005,** *Nat. Rev. Immunol.*, 5:485.

den Hertog,A.L. et al., **2006G,** *Biol. Chem.*, 387:1495-1502.

Eddy,E.M. et al., **1994**, *In The Physiology of Reproduction*, E.Knobil, ed. (New York: Raven Press), pp. 29-77.

Exely,M. et al., **2000**, *Immunology*, 100:34-37

Evans,J.P., **1999**, *Front Biosci.*, 4:D114-D131.

Flesch,F.M.et al., **2001**, *J. Cell Sci.*,114:3543-3555.

Flesch,F.M. et al., **2000**, *Biochimica et Biophysica Acta*, 1469:197-235.

Florman,H.M. et al., **2006**, *In Knobil and Neil's Physiology of Reproduction*, J.D.Neill, ed. (New York: Elsevier), pp. 55-112.

Fluharty,A.L. et al., **1974**, *Biochemical and Biophysical Research Communications*, 61:348-354.

Fornes,W.M. et al., **1995**, *Andrologia*, 27:233-237.

Franchini et al., **2008**, *Chem. Phys. Lipids.*, 152:78-85.

Frank,M., **2000**, *Prog. Neurobiol.*, 60:531-544.

Frenette,G. et al., **2002**, *Biology of Reproduction*, 67:308-313.

Frenette,G. et al., **2001**, *Molecular Reproduction and Development*, 59:115-121.

Friedrich,M.V. et al., **1999**, *J. Mol. Biol.*, 294:259-270.

Frohm,M. et al., **1997**, *J. Biol. Chem.*, 272:15258-15263.

Fujimoto,H. et al., **2000**, *Journal of Biological Chemistry*, 275:22623-22626.

Gallo,R.L. et al., **1997**, *J. Biol. Chem.*, 272:13088-13093.

Ganz,T. et al., **1999**, *Science*, 286:420-421.

Gatti,J.L. et al., **2000**, *Biol. Reprod.*, 62:950-958.

Gaudreault,E. and Grosselin,J., **2007**, *Viral Immunol.*, 20:407-420.

Giangaspero,A. et al., **2001**, *Eur. J. Biochem.*, 268:5589-5600.

Gudmundsson,G.H. et al., **1996**, *Eur. J. Biochem.*, 238:325-332.

Hammami-Hamza,S. et al., **2001**, *Mol. Hum. Reprod.*, 7:625-632.

Holt,G.D. et al., **1989**, *Journal of Biological Chemistry*, 264:12138-12140.

Holt,G.D. et al., **1990**, *Journal of Biological Chemistry* 1990:2852-2855.

Honke,K. et al., **2000**, *Proceedings of the National Academy of Science USA* 99:4227-4232.

Hsu,L.H. et al., **1983**, *Can. J. Biochem. Cell Biol.*, 61:1272-1281.

Ianaro,A. et al., **1995**, *Immunology*, 84:8

Ida,M. et al., **2004**, *J. Biochem. (Tokyo)* 135:583-588.

Ishizuka,I. et al., **1973**, *Journal of Biochemistry*, 73:77-87.

Kerr,C.L. et al., **2002**, *Biology of Reproduction* 66(6):1585-1595.

Kierszenbaum,A.L., **2002**, Histology and cell biology: an introduction to pathology. (St. Louis: Mosby, Inc.).

Kishida,J. et al., **2005**, *Tetrahedron*, 61:10559-10568

Klugerman,A. and Kornblatt,M.J., **1980**, *Can. J. Biochem.*, 58:225-229.

Knapp,A. et al., **1973**, *Biochemical and Biophysical Research Communications*, 55:179-186.

Kobayashy,K. et al., **1995**, *Oncol. Res.*, 7:529-534.

Koch,M. et al., **2005**, *Nat. Immunol.*, 6:819-826

Kolter,T. and Sandhoff,K., **2005**, *Annu. Rev. Cell Dev. Biol.*, 21:81-103.

Kornblatt,M.J. et al., **1974**, *Can. J. Biochem.*, 52:689-697.

Kupker,W. et al., **1998**, *European Society for Human Reproduction & Embryology*, 13(suppl. 1):20-26

Kurosawa,N. et al., **2000**, *European Journal of Biochemistry*, 267:344-351.

Lai,Y. et al., **2009**, *Trends Immunol.*, 30:131-141.

Laemmli,U.K., **1970**, *Nature*, 227:680-685.

Laroche,M. et al., **2007**, *Mar. Biol.*, 151:1365-1373.

Larrick,J.W. et al., **1991**, *Biochem. Biophys. Res. Commun.*, 179:170-175.

Larrick,J.W. et al., **1995**, *Infect. Immunol.*, 63:1291-1297.

Larrick,J.W. et al., **1996**, *FEBS Lett.*, 398:74-80.

Lehrer,R.I. et al., **1999**, *Curr. Opin. Immunol.*, 11:23-27.

Letts,P.J. et al., **1978**, *Biochimica et Biophysica Acta* 541:59-75.

Lingwood,C.et al., **1994**, *Molecular Reproduction and Development* 37:462-466.

Lingwood,C. et al., **1990**, *Journal of Cellular Physiology* 142:170-176.

Lingwood,C.A., **1981**, *The Journal of Cell Biology* 89:621-630.

Lingwood,C.A., **1985**, *Journal of Cell Science* 75:329-338.

Lingwood,C.A., **1986**, *Biochemistry and Cell Biology*, 64:984-992.

Lingwood,C.A. et al., **1981**, *Can. J. Biochem.*, 59:556-563.

Loffredo et al., **2010**, *J. Immunol.*, in press.

Lopez-Garzia,B. et al., **2005**, *J. Invest. Dermatol.*, 125:108-115.

Malm,J. et al., **2000**, *Infect Immun.*, 68:4297-4302.

Mamelak,D. and Lingwood,C., **2001**, *Journal of Biological Chemistry* 276:449-456.

Mohan,P.S. et al., **1992**, *Biochem. Biophys. Res. Commun.*, 182:689-696.

Molander-Melin,M. et al., **2004**, *J. Neurocytol.*, 33:417-427.

Morales,C.R. et al., **1998**, *J. Androl.*, 19:156-164.

Motoki,K. et al., **1995**, *Bioorg. Med. Chem. Lett.*, 5:705.

Moviglia,G.A. et al., **1982**, *Journal of Reproduction and Fertility*, 66:123-127.

Murakami,M. et al., **2002**, *J. Invest. Dermatol.*, 119:1090-1095.

Murakami.M. et al., **2002**, *J. Dent. Res.*, 81:845-850.

Needham,L.K. and Schnaar,R.L., **1993**, *Proc. Natl. Acad. Sci. U.S.A*, 90:1359-1363.

Nijnik,A. and Hancock,R., **2009**, *Curr. Opin. Hematol.*, 16:41-47.

Nilsson,M.F. et al, **1999**, *Infect. Immunol.*, 67:2561-2566.

Nilsson,T. and Warren,G., **1994**, *Curr. Opin. Cell Biol.*, 6:517-521.

O'Brien,J.S. and Kishimoto,Y., **1991**, *FASEB Journal*, 5:301-308.

Olson,L.D. and Gilbert,A.A., **1993**, *J. Bacteriol.*, 175:3224-3227.

Pancake,S. et al., **1992**, *The Journal of Cell Biology*, 117:1351-1357.

Parks,J.E. and Lynch,D.V., **1992**, *Cryobiology*, 29:255-266.

Pawlik,J.R. et al., **1993**, *Chem. Rev.*, 93:1911-1922.

Piel,J. et al., **2004**, *Nat. Prod. Rep.*, 21:519-538.

Popsueva,A.E. et al., **1996**, *FEBS Lett.*, 391:5-8.

Porcelli,S., **1995**, *Adv. Immunol.*, 59:1-98.

Primakoff,P. et al., **2002**, *Science*, 296:2183-2185.

Ritonja,A. et al., **1989**, *FEBS Lett.*, 255:211-214.

Roberts,D.D., **1998**, *Cancer Res.*, 48:6785-6793.

Roberts,D.D. et al, **1986**, *Journal of Biological Chemistry*, 261:3306-3309.

Rousset,E. et al., **1998**, *Infect. Immun.*, 6:5650-5658.

Saez,F. et al., **2003**, *J. Androl*, 24:149-154.

Sakac,D. et al., **1992**, *Journal of Biological Chemistry*, 267:1655-1659.

Schott,I. et al., **2001**, *Virchows Archive*, 439:90-96.

Schulte,S. and Stoffel,W., **1993**, *Proc. Natl. Acad. Sci. U. S. A*, 90:10265-10269.

Scocchi,M. et al., **1999**, *FEBS Lett.*, 57:459-464.

Shadan,S. et al., **2004**, *Biol. Reprod.*, 71:253-265.

Shirley,M.A. and Schachter,H., **1980**, *Can. J. Biochem.*, 58:1230-1239.

Smeianov,V. et al., **2000**, *Microbes Infect.*, 2:773-777.

Sorensen,O.E. et al., **2001**, *Blood*, 97-3951.

Sorensen,O.E. et al., **2003**, *J. Biol.Chem.*, 278:2854-28546.

Sorensen,O.E. et al., **2005**, *Comb. Chem. High Thruoghput Screening*, 8:273

Sosa,M.A. et al., **1996**, *Andrologia*, 28:217-221.

Sprong,H. et al., **1998**, *J. Biol. Chem.*, 273:25880-25888.

Stie,J. et al., **2007**, *J. Leukocyte Biol.*, 82:261.

Storici,P. and Zanetti,M., **1993a**, *Biochem. Biophys. Res. Commun.*, 196:1058-1065.

Storici,P. and Zanetti,M., **1993b**, *Biochem. Biophys. Res. Commun.*, 196:1363-1368.

Storici,P. et al., **1994**, *FEBS Lett.*, 337:303-307.

Suzuki,A. et al., **1973**, *Japan J. Exp. Japan Journal of Experimental Medicine*, 43:435-442.

Suzuki,Y. et al, **1993**, *Biochemical and Biophysical Research Communications*, 190:426-434.

Tadano-Aritomi,K. et al., **2003**, *J. Lipid Res.*, 44:1737-1743.

Tanphaichitr,N. et al., **2003**, *Lipid Metabolism and Male Fertility, S.De Vriese, ed.* (Champaign, IL: AOCS Press).

Tanphaichitr,N. et al, **2007**, *Frontiers in Bioscience*, 12:1748-1766.

Tanphaichitr,N. et al ., **1990**, *Biochem. Cell Biol.*, 68:528-535.

Tantibhedhyangkul,J. et al., **2002**, *Biology of Reproduction*, 67:212-219.

Towbin,H. et al., **1984**, *Journal of Immunological Methods*, 72:313-340.

Towle,M.J. et al., **2001**, *Cancer Res.*, 61:1013-1021.

Travis,S.M. et al., **2000**, *Infect. Immun.*, 68:2748-2755.

Tulsiani,D.R. et al., **1995**, *Biochem. J.*, 305 (Pt 1):41-50.

van't Hof,W. et al., **2001**, *Biol. Chem.*, 382:597-619.

Wassarman,P.M., **2005**, *J. Cell Physiol*, 204:388-391.

Disease, (The McGraw-Hill Companies), pp. 3695-3724.

Weerachatyanukul,W. et al., **2001a**, *Molecular Reproduction and Development*, 60(4):569-578.

Weerachatyanukul,W. et al., **2001b**, *Biology of Reproduction*, 64: Suppl. 1, 220, Abstract.

Weerachatyanukul,W. et al., **2003**, *Biol. Reprod.,* 69:1183-1192.

Wieprecht,T. et al., **1999**, *Biochemistry*, 36:12869-12880.

White,D. et al., **2000**, *Biology of Reproduction*, 63:147-155.

Yang,D. et al., **2002**, *Trends Immunol.*, 23:291-296.

Yamato,K. et al., **1974**, *Journal of Biochemistry*, 75:1241-1247.

Yanagimachi,R. et al.,**1985**, *Am. J. Anat.*, 172:317-330.

Yanagimachi,R., **1994**, *In The Physiology of Reproduction*, E.Knobil, ed. (New York: Raven Press Ltd.), pp. 189-317.

Yeung,C.H.et al., **1997**, *Mol. Reprod. Dev.*, 48:267-275.

von Figura,K. et al., **2001**, *In The Online Metabolic & Molecular Bases of Inherited*

Zaiou,M. et al., **2007**, *J. Mol. Med.*, 85:317-329.

Zanetti,M. et al., **1995**, *FEBS Lett.*, 374:1-5.

Zasloff,M. et al., **2002**, *Nature*, 415:389-395.

Zhao,C. et al., **2001**, *Antimicrob. Agents Chemother.*, 45:2695-2702.

19. ACKNOWLEDGEMENTS